การเพิ่มปริมาณก๊าซธรรมชาติเหลวโดยใช้การแทนที่ แบบ่ผเทของคาร์บอนไดออกไซด์

นาย นิธิฉัตร กฤษนันต์

วิทยานิพนธ์นี้เป็นส่วนหนึ่ งของการศึกษาตามหลักสูตรปริญญาวิศวกรรมศาสตรมหาบัณฑิต
สาขาวิชาวิศวกรรมปิโตรเลียม ภาควิชาวิศวกรรมเหมืองแร่และปิโตรเลียม
คณะวิศวกรรมศาสตร์ จุฬาลงกรณ์มหาวิทยาลัย
ปีการศึกษา 2553

ENHANCED CONDENSATE RECOVERY USING CO_2 DUMP FLOOD

Mr. Nitichatr Kridsanan

A Thesis Submitted in Partial Fulfillment of the Requirements
for the Degree of Master of Engineering Program in Petroleum Engineering
Department of Mining and Petroleum Engineering
Faculty of Engineering
Chulalongkorn University
Academic Year 2010

Thesis Title	ENHANCED CONDENSATE RECOVERY USING CO_2 DUMP FLOOD
By	Mr. Nitichatr Kridsanan
Field of Study	Petroleum Engineering
Thesis Advisor	Assistant Professor Suwat Athichanagorn, Ph.D.

Accepted by the Faculty of Engineering, Chulalongkorn University in Partial Fulfillment of the Requirements for the Master's Degree

.... Dean of the Faculty of Engineering
(Associate Professor Boonsom Lerdhirunwong, Dr.Ing.)

THESIS COMMITTEE

..............................Chairman
(Associate Professor Sarithdej Pathanasethpong)

Suwat Athichanagorn
...........................Thesis Advisor
(Assistant Professor Suwat Athichanagorn, Ph.D.)

..............................External Examiner
(Siree Nasakun, Ph.D.)

นิธิฉัตร กฤษนันต์ : การเพิ่มปริมาณก๊าซธรรมชาติเหลวโดยใช้การแทนที่แบบถ่ายเทของคาร์บอนไดออกไซด์ (ENHANCED CONDENSATE RECOVERY USING CO_2 DUMP FLOOD) อ. ที่ปรึกษาวิทยานิพนธ์หลัก: ผศ. ดร. สุวัฒน์ อธิชนากร, 102 หน้า.

เพื่อที่จะเพิ่มผลผลิตก๊าซธรรมชาติเหลวจากแหล่งกักเก็บก๊าซธรรมชาติที่มีก๊าซธรรมชาติเหลวเป็นส่วนประกอบ เราอาจจะใช้วิธีการอัดก๊าซเพื่อเพิ่มความดันในแหล่งกักเก็บเพื่อที่จะหลีกเลี่ยงการก่อตัวของก๊าซธรรมชาติเหลวในแหล่งกักเก็บ ซึ่งโดยปกติแล้วก๊าซคาร์บอนไดออกไซด์หรือก๊าซมีเทนจะถูกเลือกเพื่อใช้ในการอัด โดยที่การอัดก๊าซมีเทนหรือคาร์บอนไดออกไซด์นั้นไม่เพียงแต่เพื่อเพิ่มความดันของแหล่งกักเก็บแต่ยังลดจุดความดันกลั่นตัวเป็นเหตุให้การกลั่นตัวเป็นไปได้ยากอีกด้วย

แหล่งก๊าซธรรมชาติจำนวนมากในอ่าวไทยนั้นเป็นแบบเรียงตัวเป็นชั้นๆ โดยไม่เชื่อมต่อถึงกัน บางแหล่งกักเก็บมีปริมาณก๊าซคาร์บอนไดออกไซด์สูงซึ่งไม่เหมาะต่อการผลิตเนื่องด้วยเหตุผลทางเศรษฐกิจ แต่หนทางหนึ่งซึ่งจะสามารถใช้ประโยชน์ได้ก็คือทำการแทนที่แบบถ่ายเทจากแหล่งที่มีปริมาณก๊าซคาร์บอนไดออกไซด์และความดันของแหล่งกักเก็บที่มีค่าสูงไปสู่แหล่งกักเก็บก๊าซธรรมชาติที่มีก๊าซธรรมชาติเหลวเพื่อเพิ่มความดันและลดจุดความดันกลั่นตัว ซึ่งจุดประสงค์หลักในการทำการแทนที่แบบถ่ายเทนี้เพื่อเพิ่มผลผลิตก๊าซธรรมชาติเหลวโดยวิธีการป้องกันไม่ให้ก๊าซธรรมชาติเหลวกลั่นตัวในแหล่งกักเก็บ

ในงานศึกษานี้เราได้ใช้แบบจำลองแหล่งกักเก็บชนิดพิจารณาองค์ประกอบเพื่อประเมินประสิทธิภาพการแทนที่แบบถ่ายเท ซึ่งพารามิเตอร์ที่สำคัญสามชนิดที่ถูกพิจารณาในการศึกษานี้คือเวลาที่ทำการแทนที่แบบถ่ายเท องค์ประกอบในแหล่งกักเก็บที่มีปริมาณก๊าซคาร์บอนไดออกไซด์สูง และ ระยะห่างของความลึกระหว่างแหล่งกักเก็บก๊าซธรรมชาติที่มีก๊าซธรรมชาติเหลวกับแหล่งกักเก็บที่มีปริมาณก๊าซคาร์บอนไดออกไซด์สูง จากผลการจำลองพบว่าการแทนที่แบบถ่ายเทของแหล่งกักเก็บที่มีปริมาณก๊าซคาร์บอนไดออกไซด์สูงนั้นจะมีประสิทธิภาพสูงเมื่อทำการแทนที่แบบถ่ายเทก่อนที่ความดันของแหล่งกักเก็บก๊าซธรรมชาติที่มีก๊าซธรรมชาติเหลวจะต่ำกว่าจุดความดันกลั่นตัวและผลการทดลองยังแสดงให้เห็นอีกว่าผลขององค์ประกอบในแหล่งกักเก็บที่มีปริมาณก๊าซคาร์บอนไดออกไซด์สูงและระยะห่างของความลึกระหว่างแหล่งกักเก็บมีผลต่อการเพิ่มผลผลิตก๊าซธรรมชาติเหลวเล็กน้อย

ภาควิชา วิศวกรรมเหมืองแร่และปิโตรเลียม ลายมือชื่อนิสิต

สาขาวิชา วิศวกรรมปิโตรเลียม ลายมือชื่อ อ.ที่ปรึกษาวิทยานิพนธ์หลัก

ปีการศึกษา 2553

5271608921: MAJOR PETROLEUM ENGINEERING
KEYWORDS: ENHANCE / DUMP FLOOD/ GAS CONDENSATE

NITICHATR KRIDSANAN. ENHANCED CONDENSATE RECOVERY USING CO_2 DUMP FLOOD. ADVISOR: ASST. PROF. SUWAT ATHICHANAGORN, Ph.D., 102 pp.

In order to increase condensate recovery from a gas-condensate reservoir, one may inject gas to increase the reservoir pressure to avoid condensate dropout in the reservoir. Several types of gas may be chosen for this process. However, two commonly used are CO_2 or CH_4. Injecting CO_2 or CH_4 will not only increase the reservoir pressure but also decrease the dewpoint pressure, making it more difficult for gas to condense into condensate when the pressure in the reservoir declines as a result of gas production.

In the Gulf of Thailand, many gas fields are multi-stacked reservoirs. Some of these reservoirs have high CO_2 content. It is not economical to produce gas from these reservoirs. One way to make use of this high-pressure gas is to perform internal dump flood in which high CO_2 gas is flowed from the source reservoir to the target gas-condensate reservoir to increase the pressure of the target reservoir as well as to reduce the dewpoint of the reservoir fluid. The main purpose is to increase condensate recovery by preventing condensate dropout in the reservoir.

In this thesis, hypothetical reservoir models were created in order to evaluate the performance of gas dump flood. Three important variables which are timing of the flooding, composition of the source gas, and the difference in original depths of the source and target reservoirs were considered in this study. The results from reservoir simulation show that the best time to start gas dump flood is before the reservoir pressure drops below the dewpoint pressure and that the composition of the source gas and the difference in original reservoir depths have a slight effect on the recovery of condensate.

Department: Mining and Petroleum Engineering Student's signature: ....
Field of study: Petroleum Engineering Advisor's signature: Suwat Athichanagorn
Academic Year: 2010

Acknowledgements

I would like to express my sincere gratitude to my advisor Asst. Prof. Suwat Athichanagorn for his guidance and support throughout the thesis. Without his valuable comments, completion of this work would not have been possible.

I would like to thank my all faculty members in the Department of Mining and Petroleum Engineering who have offered petroleum knowledge, technical advice, and invaluable consultation.

I would like to also thank Schlumberger for providing educational license of ECLIPSE reservoir simulator to the Department of Mining and Petroleum Engineering.

My appreciation goes to my mother and sister for all the care and advice I have received and continue to receive from them. They are always closest to my joys and sorrows and always standing by me.

Contents

Page

CHAPTER

List of Tables

List of Figures

List of Abbreviations

bbl	barrel (bbl/d : barrel per day)
BHP	bottom hole pressure
C_1	methane
C_2	ethane
C_3	propane
$i\text{-}C_4$ or $I\text{-}C_4$	isobutane
$i\text{-}C_5$ or $I\text{-}C_5$	isopentane
$n\text{-}C_4$ or $N\text{-}C_4$	normal butane
$n\text{-}C_5$ or $N\text{-}C_5$	normal pentane
C_6	hexane
C_{7+}	alkane hydrocarbon account from heptanes forward
CO_2	carbon dioxide
D	darcy
EQUIL	equilibrium data specification
EOR	enhance oil recovery
EoS	equation of state
LGR	local grid refinement
LPG	liquefied petroleum gas
M	thousand (1,000 of petroleum unit)
MSCF/D	thousand standard cubic feet per day
PVT	pressure-volume-temperature
PSIA or psia	pounds per square inch absolute
SCAL	special core analysis
$SCCO_2$	supercritical carbon dioxide
STB or stb	stock-tank barrel
STB/D	stock-tank barrels per day
SWAT	water saturation
TVD	true vertical depth or total vertical depth

Nomenclature

A	cross-section area
B	formation volume factor
E	sweep efficiency
k	permeability
k_r	relative permeability
k_{rg}	gas relative permeability
k_{rw}	water relative permeability
k_{rog}	oil relative permeability for a system with oil, gas and connate water
k_{row}	oil relative permeability for a system with oil and water only
k_{rowg}	oil relative permeability for a system with oil and water at $S_g = 0$
N_c	capillary number
p	pressure
p_c	capillary pressure
q	volumetric flow rate
S	saturation
S_r	residual saturation
T	temperature
v	velocity
x	distance
z	compressibility factor

GREEK LETTER

β	Forchheimer parameter
ε	Corey exponent
ϕ	porosity
f	capillary number dependent transition function
ρ	fluid density (mass/volume)
μ	fluid viscosity
α	constant in capillary number dependent transition function
σ	interfacial tension

SUBSCRIPTS

A	areal
atm	at standard pressure
d	displacement
g	gas
i	vertical
sc	*at* standard condition
sw	distilled water
w	water
α	phase indicator for relative permeability and saturation

CHAPTER I

INTRODUCTION

Gas-condensate reservoir is considered the most complex reservoir among other types of petroleum reservoirs. A gas-condensate is a single-phase fluid in the form of gas at initial reservoir conditions. As the reservoir pressure decreases and passes through the dewpoint, liquid forms. The amount of the liquid increases as the pressure decreases during retrograde condensation. When condensate liquid forms in a gas-condensate reservoir, some condensate liquid is immobile because capillary forces act upon the fluids and condensate saturation is less than the critical saturation. As a consequence, valuable condensate is lost in the reservoir. At a near-well region, the condensate saturation is greater than the critical saturation, so both gas and condensate flow. However, condensate saturation here is highest because lowest pressure occurs at the bottomhole. The oil relative permeability increases with saturation. The decrease in gas relative permeability near the wellbore illustrates the condensate blockage effect. Consequently, additional pressure drop due to condensate blockage can cause a loss of well productivity.

When normal depletion leaves valuable condensate fluids in the reservoir, condensate blockage can be very important for well productivity. Thus, many recovery solutions such as gas cycling, gas injection can be planed ahead to manage the gas-condensate reservoir. The main objective is to recover more condensate. Since the price of natural gas has risen to the value that makes reinjection less attractive strategy, alternatively worthless gas such as CO_2 instead of natural gas may be a good candidate.

In the Gulf of Thailand, we usually find many multi-stacked gas or gas-condensate reservoirs. Some gas reservoirs contain high CO_2 %mole while the others do not. In many cases, we do not produce the reservoir containing high CO_2 %mole because of economic reason. However, the internal gas dump flood is a potential solution to exploit the high CO_2 %mole reservoir to flood into a gas-condensate reservoir for enhanced condensate recovery.

1.1 Outline of Methodology

This research is to study the mechanism of gas dump flood in gas-condensate reservoir associated with pressure maintenance and revaporization with an emphasis on flow behavior analysis and condensate recovery. Although some research and development have been performed in this area, there still exist many important issues to be resolved. Specifically, this work focuses on the following aspects:

- Producing schemes. Different timings of gas dump flood strategy may impact gas production and condensate recovery. Optimal injection will be determined for best condensate production.
- Composition variation. The objective of this part is to study how the concentration of CO_2 in a source reservoir affects phase behavior of target reservoir during production.
- Depth or pressure difference. The reservoirs in multi-stacked reservoirs are located at different depths or pressures. This difference may have an effect to flooding mechanism such as cross flow rate, higher pressure losses in the wellbore.

In the gas dump flood scenarios, we also study effect of composition variation on vertical flow performance from source reservoir to target reservoir which has a different pressure loss in tubing when the compositions and depths are not the same. The abandonment rates were set by condensate production rate and gas production rate.

1.2 Thesis Outline

This thesis paper proceeds as follows.

Chapter II presents a literature review on core flooding experiment to investigate fluid behavior, condensate blockage effect around the well and the associated impairment in gas productivity and condensate recovery. The chapter includes advantages and limitations of existing technique of CO_2 injection into gas-condensate reservoir to enhance hydrocarbon recovery.

Chapter III describes the theory of gas-condensate reservoir such as gas-condensate phase behavior and flow regime behavior.

Chapter IV describes the simulation model used in this study.

Chapter V discusses the results of reservoir simulation obtained from different values of controlled variables which are time to start gas dump flood, CO_2 concentration in source reservoir and difference in depths between source and target reservoirs.

Chapter VI provides conclusions and recommendations for further study.

CHAPTER II

LITERATURE REVIEW

This chapter discusses some works related to core flooding experiment which was conducted to investigate the fluid behavior, condensate blockage effect around the well and the associated impairment in gas productivity and condensate recovery. Some works are significant for generating the most realistic simulation model which will be used to determine optimal production strategy. Most of the following literatures discuss related works in CO_2 flooding into gas-condensate reservoirs using a compositional reservoir simulator.

2.1 Previous works

Al-Abri et. al. [1] presented results from experimental work on CO_2-condensate and CO_2-methane relative permeabilities. They used high-pressure high-temperature equipment to perform experiments in order to determine relative permeabilities at reservoir conditions. The coreflooding experiments were conducted by injecting different supercritical CO_2 ($SCCO_2$)-methane concentrations. The CO_2 percentage in the methane was increased successively from 10% to 25%, 50% and 75%. In their results, the greater the percentage of $SCCO_2$ in the injection gas mixture, the higher the ability of the gas to displace the condensate before it breaks through. The relative permeability curves improve as the CO_2 concentration in the injection gas increases. Consequently, the mobility ratio decreases, giving rise to a more stable displacement front.

Shi et. al. [2] studied the behavior of condensate composition variation, condensate saturation build-up and condensate recovery during a gas-condensate production process. The authors performed core flooding experiments and compositional simulation to investigate the composition and condensate saturation variations in the reservoir. Different production strategies were compared, and the optimum production sequences were suggested for maximum gas recovery. In their simulation results, high total gas production can be achieved temporarily by using low BHP. However, lower BHP might not be a better strategy to minimize the condensate blockage or to enhance the ultimate liquid recovery. Therefore, they concluded that there is no standard way to optimize the production strategy or the optimal approach is likely to be dependent on the original composition.

Tangkaprasert [3] studied the behavior of CO_2 injection in gas-condensate reservoir using a reservoir simulator. Gas injection allows enhanced condensate recovery by reservoir pressure maintenance and liquid revaporization. In order to optimize the injection strategy, he created several scenarios to determine the most appropriate injection timing. The result is that the maximum oil recovery can be obtained by starting the injection shortly after the bottomhole pressure drops below the dewpoint pressure.

Shtepani [4] performed an experiment on CO_2 core flood displacement. The objective of his experiment is to investigate several factors affecting the mechanism, stability on the breakthrough and ultimate recoveries using P-x experiment. P-x experiment was performed on four different scenarios: 20, 40, 60 and 80 %mole of CO_2 mixtures. From his result, at 80% mole CO_2 injection, no condensate liquid occurs. The mixture is a single phase gas only. Therefore, properties of depleted gas-condensate reservoirs and CO_2 are favorable for re-pressurization and enhanced gas recovery processes.

Shi and Horne [5] conducted a study to determine appropriate production strategy to improve productivity from gas-condensate reservoirs. They performed a core flooding experiment and reservoir simulation. Their research provided the effect of bottomhole pressure, relative permeability and production. These parameters were compared and summarized to obtain the optimum strategy to maximize the gas recovery. From experimental results, they concluded that the composition and condensate saturation change significantly as a function of interfacial tension and relative permeability. Re-pressurizing might not be a good strategy for some cases to remove the liquid accumulation in the reservoir. In their simulation results, the total gas production can be achieved by lowering the BHP.

Chang et. al. [6] presented the model of oil recovery process involving CO_2 injection while taking into account the effect of CO_2 solubility in water. A new empirical correlation was introduced for estimating CO_2 solubility in water and NaCl brine, the water formation volume factor of CO_2-saturated water, water compressibility, and water viscosity. The calculation of solubility in formation water can also be adjusted further for the effects of salinity to obtain the solubility of CO_2 in brine.

The authors also investigated the effects of CO_2 solubility in water using a reservoir simulator. Two water alternating gas (WAG) injection cases were designed. Case A was operated as the secondary CO_2 flooding while case B was operated as the tertiary CO_2 flooding. The simulation results showed that about 10% of the CO_2 injected was dissolved in the water and was unavailable for mixing with oil. This might be considered “lost” to the aqueous phase.

Sengul [7] illustrated framework of CO_2 sequestration and vital aspects such as site selection, reservoir characterization, modeling of storage and long term leakage monitoring techniques. He concluded that CO_2 capture and storage (CCS) offers possibilities for making further use of fossil fuels more compatible with climate change and mitigation policies. Technologies required for CO_2 capture and storage, monitoring, verification are widely available today.

Sengul [7] also concluded that the probability of CO_2 leakage in oil and gas reservoirs is very low. However, brine formations, which generally are not well characterized and do not have caprocks or seals will require significant effort to evaluate potential risks, and these risks must be taken seriously.

Al-Hashami et. al. [8] investigated the effects of gas mixing, CO_2 diffusion and CO_2 solubility in formation water in the process of injecting CO_2 into gas reservoir using a compositional reservoir simulator. CO_2 dispersion effect in which the diffusion coefficient is high will cause an early CO_2 breakthrough. However, when the diffusion coefficient at reservoir conditions is smaller than 10^{-6} m^2/sec, the effect of diffusion can be ignored; hence, the mixing of CO_2 and methane is totally convective flow.

Regarding the effect of CO_2 solubility in water, CO_2 breakthrough time is delayed compared to the case without considering CO_2 solubility in water. Thus, the dissolution of CO_2 in formation water has some positive effect on CO_2 storage which can delay CO_2 breakthrough and store more CO_2 in the reservoir.

CHAPTER III

THEORY AND CONCEPT

In this chapter, we explore several key concepts about the flow behavior of the gas-condensate system and define related theories involved with the mechanism of gas flooding in a gas-condensate reservoir. Previous prospective researches on these issues are reviewed.

3.1 Review of Gas-Condensate Reservoir

Reservoir fluids can be divided into five types; black oil, volatile oil, retrograde gas, wet gas and dry gas. Each type of reservoir fluids has unique characteristics which can be confirmed only by observation in the laboratory. The characteristics used to identify the type of reservoir fluid are the initial producing gas oil ratio, the gravity of the stock tank liquid, the color of the stock tank liquid, oil formation volume factor, and mole fraction of hepthane plus.

Gas-condensate reservoir is considered the most complex reservoir among other types of petroleum reservoirs. The initial reservoir condition is a single phase gas. One unique phenomenon in near wellbore region of gas-condensate reservoir is condensate blockage. As reservoir pressure declines and passes though the dewpoint, condensate drops out of the gas. The condensate saturation is highest near the wellbore because the pressure is lowest. Condensate liquid can be produced into the wellbore. However, if the gas does not have sufficient energy to carry the liquid to surface, liquid loading in the wellbore occurs because the liquid is denser than the gas phase. If the liquid falls back down to the bottom of the wellbore, the liquid percentage will increase and may eventually restrict production.

3.1.1 Gas-Condensate Phase Behavior

Gas-condensate or retrograde gas is one of the various types of the reservoir fluid which has unique characteristics of phase diagram as illustrated in Figure 3.1.

The region of retrograde condensate occurs at temperature between the critical temperature (T_C) and the cricondentherm. The cricondentherm is the highest temperature on saturated envelope.

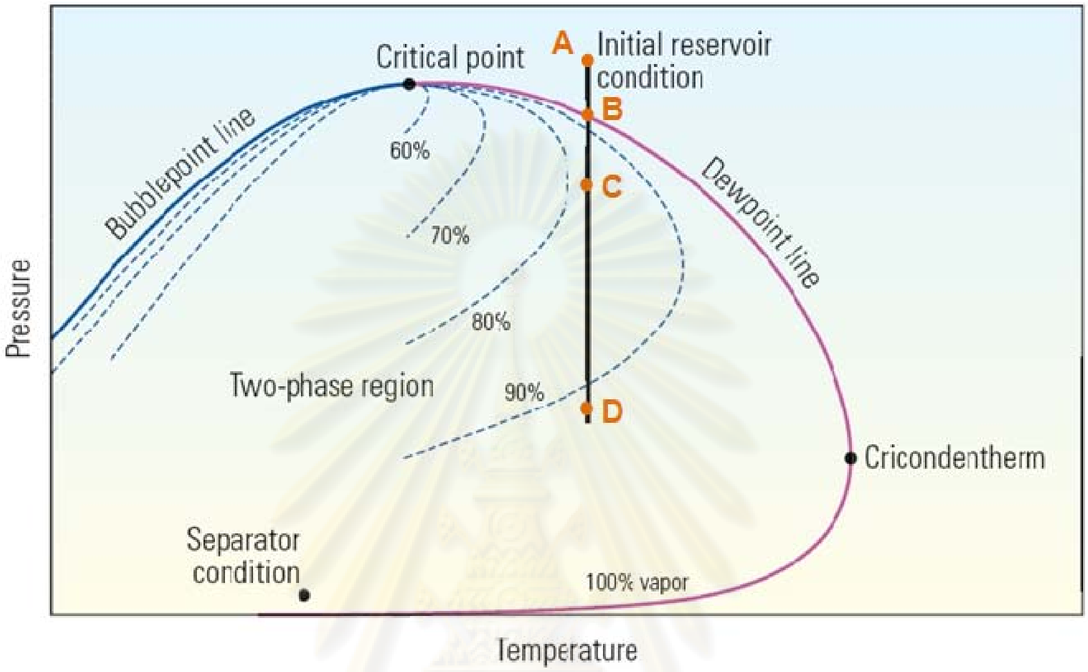

Figure 3.1: Pressure-Volume-Temperature diagram of condensate (after Fan et. al. [9]).

Gas-condensate is a single-phase gas at original reservoir condition (point A). At dewpoint pressure (point B), the fluid will start to separate into gas and liquid that is called a retrograde condensate. The liquid dropout in the pore space will lead to the formation of a liquid phase and a consequent reduction in the gas production of the well. This phenomenon continues until a point of maximum liquid volume is reached (point C). Lowering the pressure furthermore will cause the revaporization process (point D) but this process is typically below the economic life of the field, and this stage will not be reached.

The amount of liquid phase present depends not only on the pressure and temperature but also on the composition of the reservoir fluid. The condensate gas can be classified into three types; poor, middle and rich content condensate gas. The classifications and the physical characteristics are listed in Table 3.1.

Table 3.1: Physical characteristics of condensate gas (after Yisheng et. al. [10]).

Fluid type	Heavier hydrocarbon content C_7+	Reservoir fluid density (g/cm^3)	Production GOR (m^3/m^3)	Condensate content (g/m^3)
Poor	0.5 – 2.0	0.20 – 0.25	18000 - 5000	<150
Middle	2.0 – 4.0	0.25 – 0.30	5000 - 2000	150 - 350
Rich	4.0 – 9.0	0.30 – 0.45	2000 - 1000	250 - 600
Near critical	9.0 – 12.5	0.45 – 0.50	1000 - 700	600 - 800

A rich gas-condensate forms a higher percentage of liquid than a lean gas-condensate. The phase diagrams of poor, middle and rich content condensate gas are shown in Figures 3.2, 3.3 and 3.4, respectively.

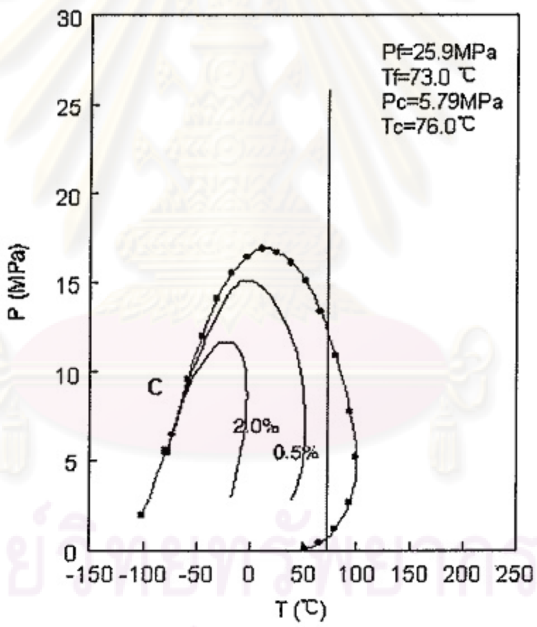

Figure 3.2: Pressure-Volume-Temperature diagram of poor condensate content (after Yisheng et. al. [10]).

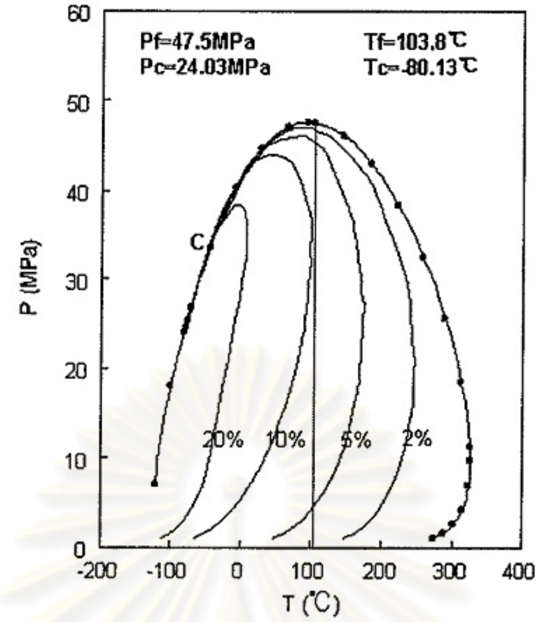

Figure 3.3: Pressure-Volume-Temperature diagram of middle condensate content (after Yisheng et. al. [10]).

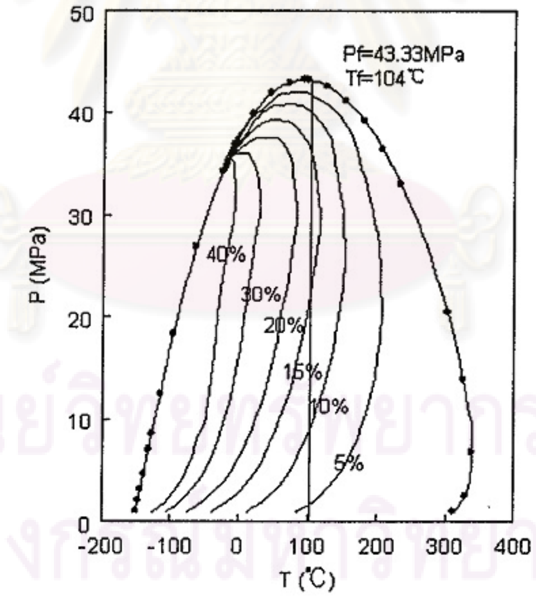

Figure 3.4: Pressure-Volume-Temperature diagram of rich condensate content (after Yisheng et. al. [10]).

3.1.2 Flow Regime Behavior

Fluid flow towards the well in a gas-condensate reservoir during depletion can be divided into three main flow regions. The two regions closet to the producing well exist when the pressure is below the dewpoint pressure and the third region exists when its pressure is above the dewpoint pressure as shown in Figures 3.5 and 3.6.

- Near-wellbore (Region 1): The condensate saturation of this region is greater than the critical condensate saturation. Both gas and condensate flow simultaneously at different velocities. The oil relative permeability increases with saturation while gas relative permeability decreases, illustrating the blockage effect.
- Condensate buildup (Region 2): Region where the condensate is dropping out of the gas. The condensate saturation of this region is less than the critical saturation. Only gas phase is flowing.
- Single phase gas (Region 3): This region is away from the producing well where only gas phase is present and flowing. Gas velocity in this region is generally low because the cross sectional area is high. Composition in this region is equal to the original reservoir gas.

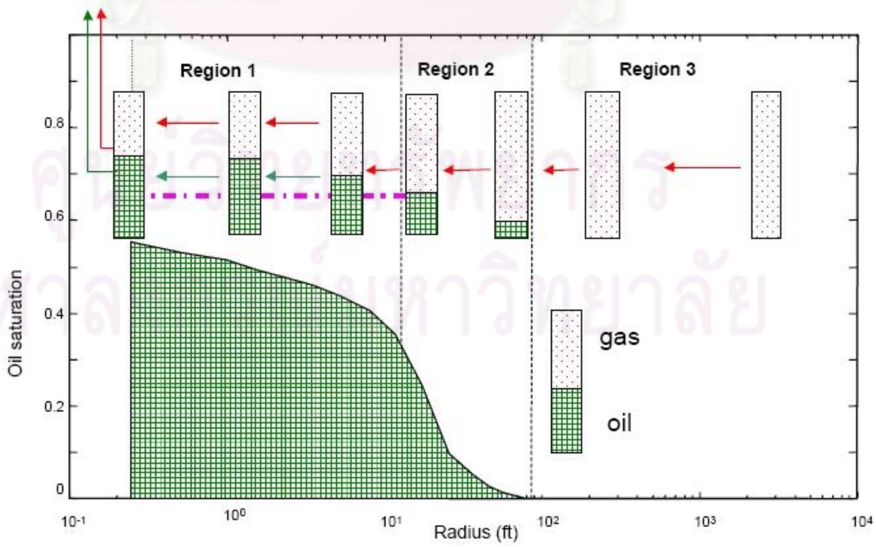

Figure 3.5: Three regions of gas-condensate fluid flow behavior (after Roussennac et. al. [11]).

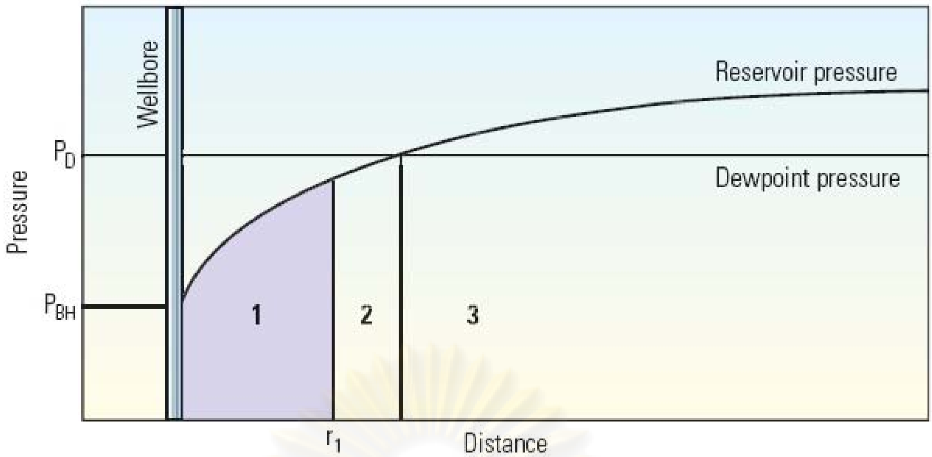

Figure 3.6: Three regions of gas-condensate pressure profile (after Fan et. al. [9]).

3.1.3 Fluid Composition Change

In gas-condensate system, the buildup of condensate is due to the pressure drop below the dewpoint pressure. The heavier components tend to drop out first and then become the condensate liquid. The phase diagram of the reservoir fluids is shifted clockwise to a system with higher critical temperature as shown in Figure 3.7.

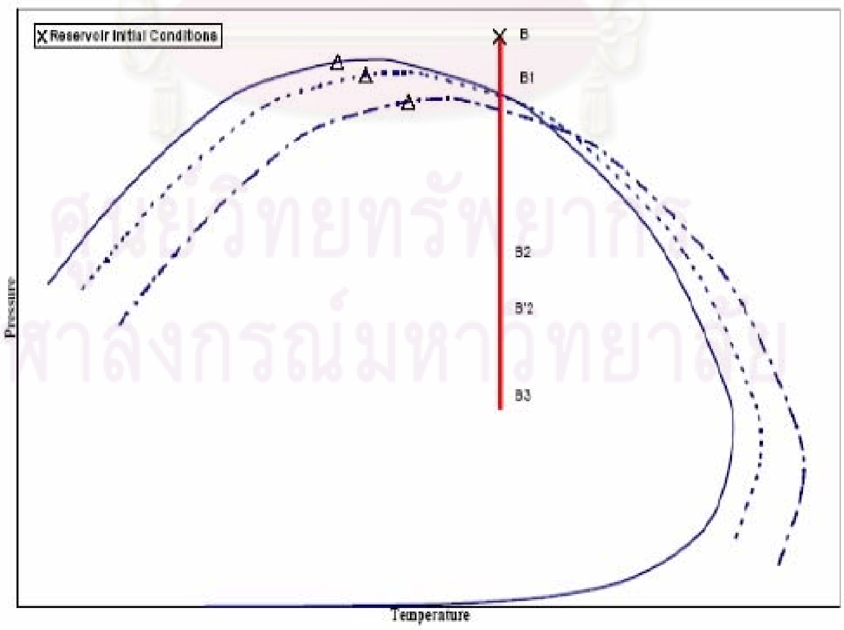

Figure 3.7: Shift of phase envelope with composition change
(after Roussennac [11]).

3.1.4 Non-Darcy Flow and Positive Coupling

In near wellbore region of gas-condensate reservoirs, there are two phenomena that affect the well productivity and cannot be expressed by Darcy equation which are non-Darcy flow and positive coupling.

Non-Darcy flow is typically observed in high-rate gas wells when the flow converging to the wellbore reaches flow velocities exceeding the Reynolds number for laminar or Darcy flow, and results in turbulent flow. The effect of non-Darcy flow can be treated by the Forchheimer equation with an empirical correlation. Forchheimer [12] proposed the following quadratic equation to express the relationship between pressure drop and velocity in a porous medium:

$$\frac{dp}{dx} = \left(\frac{\mu}{kk_r A}\right)q + \beta\rho\left(\frac{q}{A}\right)^2 \tag{3.1}$$

where:

q	is the volumetric flow rate
k	is the rock permeability
k_r	is the relative permeability
A	is the area through which flow occurs
μ	is the fluid viscosity
ρ	is the fluid density
β	is the Forchheimer parameter
$\frac{dp}{dx}$	is the pressure gradient normal to the area

Another phenomenon which is known as positive coupling occurs when the flow velocity is high and the interfacial tension between the flowing phases is low. In this case, capillary forces may no longer dominate the distribution of the phases on a pore scale. Subsequently, macroscopic flow properties become dependent on the ratio of viscous to capillary forces on a pore scale, denoted by the capillary number N_c.

$$N_c = \frac{k\left|\nabla P\right|}{\phi\sigma} \tag{3.2}$$

where:

σ is interfacial tension

ϕ is porosity

3.2 CO_2 Mixing in Gas-Condensate Reservoir

Re-pressurization and pressure maintenance are the most common methods to enhance gas and condensate recovery. By pressurizing the reservoir so that the reservoir pressure is above the dewpoint pressure, condensate blockage can be prevented. For gas dump flood into gas-condensate fields, high viscosity of CO_2 provides a favorable mobility ratio for the displacement of methane, leading to fewer tendencies of the injected gas to finger. Revaporization will remove the condensate blockage by changing the phase behavior of the reservoir fluid. The admixture of CO_2 to gas-condensate fluid will reduce the percent liquid and improve productivity and condensate recovery.

3.2.1 Flooding Patterns and Sweep Efficiency

The movement of fluids is controlled by the arrangement of injection and production wells. There are several patterns of production and injection wells for enhanced recovery project as depicted in Figure 3.8.

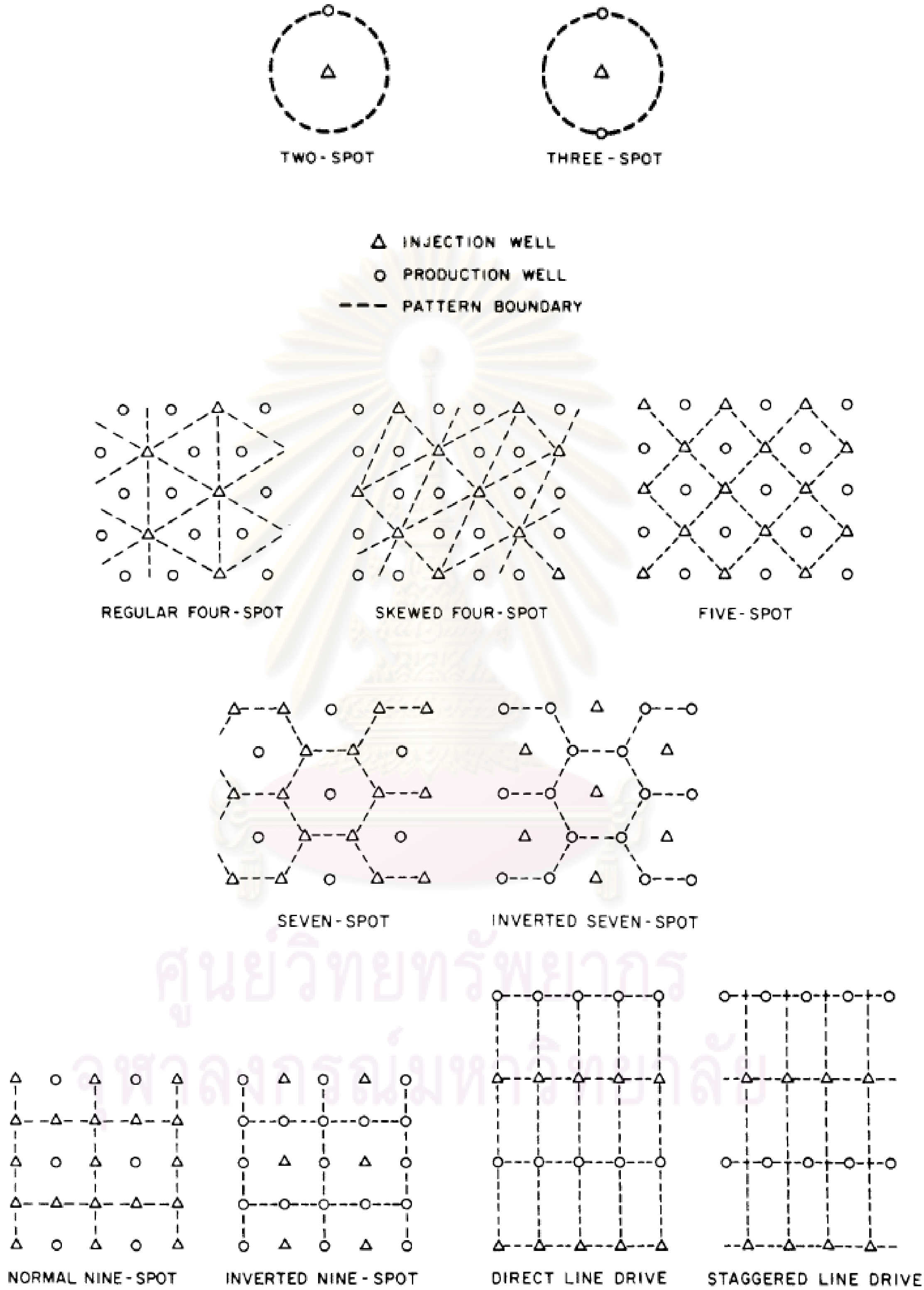

Figure 3.8: Flooding pattern. (after Willhite [13])

Different flooding patterns will result in different areal sweep efficiencies. The areal sweep efficiency at breakthrough was determined by various experimental techniques. The value of such areal sweep efficiency was calculated for a mobility ratio of unity. Table 3.2 presents the percentage of areal sweep efficiency at breakthrough calculated at unity mobility ratio for different flooding patterns. There is satisfactory agreement among most investigators that the five-spot flooding pattern gives the highest sweep efficiency.

Table 3.2: Areal sweep efficiency for various flooding patterns (after Forrest[14]).

Flooding Pattern	**Mobility Ratio**	**Areal sweep efficiency at breakthrough (%)**
Isolated two-spot	1.0	52.5 – 53.8
Isolated three-spot	1.0	78.5
Skewed four-spot	1.0	55.0
Inverted five-spot	1.0	80.0
Normal seven-spot	1.0	74.0-82.0
Inverted seven-spot	1.0	82.2

The overall efficiency at breakthrough is defined as

$$E = E_A \times E_i \times E_d \tag{3.3}$$

where

E_A = areal sweep efficiency, is the area swept in a model divided by total model reservoir area.

E_i = invasion or vertical sweep efficiency, is the hydrocarbon pore space invaded (affected, contacted) by the injection fluid divided by the hydrocarbon pore space enclosed in all layers behind the injected fluid.

E_d = displacement efficiency, is the volume of hydrocarbons displaced from individual pores or small groups of pores divided by the volume of hydrocarbon in the same pores just prior to displacement.

Dump and production well arrangement is selected by considering the highest areal sweep efficiency. Five-spot flooding pattern has been studied and reported to have the highest sweep efficiency at breakthrough. Figure 3.9 shows the schematic of five-spot flooding pattern. In five-spot flooding pattern, the injection well is located at the center of a square defined by four production wells. In this study, five-spot flooding pattern is changed to quarter five-spot because it obtains the same results as well as reduces the simulation model size.

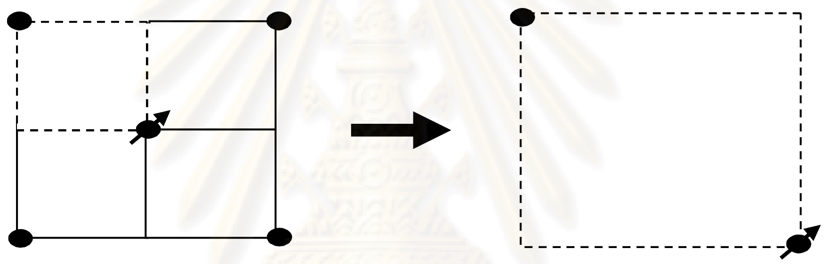

Figure 3.9: Five-spot flooding pattern.

3.2.2 Miscible Fluid Displacement

Miscibility fluid displacement is defined as a displacement process where the effectiveness of the displacement results primarily from miscibility between the displaced and displacing fluids. In this process, the displacing fluid is miscible, or will mix in all proportions with the displaced fluid. Three basic types of miscible fluid displacement are high pressure dry gas drives, enriched gas drives, and miscible slug drives. The first two employ more volatile components in the reservoir to aid in the development or creation of the miscible zone. In miscible slug injection, a slug or bank of liquefied petroleum gas (LPG) followed by scavenging gas is injected into the reservoir. This slug displaces the reservoir fluid from the swept portions of the reservoir.

CHAPTER IV

SIMULATION RESERVOIR MODEL

In order to determine optimal production and dump flooding strategy of gas dump flood to enhance condensate recovery, reservoir simulator was used as a tool to predict gas and condensate production under different strategies. As a result, the best strategy can be obtained.

The reservoir simulator ECLIPSE 300 specializing in compositional modeling was used in this study because it provides more accurate calculation of liquid dropout in the porous media by using flash calculation. For the simulation method, the adaptive implicit (AIM) mode was selected. We can divide the reservoir simulation model in to four main sections as follows:

1. **Grid section.** In this section the geometry of the reservoir and its permeability and porosity were specified.

2. **Fluid section.** The gas-condensate reservoir and source reservoir composition were specified in this section. The physical properties of each component and the EOS used in flash calculation were also specified. Initial reservoir condition was also included in this section.

3. **SCAL section.** In special core analysis or SCAL section, oil relative permeability in gas at connate water as a function of gas saturation, oil relative permeability in water as a function of water saturation were specified.

4. **Wellbore section.** The wellbore model was constructed and used to calculate the vertical flow performance.

This chapter describes in details on how properties are gathered in each section. The detail of the simulation input is shown in Appendices A and B.

4.1 Grid Section

In this study, we generated two reservoirs which are gas-condensate reservoir and source reservoir (high CO_2 content). Both reservoirs were constructed using Cartesian coordinate under plane geometry and homogeneous conditions. The dimension of each reservoir is 2000 ft x 2000 ft x 100 ft. The number of grid blocks of each reservoir is 25 x 25 x 5. The top of gas-condensate reservoir is located at a depth of 6,000 ft, and top of the source reservoir was varied in order to consider the effect of depth at 7,000 and 8,000 ft. The porosity of the reservoir was assumed to be 17.0%. The horizontal permeability was set at 50 mD, and the vertical permeability was 5 mD. Figures 4.1, 4.2, and 4.3 display the model used in this study in the top view, side view and 3D view, respectively.

4.1.1 Local Grid Refinement

Local grid refinement (LGR) was used around the dump flood and production wells in order to obtain accurate calculation of liquid dropout around the wellbores. In the reservoir simulator, we need to specify LGR name, coordinate, and the number of refined cells. The details of LGR are shown in Table 4.1.

Table 4.1: Description of local grid refinement

LGR name	LGR coordinate			Number of refined cells		
	I	J	K	X	Y	Z
Producer	24-25	24-25	1-5	8	8	5
Dump_FL	1-2	1-2	1-5,7-11	8	8	5

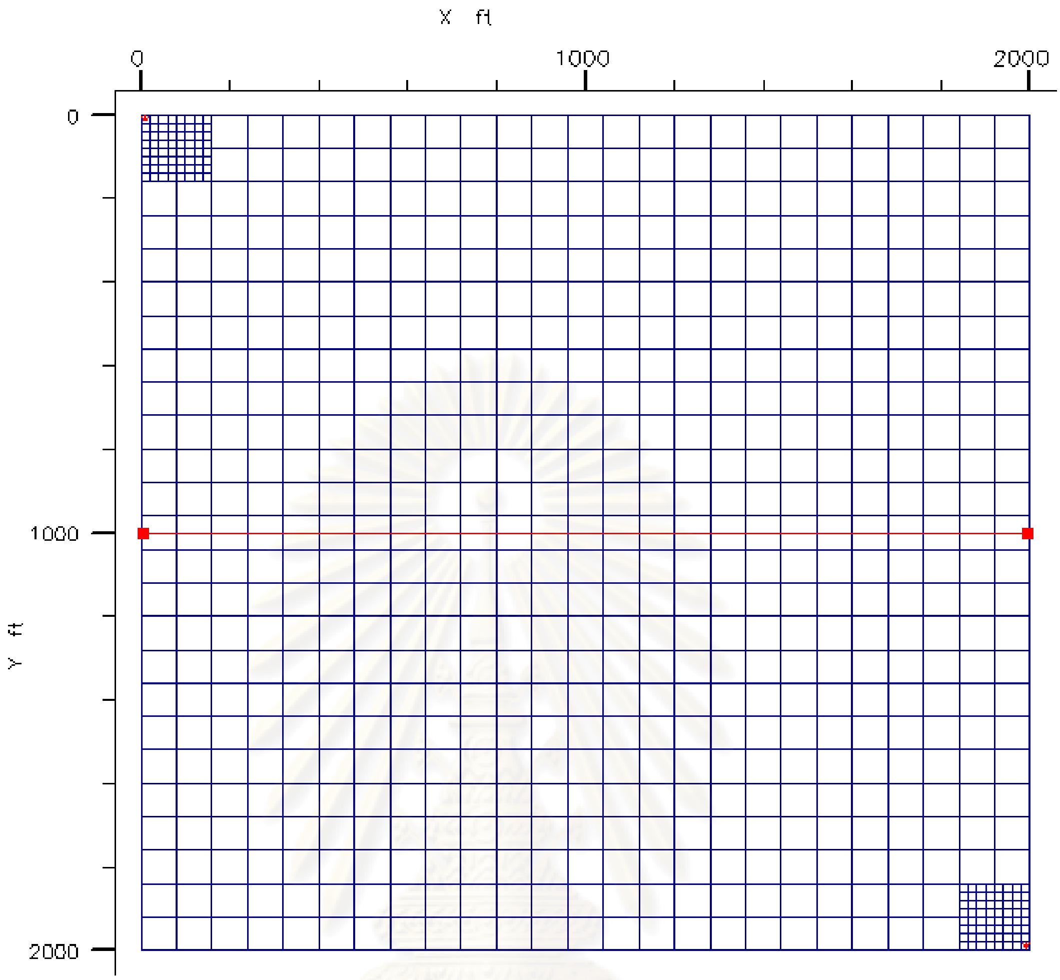

Figure 4.1: Top view of the reservoir model.

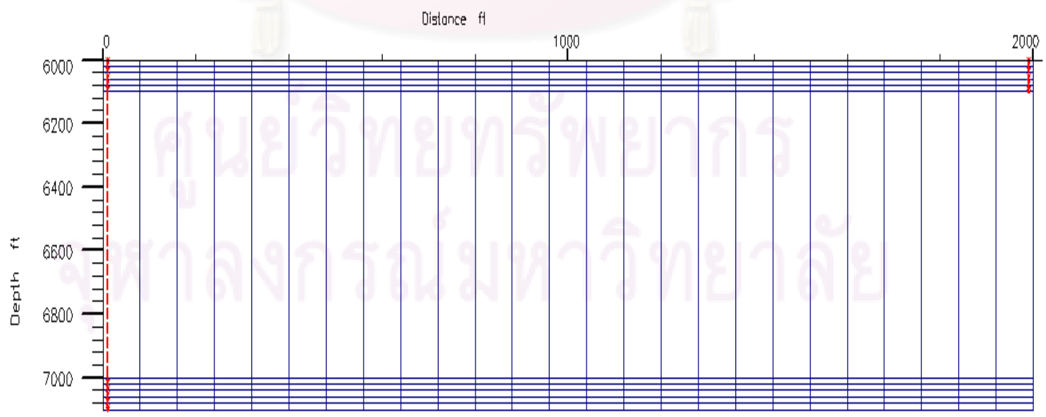

Figure 4.2: Side view of the reservoir model.

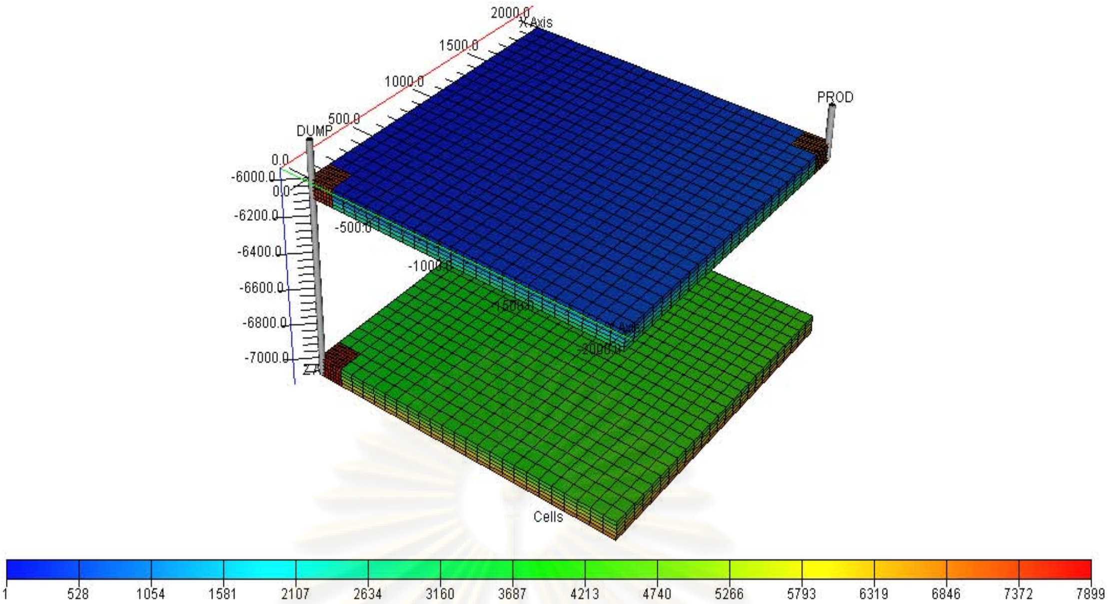

Figure 4.3: 3D view of the reservoir model.

4.2 Fluid Section

The initial fluid conditions such as datum depth, pressure at datum depth, and water-oil contact depth was specified in Equilibration Data Specification (EQUIL) section which was used to generate consistent oil and gas compositions for each cell. The equation of state used in this study is Peng-Robinson. A typical composition of gas-condensate found in the Gulf of Thailand was used for the gas-condensate reservoir model while a binary-component system (C_1/CO_2) was used for the source reservoir model. Four different mixtures (80:20, 60:40, 40:60, and 20:80 %mole of $C_1:CO_2$) were investigated in this study. Table 4.2 illustrates the fluid composition in the gas-condensate reservoir.

Table 4.2: The initial composition of the reservoir fluid

Component	Mole fraction
Carbon dioxide	0.012302
Methane	0.599910
Ethane	0.084326
Propane	0.063988
Isobutane	0.034127
Normal butane	0.038989
Isopentane	0.014286
Normal pentane	0.013988
Hexane	0.072718
Hepthane plus	0.065366

The physical properties of each component and the binary interaction coefficients of this system are shown in Tables 4.3 and 4.4, respectively.

Table 4.3: Physical properties of each component

Component	Boiling points (°R)	Critical pressure (psia)	Critical temp. (°R)	Critical volume (ft³/lb-mole)	Molecular weight	Acentric factor
CO_2	350.46	1071.3	548.46	1.5057	44.01	0.225
C_1	200.88	667.78	343.08	1.5698	16.043	0.013
C_2	332.28	708.34	549.77	2.3707	30.07	0.0986
C_3	415.98	615.76	665.64	3.2037	44.097	0.1524
i-C_4	470.34	529.05	734.58	4.2129	58.123	0.1848
n-C_4	490.86	550.66	765.36	4.0847	58.123	0.201
i-C_5	521.80	491.58	828.72	4.9337	72.15	0.227
n-C_5	556.56	488.79	845.28	4.9817	72.15	0.251
C_6	606.69	436.62	913.50	5.6225	86.177	0.299
C_{7+}	734.08	403.29	1061.3	7.509	115	0.38056

Table 4.4: Binary interaction coefficient between components

	CO_2	C_1	C_2	C_3	i-C_4	n-C_4	i-C_5	n-C_5	C_6	C_{7+}
CO_2	0.000	0.1000	0.100	0.100	0.100	0.100	0.100	0.100	0.1000	0.1000
C_1	0.100	0.0000	0.000	0.000	0.000	0.000	0.000	0.000	0.0279	0.0378
C_2	0.100	0.0000	0.000	0.000	0.000	0.000	0.000	0.000	0.0100	0.0100
C_3	0.100	0.0000	0.000	0.000	0.000	0.000	0.000	0.000	0.0100	0.0100
i-C_4	0.100	0.0000	0.000	0.000	0.000	0.000	0.000	0.000	0.0000	0.0000
n-C_4	0.100	0.0000	0.000	0.000	0.000	0.000	0.000	0.000	0.0000	0.0000
i-C_5	0.100	0.0000	0.000	0.000	0.000	0.000	0.000	0.000	0.0000	0.0000
n-C_5	0.100	0.0000	0.000	0.000	0.000	0.000	0.000	0.000	0.0000	0.0000
C_6	0.100	0.0279	0.010	0.010	0.000	0.000	0.000	0.000	0.0000	0.0000
C_{7+}	0.100	0.0378	0.010	0.010	0.000	0.000	0.000	0.000	0.0000	0.0000

In this study, the reservoir temperature was assumed to be constant at 293 ^{o}F and the initial reservoir pressure of gas-condensate reservoir was 3,000 psi. With this reservoir pressure, reservoir temperature and fluid composition, the phase behavior of gas-condensate reservoir and binary C_1:CO_2 system is displayed in Figure 4.4 and 4.5, respectively.

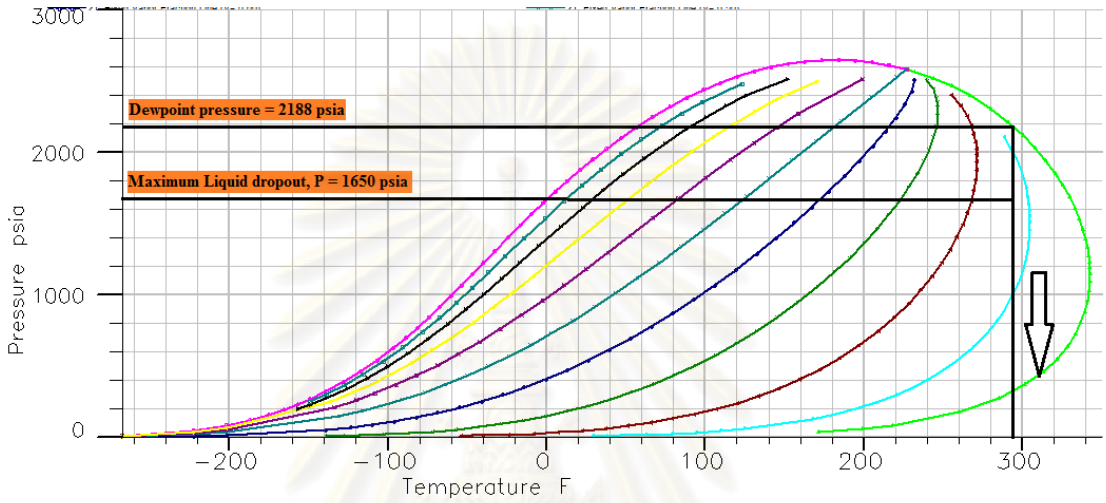

Figure 4.4: Phase behavior of the gas-condensate reservoir fluid system.

This phase behavior was calculated by PVTi program in ECLIPSE simulator. The dew point pressure is 2,188 psi and the maximum liquid dropout of 12% occurs when the reservoir pressure drops to 1,650 psi.

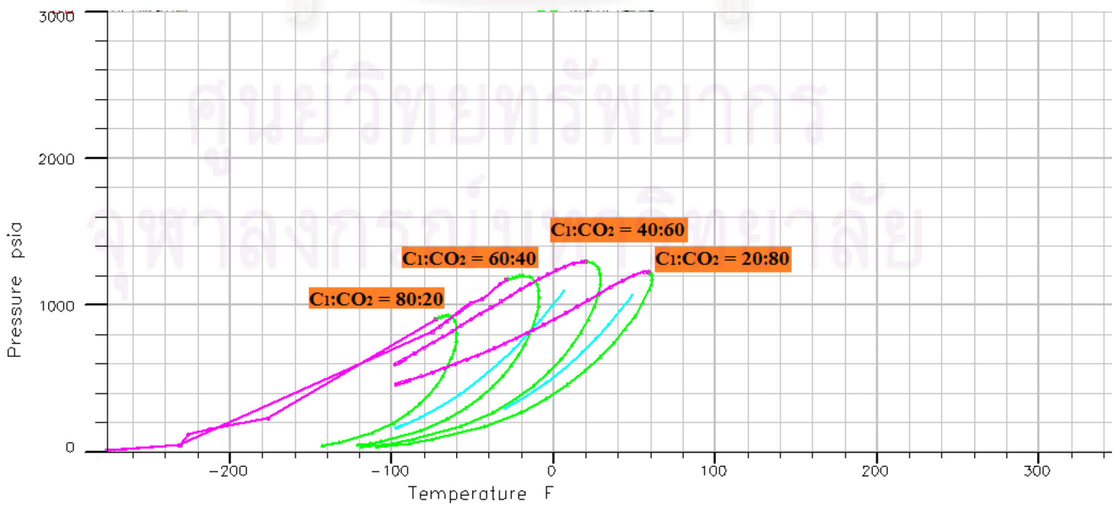

Figure 4.5: Phase envelope of binary C_1:CO_2 system.

In order to have a better understanding of the effect of CO_2 concentration on behavior of reservoir fluid, phase envelopes of reservoir fluid mixed with different concentrations of CO_2 as shown in Table 4.5 are constructed and shown in Figure 4.6. The diagram illustrates that CO_2 lowers the dewpoint pressure and cricondentherm of the mixture. This means the mixture is more likely to be single-phase gas when a large amount of CO_2 is injected.

Table 4.5: Prediction of fluid composition when gas condensate mixes with different %moles of C_1 and CO_2

Component	Mole Fraction				
	z_i	z_i+20%CO_2	z_i+40%CO_2	z_i+60%CO_2	z_i+80%CO_2
CO_2	0.012302	0.199000	0.394740	0.580	0.790
C_1	0.599910	0.681590	0.508620	0.350	0.174
C_2	0.084326	0.024876	0.015259	0.013	0.007
C_3	0.063988	0.019900	0.015259	0.013	0.007
IC_4	0.034127	0.009950	0.010172	0.005	0.003
NC_4	0.038989	0.009950	0.010172	0.005	0.003
IC_5	0.014286	0.004975	0.008138	0.004	0.001
NC_5	0.013988	0.004975	0.007121	0.004	0.001
C_6	0.072718	0.024876	0.015259	0.013	0.007
C_{7+}	0.065366	0.019900	0.015259	0.013	0.007

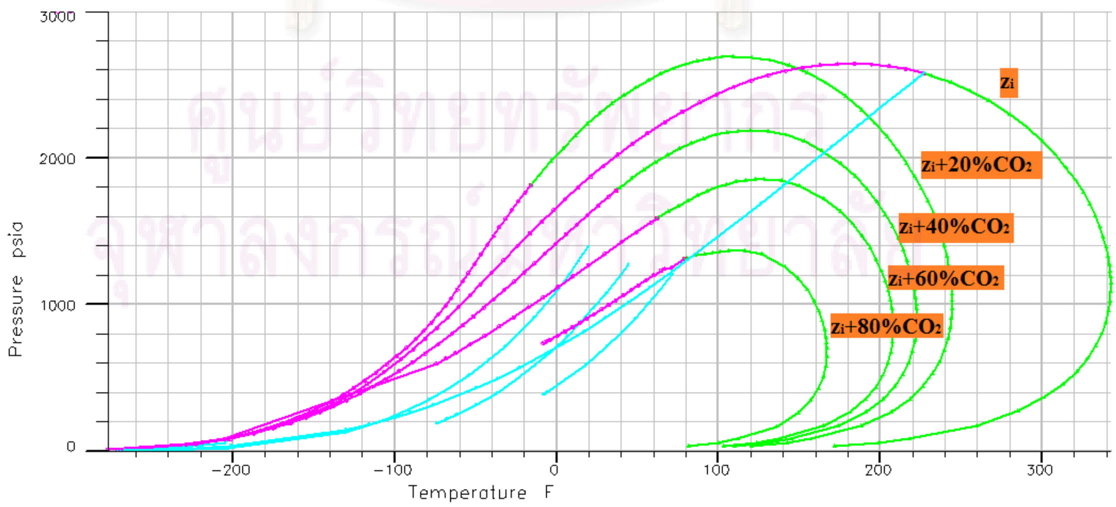

Figure 4.6: Phase behavior of reservoir fluid mixed with different concentrations of CO_2.

4.3 SCAL (Special Core Analysis) Section

Two tables of relative permeabilities (k_r) and capillary pressures (p_c) as functions of saturation in ECLIPSE allow us to enter gas/oil relative permeabilities and gas/water relative permeabilities into the software as depicted in Tables 4.6 and 4.7, respectively. These functions are shown in Figures 4.7 and 4.8.

k_{rg} is relative permeability to gas
k_{ro} is relative permeability to oil
k_{rw} is relative permeability to water
S_w is saturation of water
S_g is saturation of gas
p_c is capillary pressure

Table 4.6: Gas and oil relative permeabilities

S_g	k_{rg}	k_{ro}
0	0	0.897
0.03515	7.63E-05	0.705923
0.0703	0.00061	0.544104
0.10545	0.002059	0.409125
0.1406	0.00488	0.298553
0.17575	0.009531	0.209941
0.2109	0.01647	0.140865
0.24605	0.026154	0.0889
0.2812	0.03904	0.051603
0.31635	0.055586	0.026534
0.3515	0.07625	0.011275
0.38665	0.101489	0.003398
0.4218	0.13176	0.000433
0.45695	0.167521	0
0.4921	0.20923	0
0.52725	0.257344	0
0.5624	0.31232	0
0.59755	0.374616	0
0.6327	0.44469	0
0.66785	0.522999	0
0.703	0.61	0

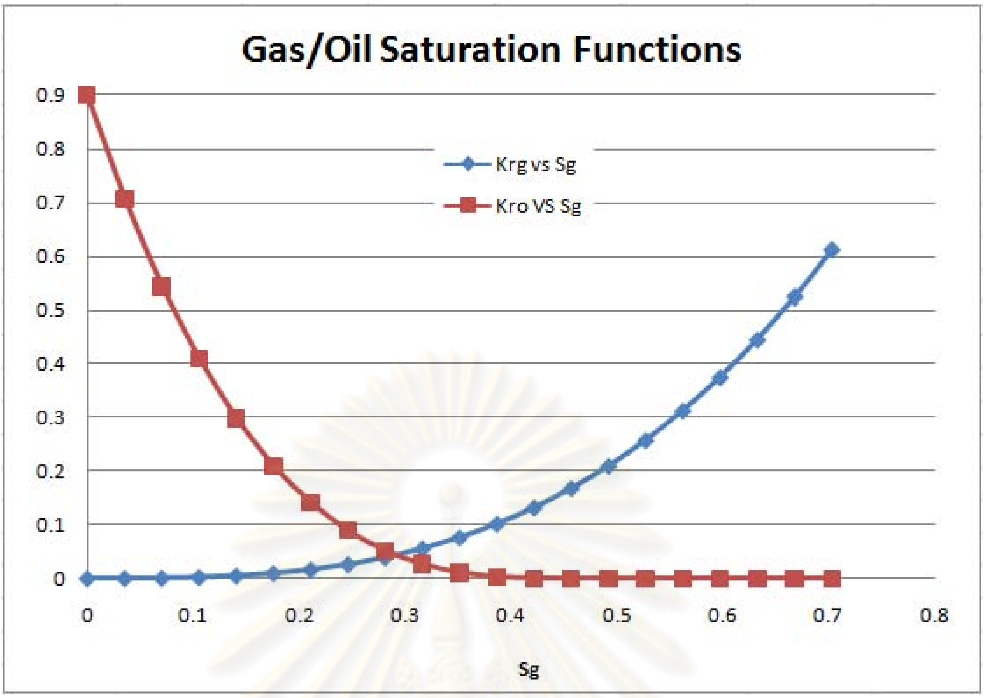

Figure 4.7: Gas and oil relative permeabilities.

Table 4.7: Oil and water relative permeabilities

S_w	k_{rw}	k_{ro}
0.297	0	0.897
0.319026	1.76E-05	0.769065
0.341051	0.000141	0.653913
0.363077	0.000476	0.55087
0.385102	0.001128	0.459264
0.407128	0.002203	0.378422
0.429154	0.003807	0.307671
0.451179	0.006045	0.246339
0.473205	0.009024	0.193752
0.49523	0.012849	0.149238
0.517256	0.017625	0.112125
0.539282	0.023459	0.081739
0.561307	0.030456	0.057408
0.583333	0.038722	0.038459
0.605358	0.048363	0.024219
0.627384	0.059484	0.014016
0.649410	0.072192	0.007176
0.671435	0.086592	0.003027
0.693461	0.102789	0.000897
0.715486	0.12089	0.000112
0.737512	0.141	0
1	1	0

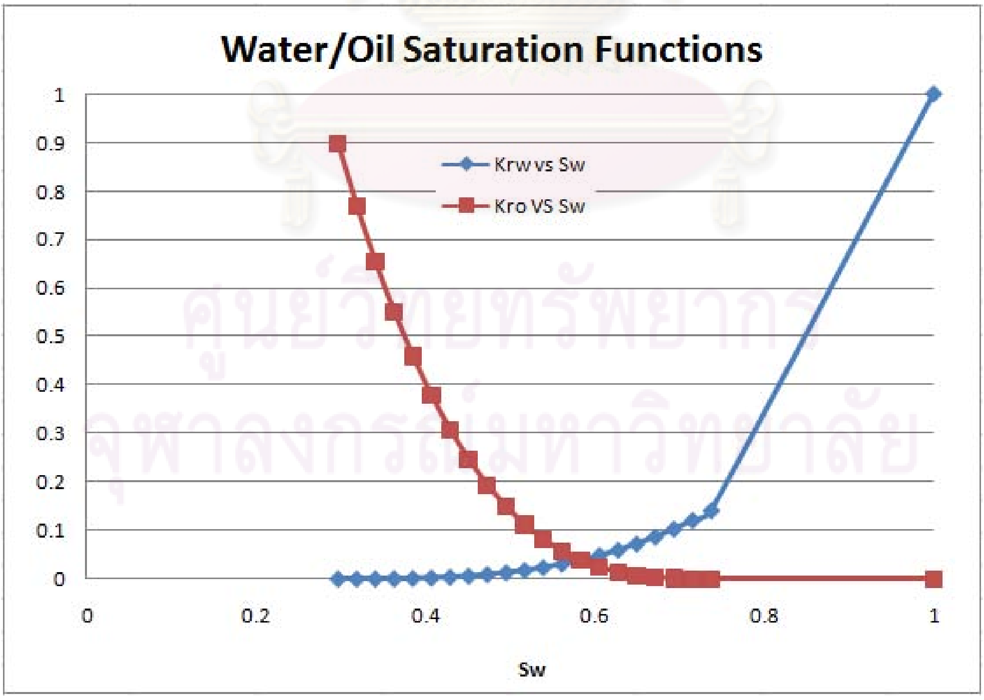

Figure 4.8: Oil and water relative permeabilities.

4.4 Wellbore Section

The production and source wells in this study have the same tubing outside diameter of 3-1/2 inches with an inside diameter of 2.992 inches. The perforation interval is from the top to the bottom of the reservoir. The schematic of wellbore configuration of production well and source well are shown in Figures 4.9 and 4.10, respectively.

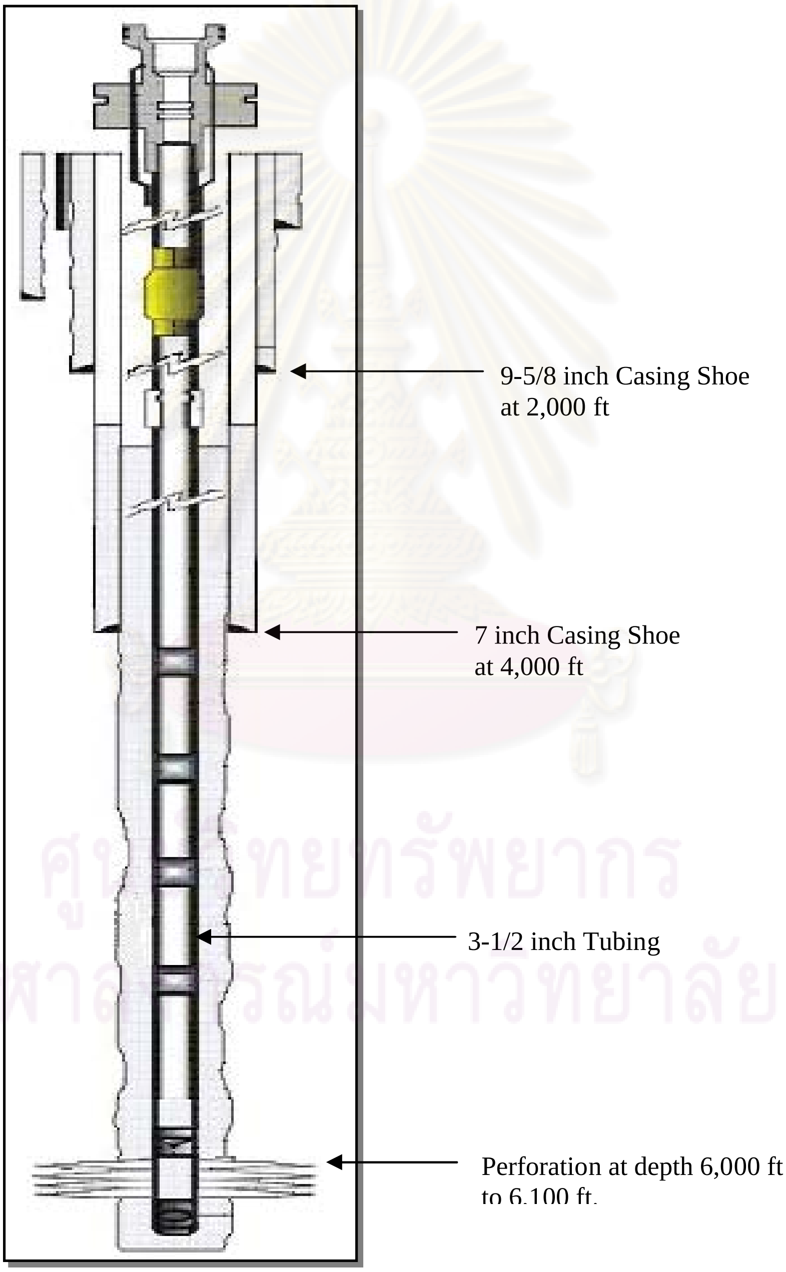

Figure 4.9: Casing and tubing flow model for the production well.

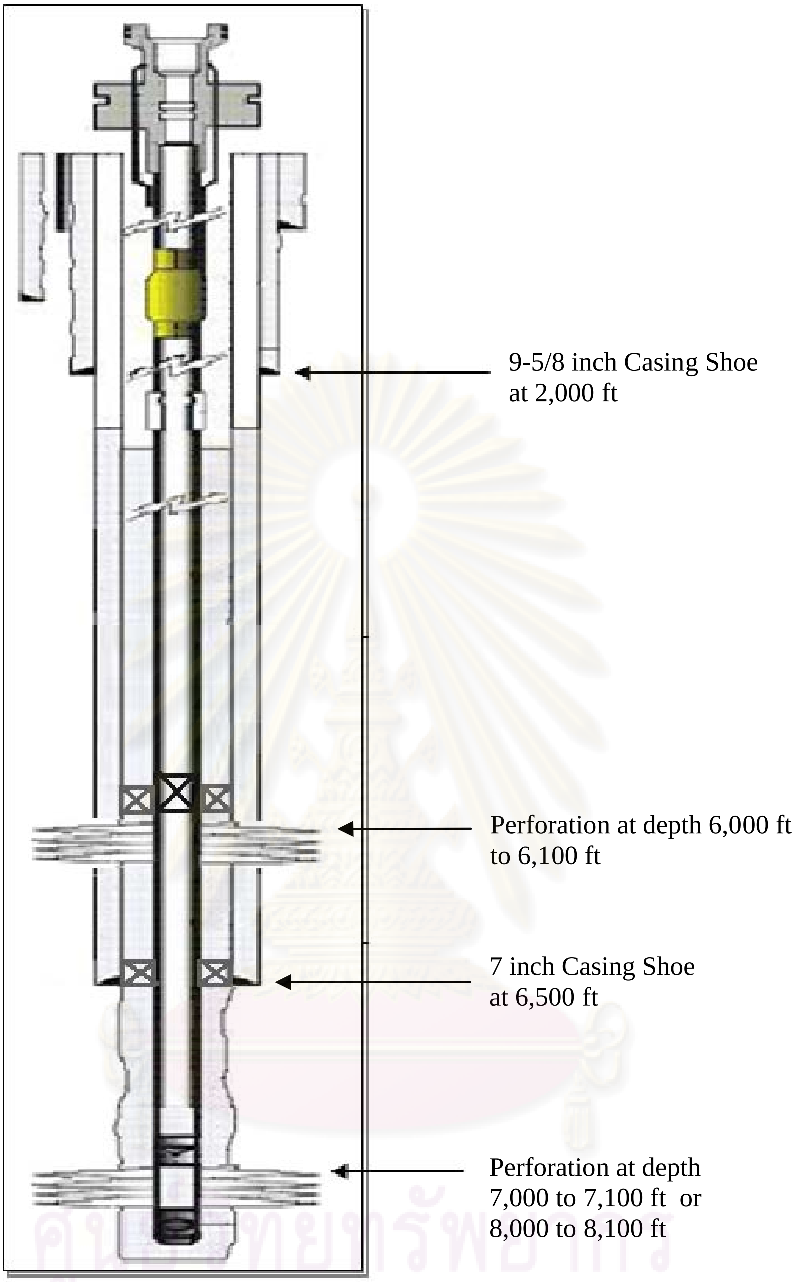

Figure 4.10: Casing and tubing flow model for the source well.

4.4.1 Vertical Flow Performance

In this study, multiple sets of vertical flow performance(VFP) curves were generated by production and system performance analysis software (PROSPER) for the variety of composition in the source to traget reservoirs. Each set of VFP curves is for specific CO_2 concentration and depth difference between source and target reservoirs. The chosen vertical flow correlation is Fancher Brown. The bottomhole flowing pressure is calculated based on the tubing head pressure, gas rate, and gas oil ratio of the producing well and source well for their respective section. The details of vertical flow performance curves used in this study are shown in Appendix B.

CHAPTER V

SIMULATION RESULTS AND DISCUSSIONS

This chapter starts by introducing the production of gas-condensate reservoir with natural depletion. After that, gas dump flood was implemented for pressure maintenance and revaporization to prevent condensate dropout in the reservoir. After introduction of gas dump flood, simulation runs under different scenarios were performed by considering three main variables affecting condensate recovery. The results are discussed in terms of condensate recovery and the effect of each variable. We also analyze and discuss the results of gas dump flood compared with conventional CO_2 injection.

A target tubing head pressure of 500 psia with vertical flow performance VFP NO.1 (see Appendix B) was used for the production well. This limit is a common tubing head pressure used in Gulf of Thailand when a booster compressor is not installed. For the source well, an appropriate vertical flow performance (see Appendix B) according to the percent mole in each composition of source reservoir and difference in depth between source and target reservoirs was used. In gas dump flood process, there is no limitation on cross flow from the source to target reservoirs. The fluid is allowed to flow naturally from the source to target reservoirs. The abandonment rates were defined by assuming a typical daily operating cost at minimum gas rate of 100 MSCF/D and minimum oil production rate of 10 STB/D.

5.1 Production with Natural Depletion

The objective of this scenario is to investigate the problem of condensate build up in gas-condensate reservoir when normal depletion leaves valuable condensate fluids in a reservoir and condensate blockage can cause a loss of well productivity.

The production well is placed at coordinate (8, 8) in LGR grid representing the producer (located at coordinate (25, 25) in the global grid) as shown in Figure 5.1. This location of production well is similar to gas dump flood case which is discussed in section 5.2 in order to compare their performance. The maximum gas production rate which is set at 10,000 MSCF/D is used as the control variable. The gas production rate is kept constant as long as the reservoir pressure can sustain such rate with a tubing head pressure limit of 500 psia and vertical flow performance VFP NO.1 (see Appendix B).

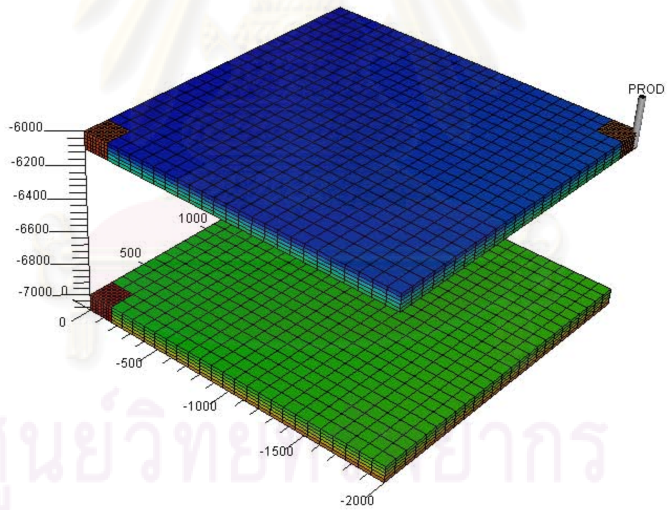

Figure 5.1: Location of production well in 3D reservoir model.

Gas production rate and condensate production rate from the simulation is shown in Figures 5.2 and 5.3, respectively. At early times, gas and condensate production rates are constant while the bottomhole pressure declines (see Figure 5.4). After the bottomhole pressure drops below the dewpoint pressure of 2,188 psi, the condensate production rate declines and liquid starts to condense in the pore space as shown in Figure 5.5

Figure 5.5 illustrates the detail of condensate build-up around the wellbore. The condensate saturation around the wellbore increases as the pressure becomes lower. At early times of condensate accumulation, condensate cannot flow in the reservoir. This condensate accumulation around the wellbore are called condensate blockage which causes the problem of gas flow performance. When the condensate saturation reaches 0.297, condensate starts to flow. The condensate saturation in Figures 5.5 and 5.6 decreases at late time period because condensate revaporizes as the pressure drops to low values. Figure 5.7 is used to explain in details that when the pressure drops with constant reservoir temperature (293 ˚F), liquid is transformed to vapor. Since there is now a higher amount of gas in the reservoir and gas is less viscous than condensate, a higher volume of gas flows out of the reservoir, contributing to higher flow rates of gas and condensate (since revaporized gas will condense into condensate again at standard conditions). Finally, simulation run stops because the gas or condensate production rate reaches abandonment rates.

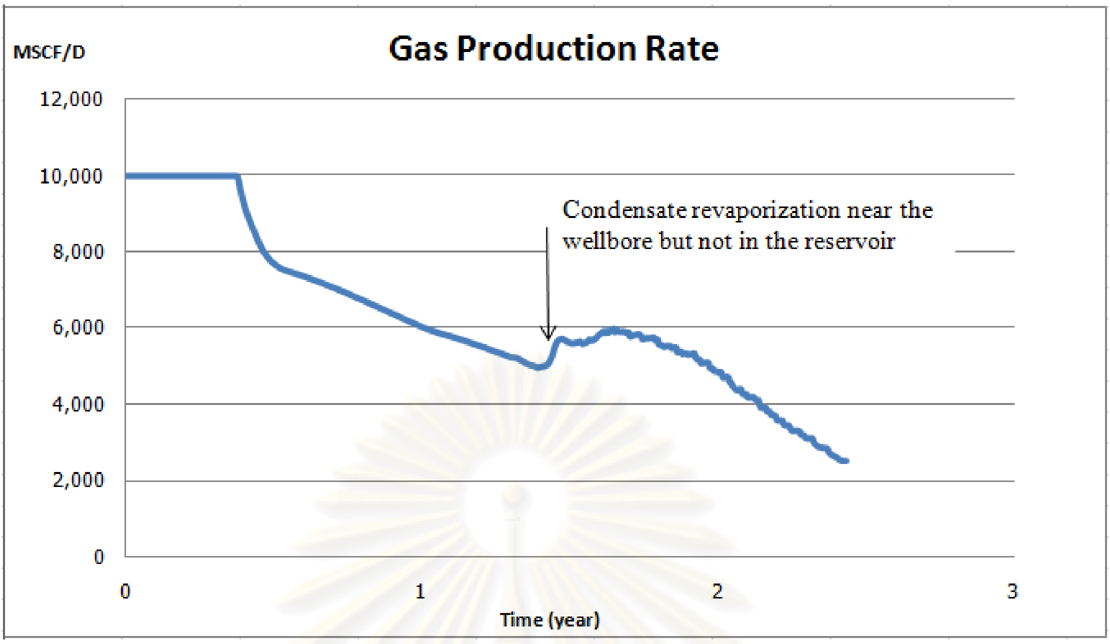

Figure 5.2: Gas production rate for natural depletion.

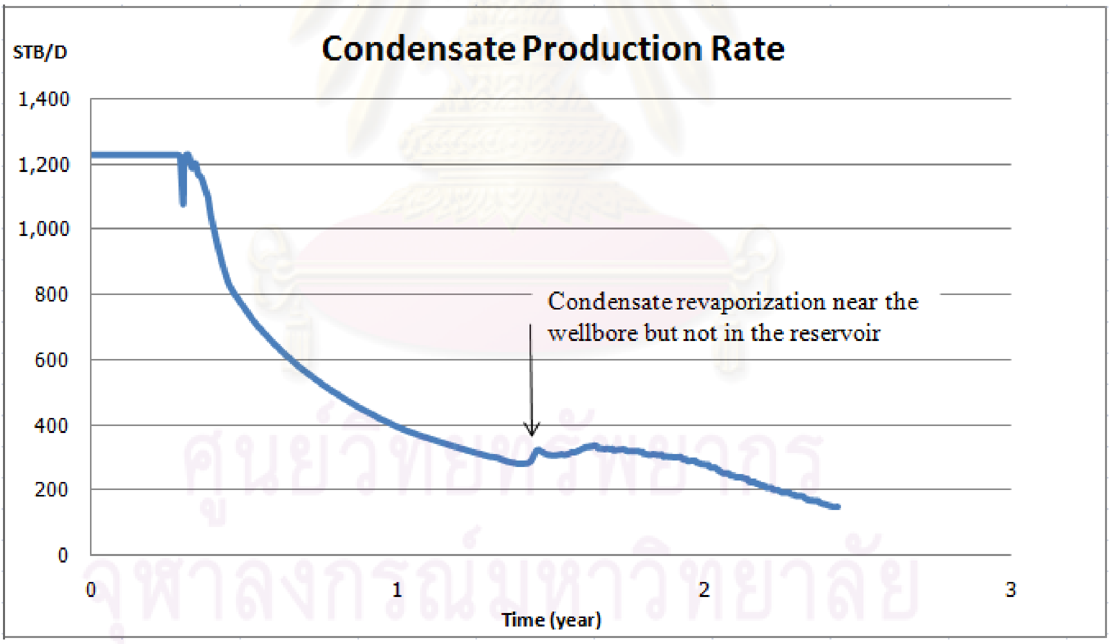

Figure 5.3: Condensate production rate for natural depletion.

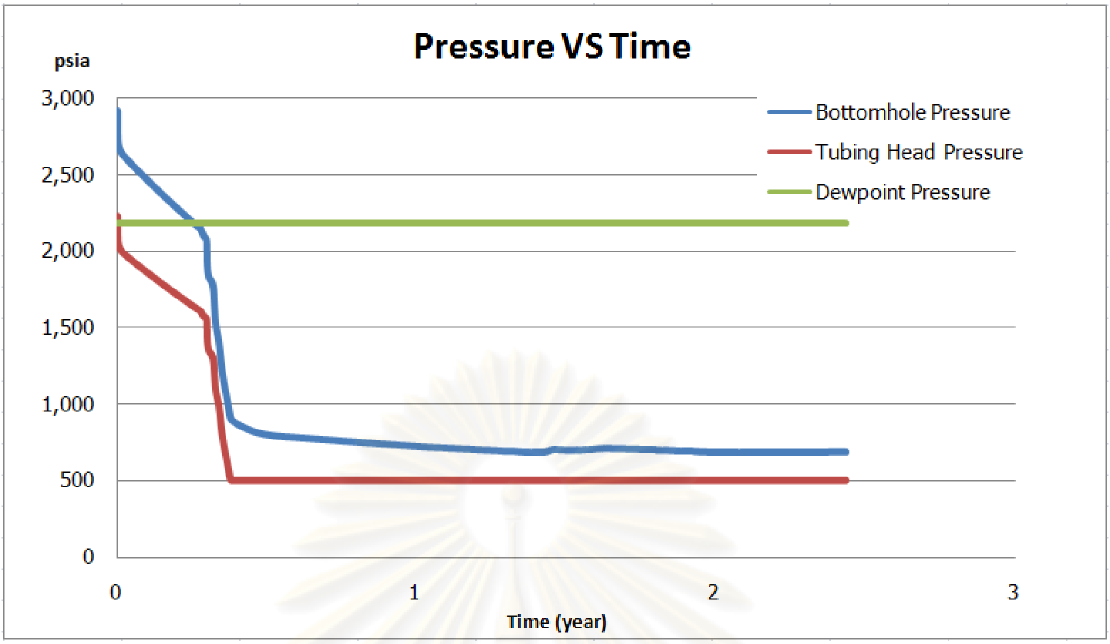

Figure 5.4: Tubing head pressure and bottomhole pressure for producing with natural depletion.

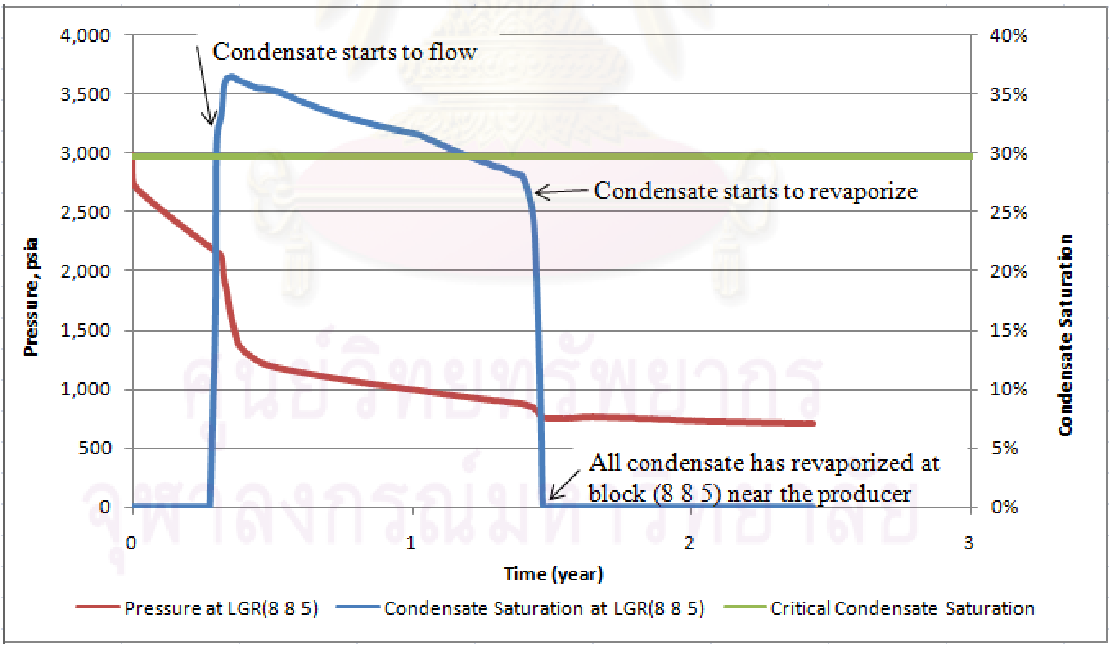

Figure 5.5: Block pressure and condensate saturation at grid (8, 8, 5) in LGR grid representing the producer for natural depletion.

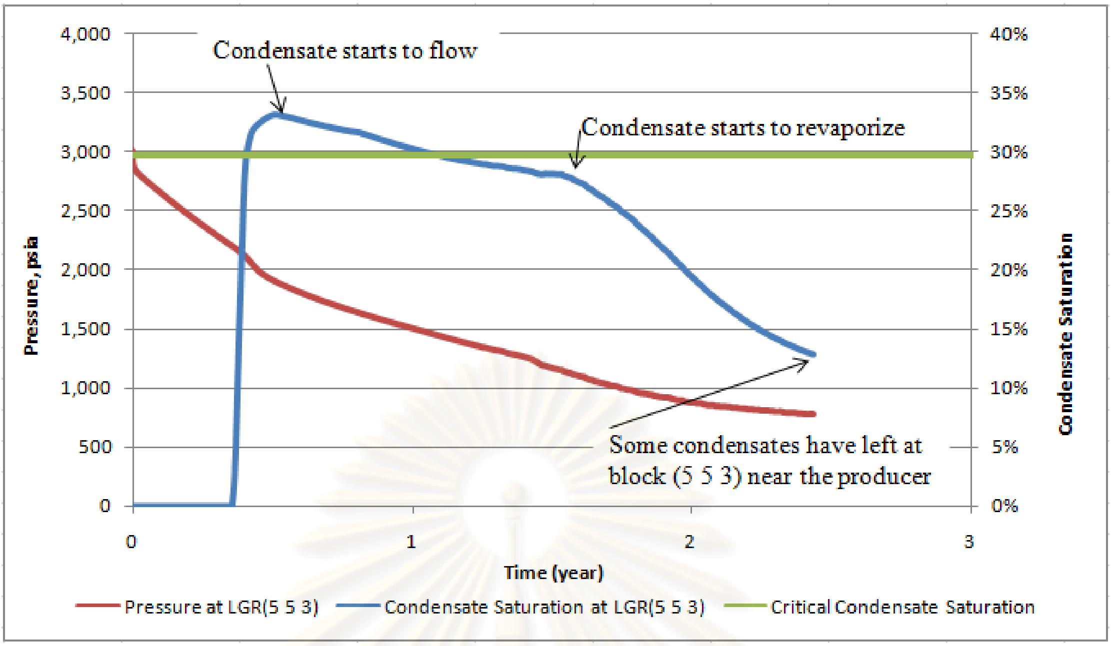

Figure 5.6: Block pressure and condensate saturation at grid (5, 5, 3) in LGR grid representing the producer for natural depletion.

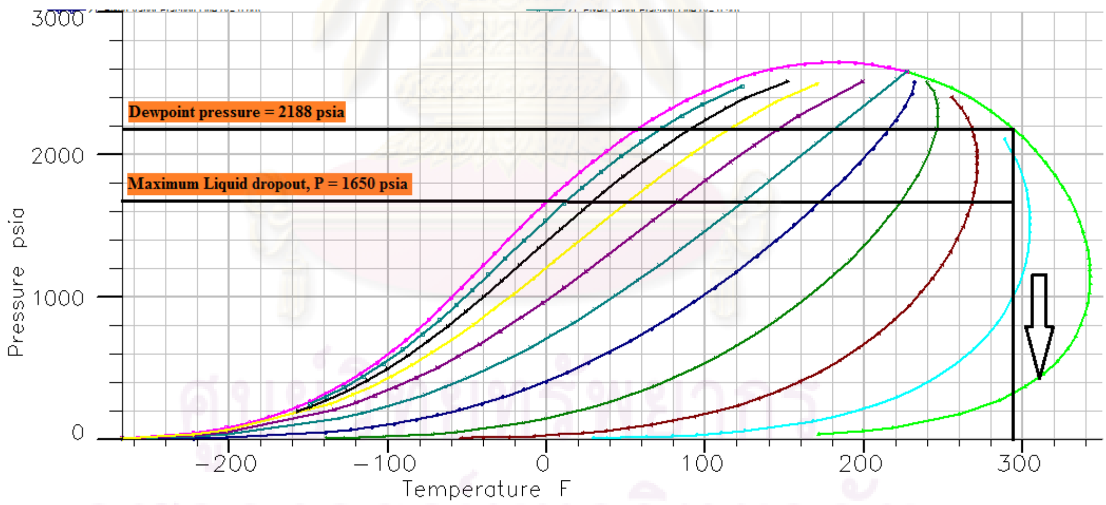

Figure 5.7: Phase behavior of the gas-condensate reservoir fluid system.

Figure 5.8a shows the condensate saturation at the beginning of natural depletion case. The dark blue color represents zero condensate saturation. Then, liquid dropout occurs around the wellbore after the bottomhole pressure reaches the dewpoint pressure as shown in Figure 5.8b. In Figure 5.8c, the liquid dropout propagates further, covering the entrie reservoir. Note that the liquid dropout around the wellbore is mobile at this point since its saturation is higher than the critical condensate saturation. After that, the condensate saturation in the reservoir decreases because the liquid dropout starts to revaporize.

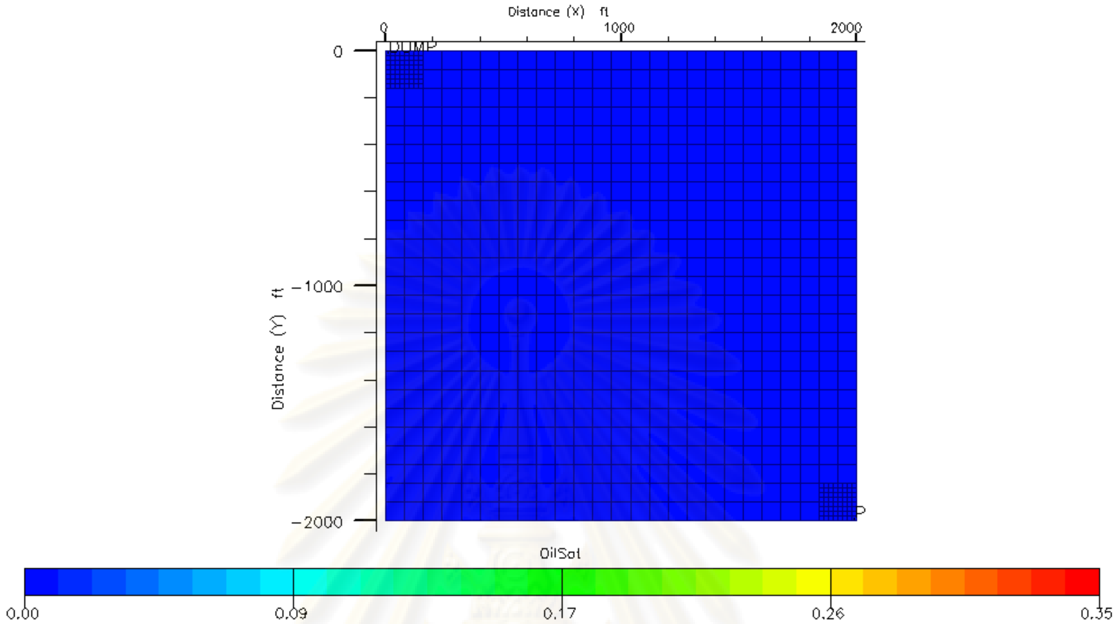

(a) Original saturation.

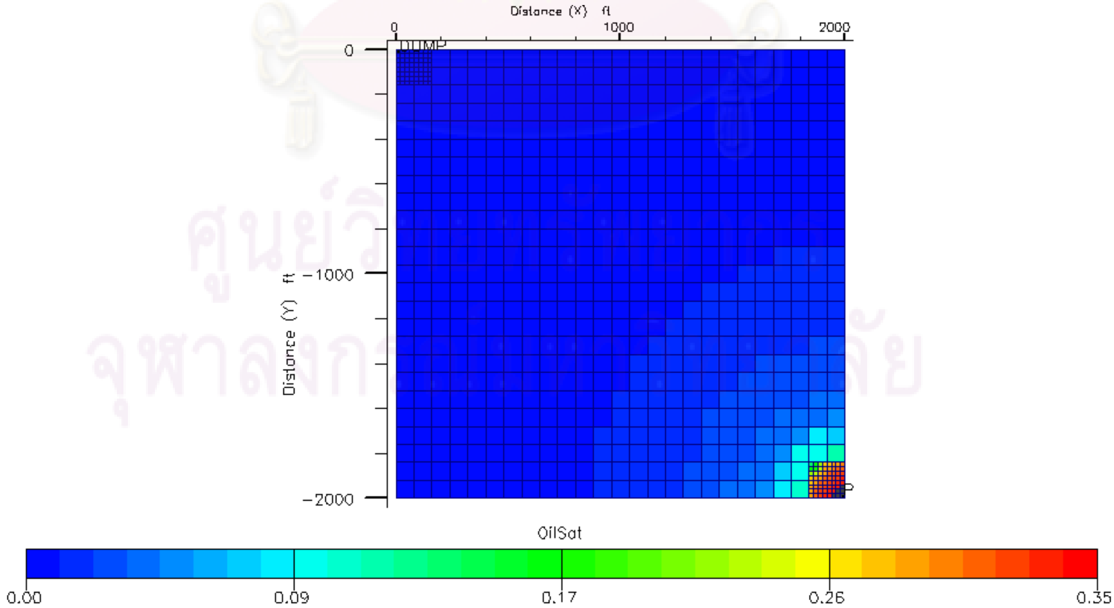

(b) Liquid starts to drop out around the wellbore.

Figure 5.8: Condensate saturation when producing with natural depletion.

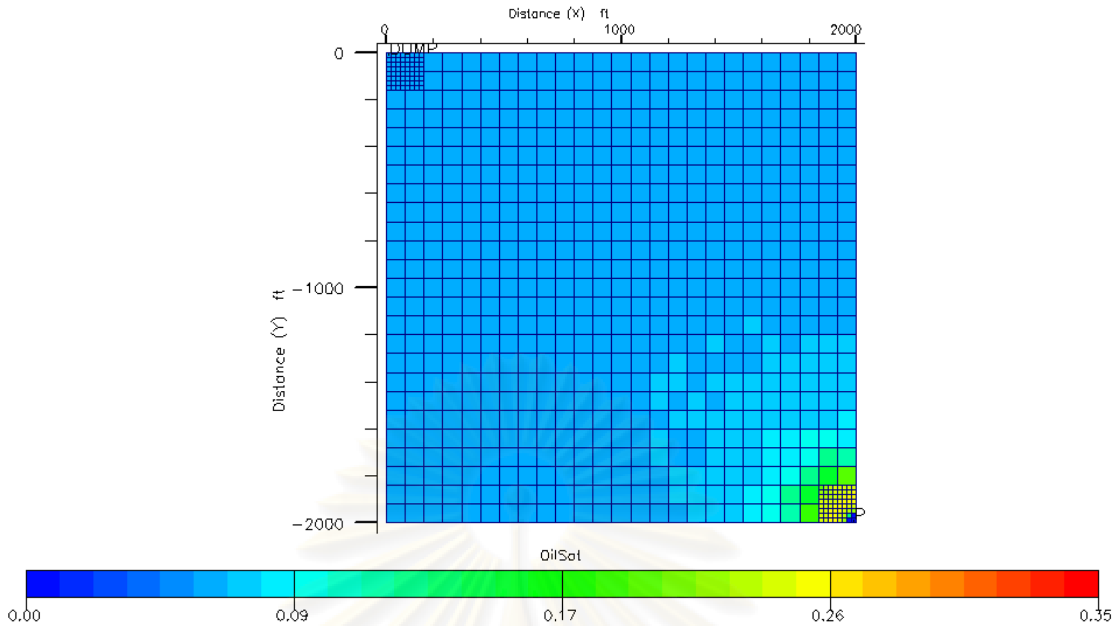

(c) Liquid dropout occurs in the entire of the reservoir.

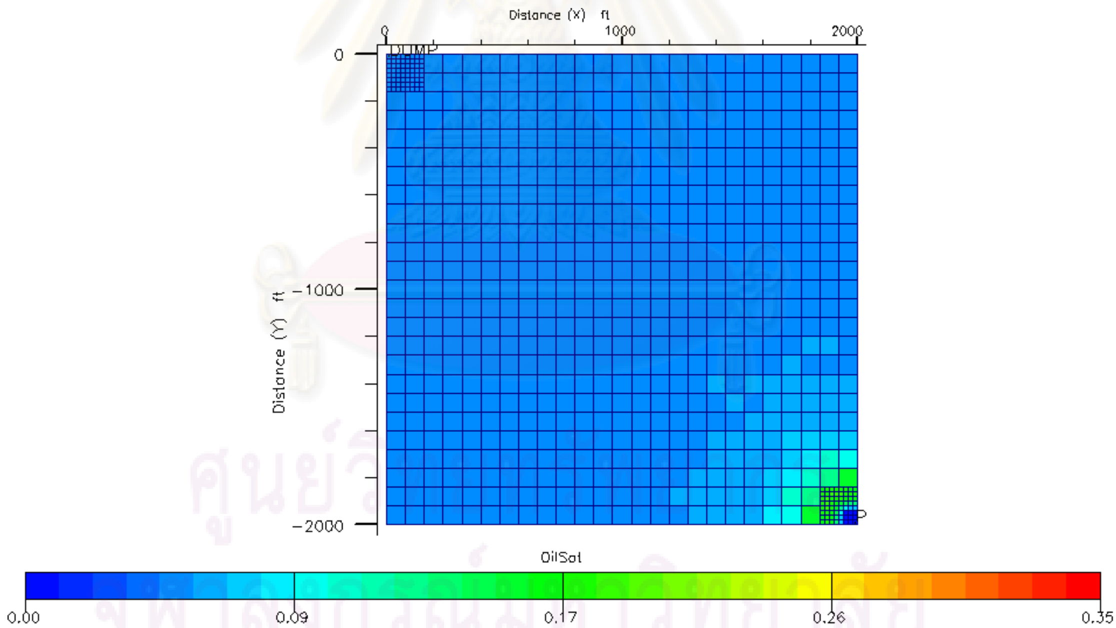

(d) End of the production.

Figure 5.8: Condensate saturation when producing with natural depletion (continued).

In this scenario, we can see that production with natural depletion does not effectively recover condensate and gas from the reservoir. At early time, the bottomhole pressure declines very quickly until it reaches the BHP limit calculated by vertical flow performance. Then, gas production rate declines until it reaches the abandonment rates. As a result, only 47% of condensate and 71% of hydrocarbon gas can be recovered.

5.2 Gas Dump Flood Mechanism

In the Gulf of Thailand, many gas fields are multi-stacked reservoirs. Some of these reservoirs have high CO_2 content. In many cases, it is not economical to produce gas from these reservoirs. One way to make use of this high-pressure gas is to perform internal dump flood in which high CO_2 gas is flowed from the source reservoir to the target gas-condensate reservoir to increase the pressure of the target reservoir as well as to reduce the dewpoint of the reservoir fluid. The main purpose is to increase condensate recovery by preventing condensate dropout in the target reservoir.

The objective of this section is to investigate the performance of gas dump flood process. In this case, gas dump flood is started when the pressure of the target reservoir is equal to the dewpoint pressure of 2,188 psia. The source reservoir containing 40% mole of C_1 and 60% of CO_2 is located 2,000 ft below the target reservoir. The production well is placed at coordinate (8, 8) in LGR grid representing the producer (located at coordinate (25, 25) in the global grid), and the source well is placed at coordinate (1, 1) in LGR grid representing the connection between source and target reservoirs (located at coordinate (1, 1) in the global grid) in order to simulate a quarter five-spot pattern. The gas from the source reservoir is allowed to flow to the target reservoir naturally without any control. The simulation stops if the gas or condensate production rate from the production well drops below the abandonment rates.

Figures 5.9 and 5.10 show gas production rate and condensate production rate with and without gas dump flood, respectively. For production without the gas dump flood, we get short plateau followed by decline for gas and condensate production. For gas dump flood, initially, the same kind of plateau and decline in gas and condensate production rate is seen. After we start the gas dump flood when the reservoir pressure is equal to the dewpoint pressure, the gas and condensate production rates increase as a result of pressure maintenance as indicated by circle 1 in Figures 5.9 and 5.10. The gas rate is increased to the maximum rate of 10,000 Mscf/d and maintained constant for almost a year. For condensate rate, it initially increases to a value higher than the original condensate plateau rate because of revaporization of condensate dropout around the wellbore. After that, it stabilizes at the plateau rate for a while. Then both gas and condensate decline again. In green circle number 2, sufficient amount of flooding gas has reached the production well, making the dewpoint pressure of the new mixture lower than the bottomhole pressure. The phase diagram of the mixture is illustrated in Figure 5.11. The diagram illustrates that CO_2 lowers the dewpoint pressure and cricondentherm of the mixture. This means the mixture is more likely to be single-phase gas when a flooding gas mixes with the target reservoir fluid. Then, the resistance to flow is reduced due to the reduction of condensate blockage. This results in increase in gas and condensate production rate.

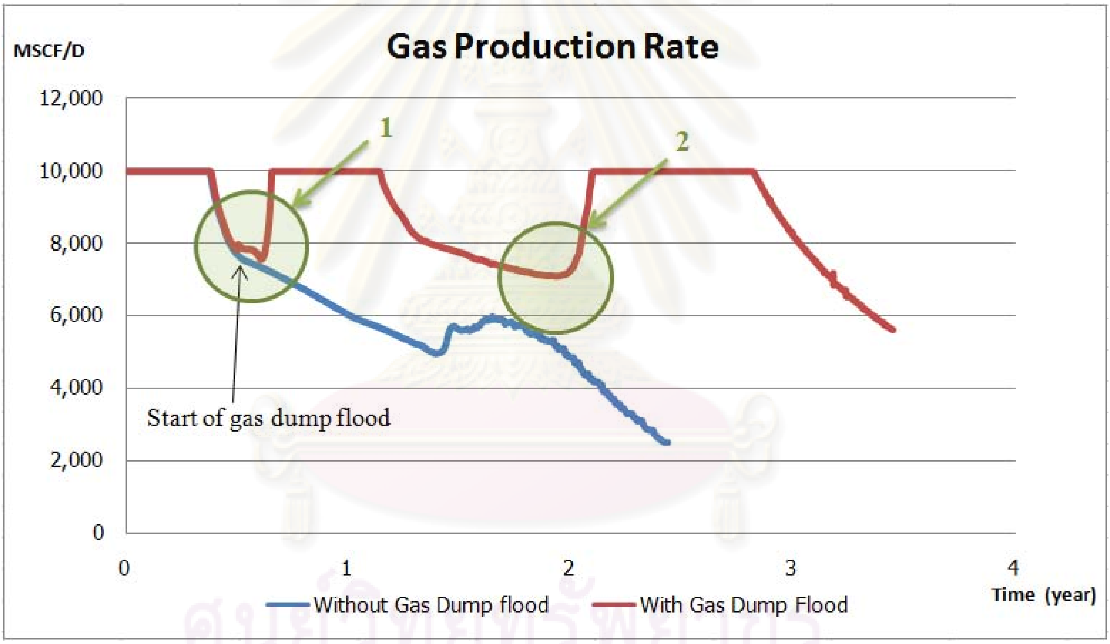

Figure 5.9: Gas production profile for production with and without gas dump flood.

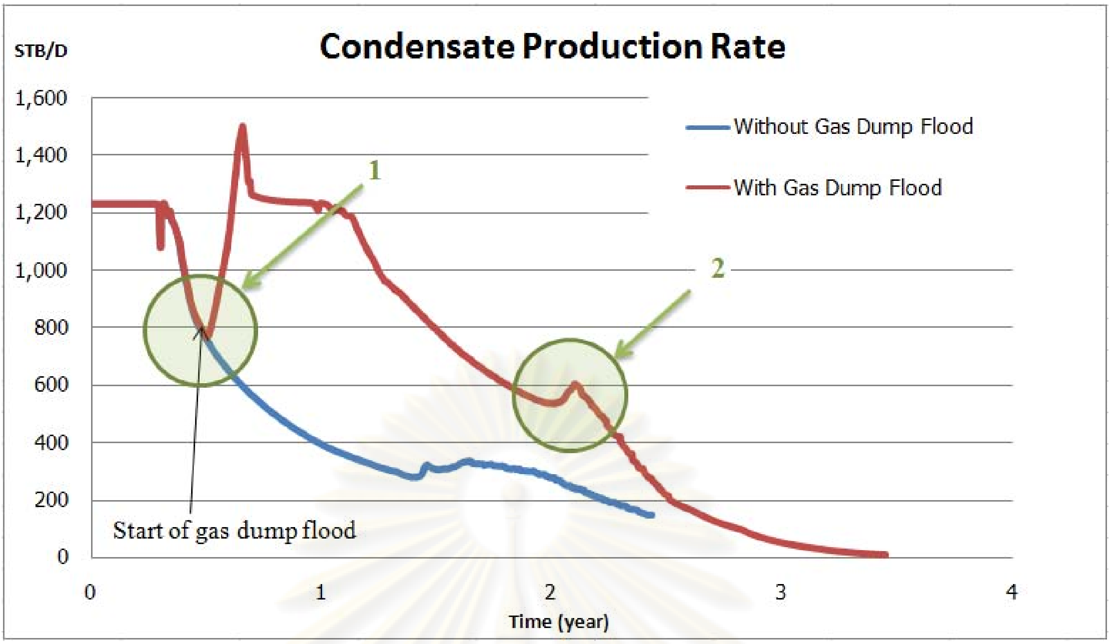

Figure 5.10: Condensate production profile for production with and without gas dump flood.

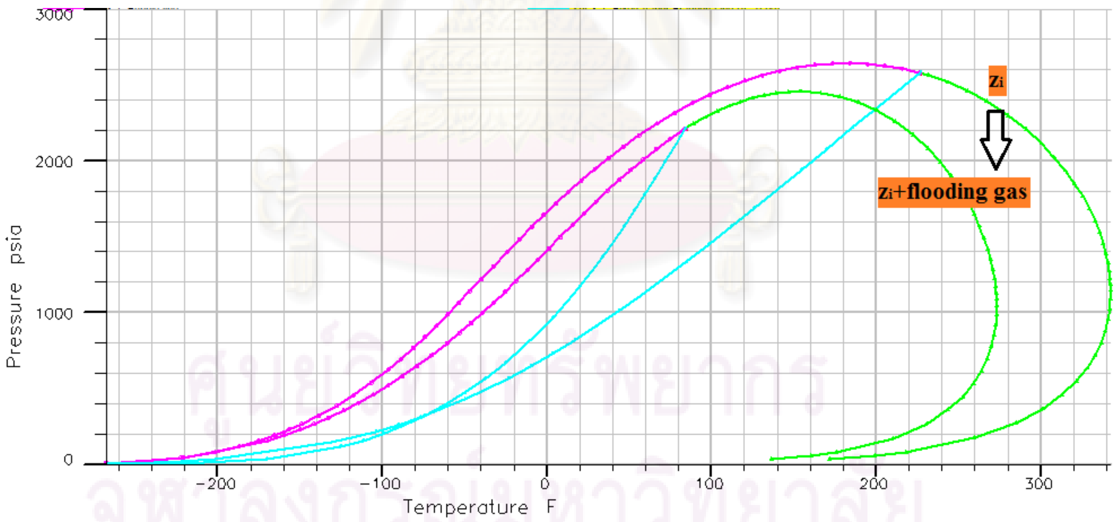

Figure 5.11: Changing phase behavior of the gas-condensate reservoir fluid mixed with flooding gas.

Figure 5.12 depicts the cross flow profile from the source reservoir to the target reservoir. At the initial period of gas dump flood, the highest cross flow rate occurs because of large pressure difference between the source and the target reservoirs. Then, the rate declines rapidly to a more stable rate because of pressure equilibrium between the two reservoirs. The cross flow rate increases again when the flooding gas starts to break through the producing well.

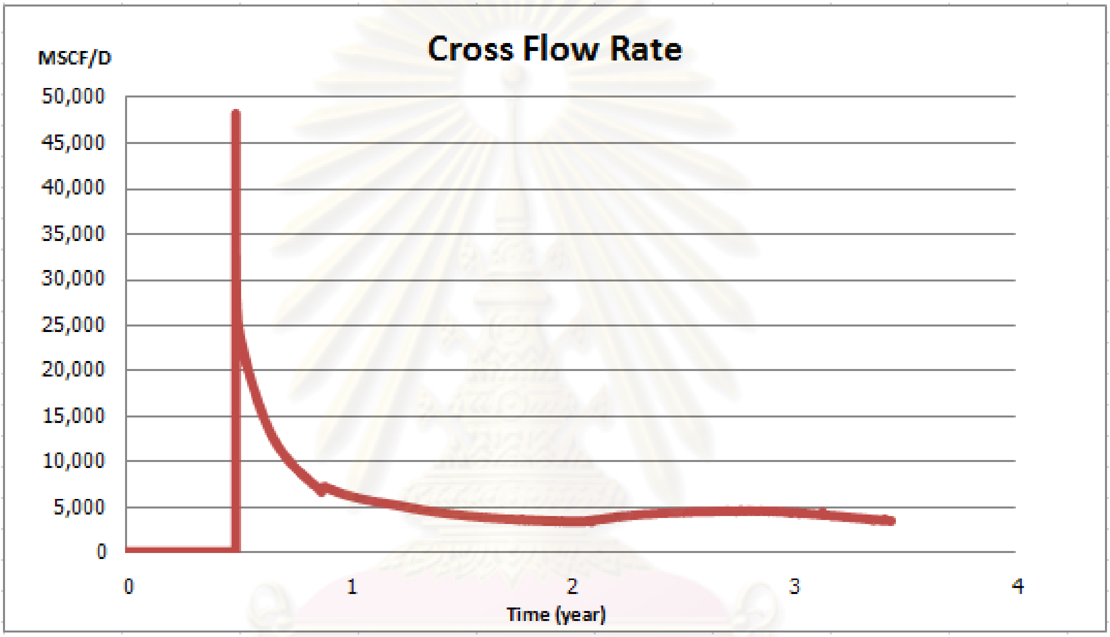

Figure 5.12: Cross flow rate of gas dump flood process.

Figure 5.13 shows CO_2 concentration profile at the production well. At late times, flooding gas containing high CO_2 concentration reduces the dewpoint pressure of the fluid in the target reservoir. Consequently, revaporization of condensate dropout around wellbore occurs.

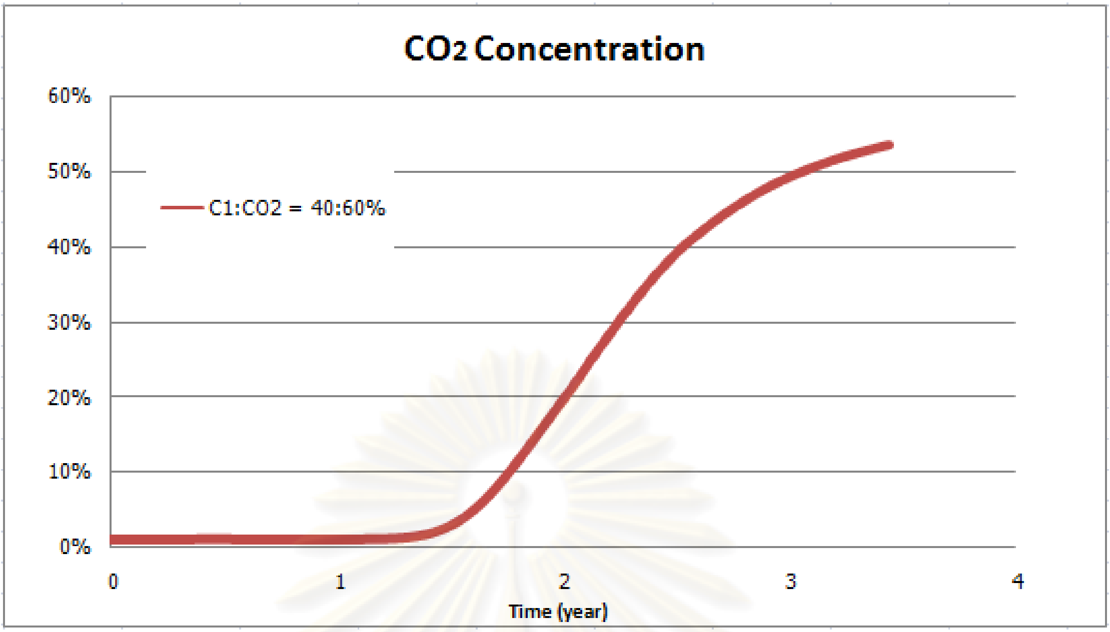

Figure 5.13: CO_2 concentration at producing well of gas dump flood process.

Figure 5.14 illustrates the condensate saturation versus time for gas production with and without gas dump flood. When performing gas dump flood, condensate saturation around the wellbore reduces because the flooding gas supports the bottomhole pressure of the producer in the target reservoir as shown in Figure 5.15, causing condensate to revaporize. However, the condensate saturation late rises up again because the flooding gas cannot maintain the pressure of the target reservoir.

Due to the fact that pressure nears the production well has a lower value than the pressure away from the production well as depicted in Figure 5.16, the condensate saturation nears the production well (LGR 8 8 5 is located closer the producer than LGR 5 5 3) tends to have higher value as shown in Figure 5.17. However, after we start gas dump flood, the block pressure shown in Figure 5.16 is not increased immediately because of delay in pressure support from the source well to production well.

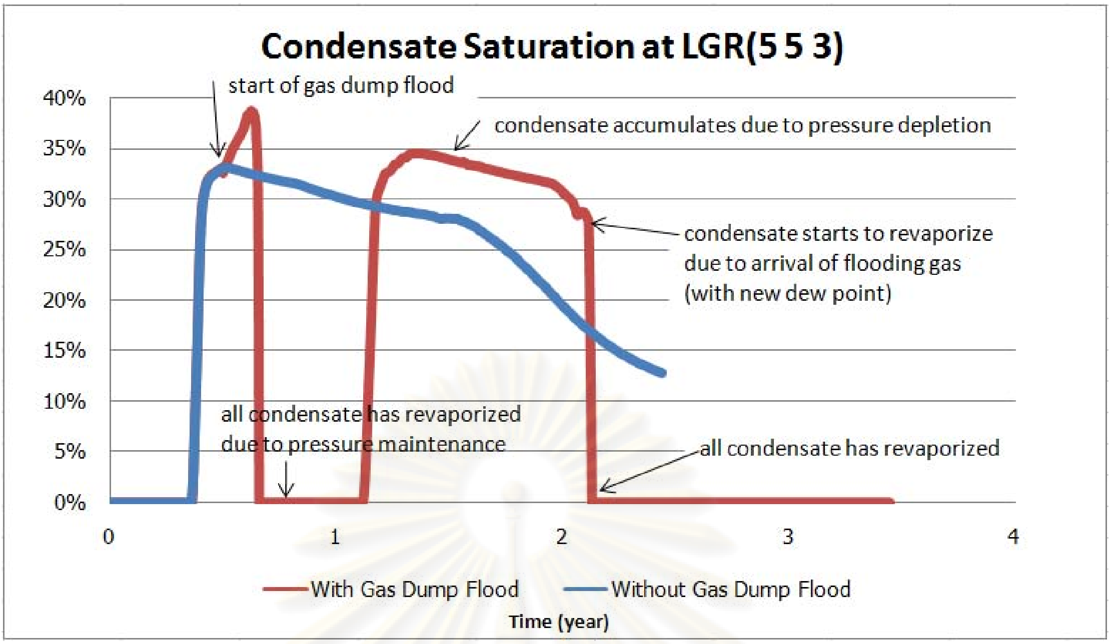

Figure 5.14: Condensate saturation at LGR (5 5 3) of producing well with and without gas dump flood.

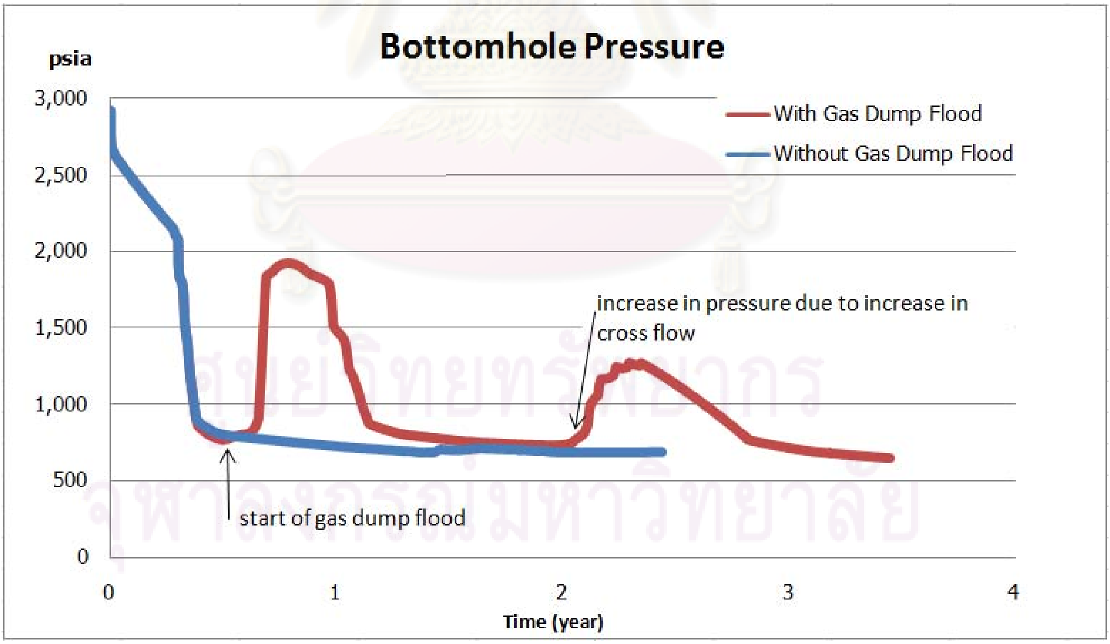

Figure 5.15: Bottomhole pressure of producing well with and without gas dump flood.

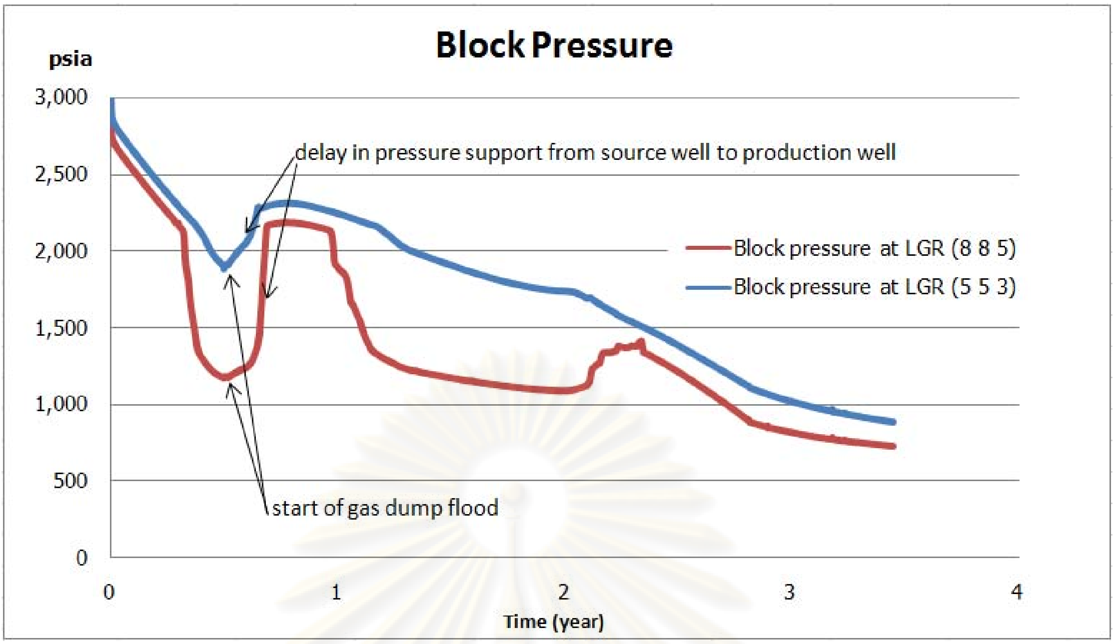

Figure 5.16: Block pressure at LGR (5 5 3) and (8 8 5).

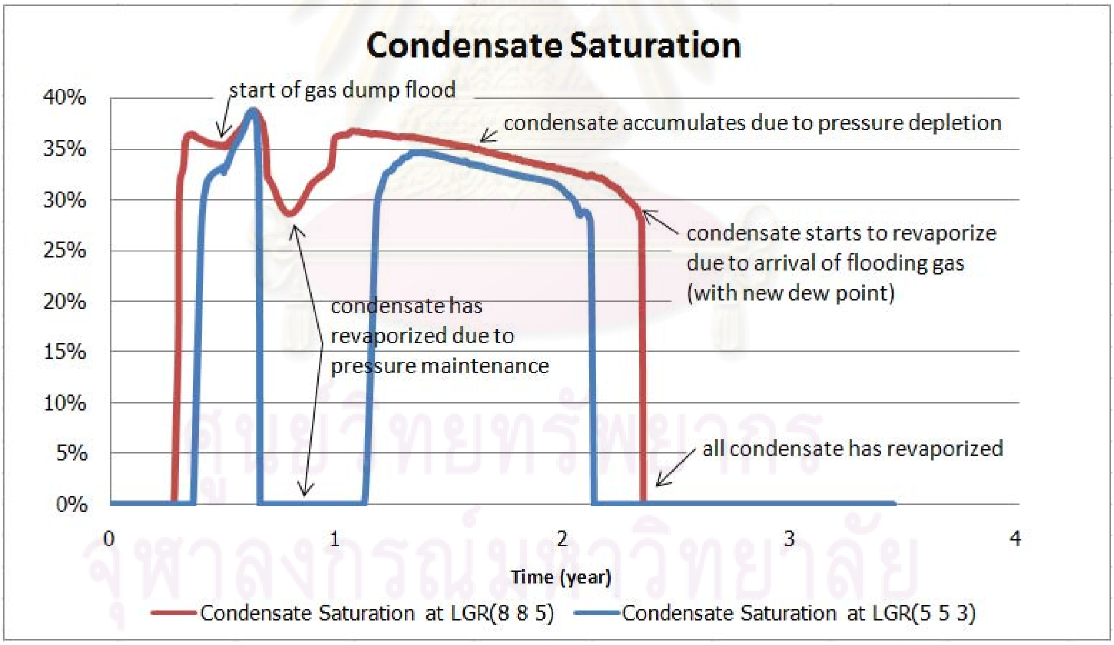

Figure 5.17: Condensate saturation at LGR (5 5 3) and (8 8 5).

When producing with gas dump flood, the reservoir pressure can be maintained to prevent liquid from dropping out. In addition, flooding gas can reduce the dewpoint of the reservoir fluid. Figure 5.18a shows condensate saturation in the grid blocks at the beginning of the gas dump flood. Initially, there is no liquid in each grid block. In Figure 5.18b, the liquid dropout occurs around the wellbore as the pressure in the grid blocks around the wellbore drops below the dewpoint pressure. During revaporization from gas dump flood, flooding gas starts to invade into the grid blocks and revaporizes condensate as shown in Figure 5.18c. We can see that the condensate saturation in the grid blocks closer to the producer is around 0.35, and the condensate saturation in the grid blocks closer to the injector is around zero. After continuous flooding, all liquid around the wellbore is revaporrized and condensate saturation in most grid blocks reduce to zero as shown in Figure 5.18d.

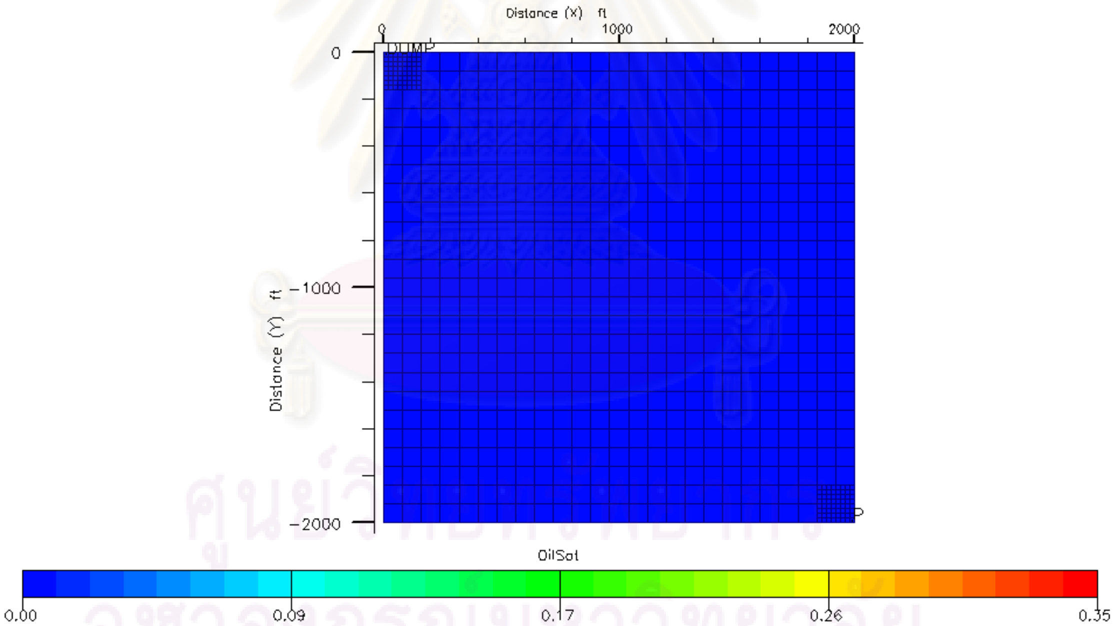

(a) Original saturation.

Figure 5.18: Condensate saturation when producing with gas dump flood.

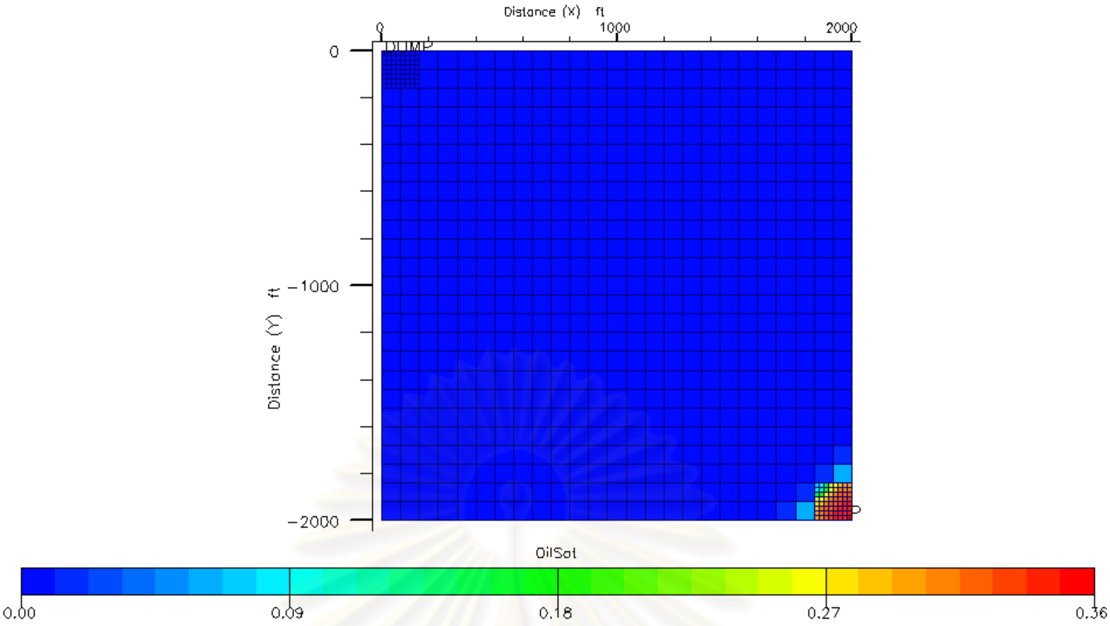

(b) Liquid starts to drop out around the wellbore.

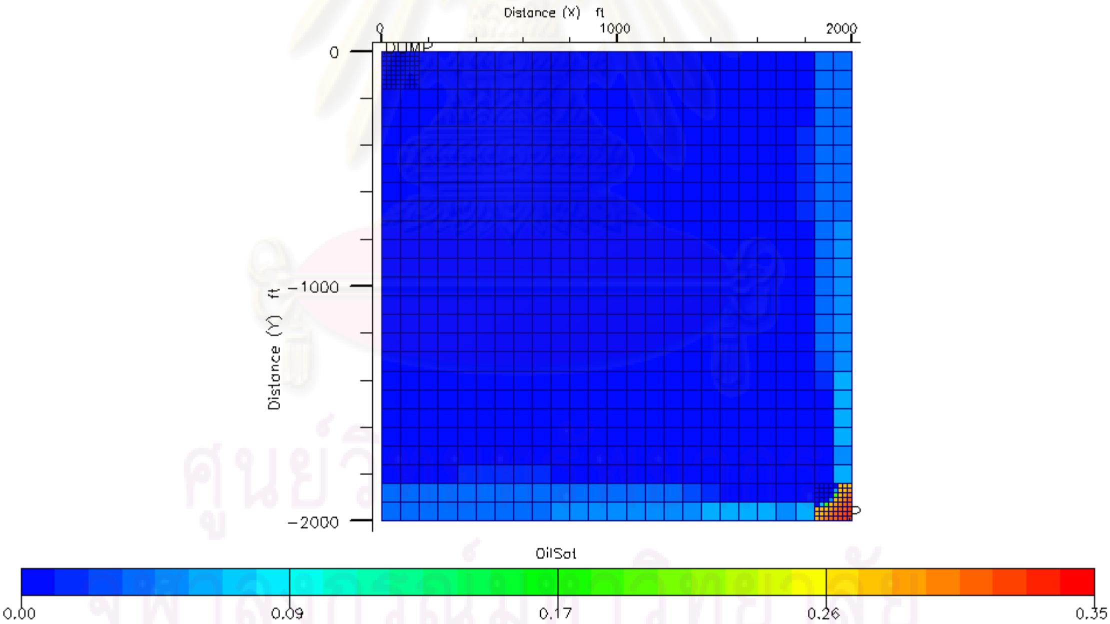

(c) Flooding gas starts to revaporize liquid dropout around the wellbore.

Figure 5.18: Condensate saturation when producing with gas dump (continued).

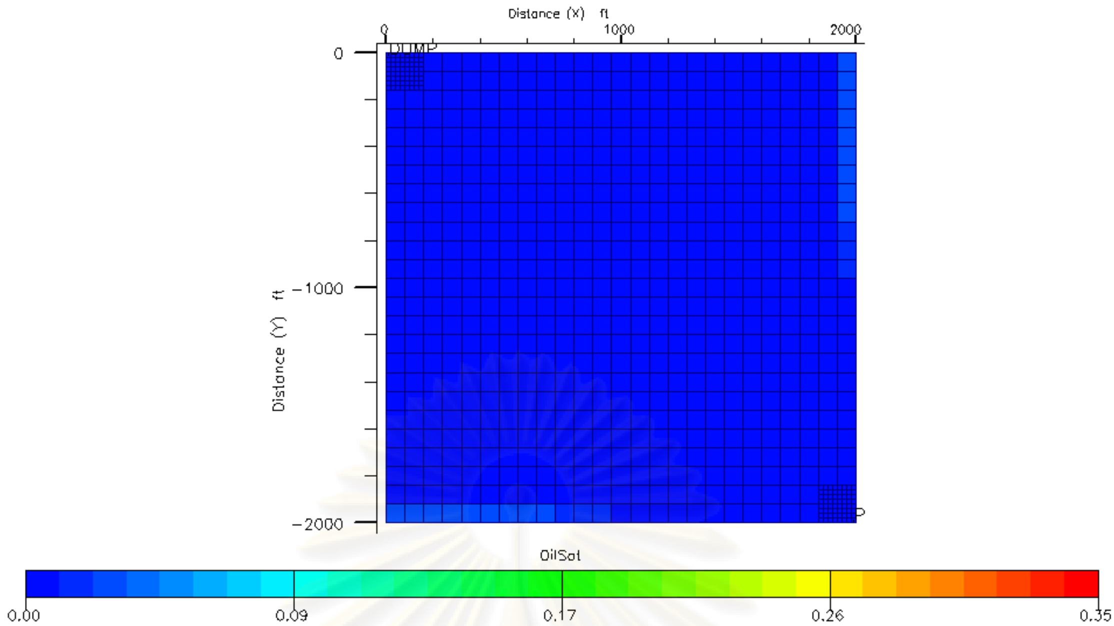

(d) End of the production.

Figure 5.18: Condensate saturation when producing with gas dump (continued).

In this scenario, the production with gas dump flood can effectively recover condensate and gas from the reservoir. The condensate dropout around the wellbore causing condensate blockage problem is reduced and prevented by mean of pressure support and reduction of dewpoint pressure of the fluid in the target reservoir.

5.3 Effect of Starting Time of Gas Dump Flood

The objective of this section is to find the optimal time to start gas dump flood. The gas-condensate reservoir is produced together with gas dump flood, started at different times. In this study, we use the following starting times for gas dump flood:

- At the beginning
- When the reservoir pressure is 300 psi higher than the dewpoint pressure
- When the reservoir pressure is equal to the dewpoint pressure (2,188 psi)
- When the reservoir pressure is 1,000 psi lower than the dewpoint pressure

For all cases, the source reservoir containing 40% mole of C_1 and 60% of CO_2 is located at 1,000 ft below the target reservoir. The condensate and gas production rates, condensate saturation, total condensate and gas productions and production life are discussed.

As shown in Figure 5.19, the gas production rate in natural depletion case declines when the bottomhole pressure reaches the limit calculated from vertical flow performance. In all cases of gas dump flood, the gas production rate increases as a result of pressure maintenance. However, if gas dump flood is started when the reservoir pressure is 1,000 psi lower than the dewpoint pressure, the gas production rate cannot rebound to the maximum rate because the pressure from the source reservoir is not high enough to bring back the gas production of the target reservoir which already has low pressure.

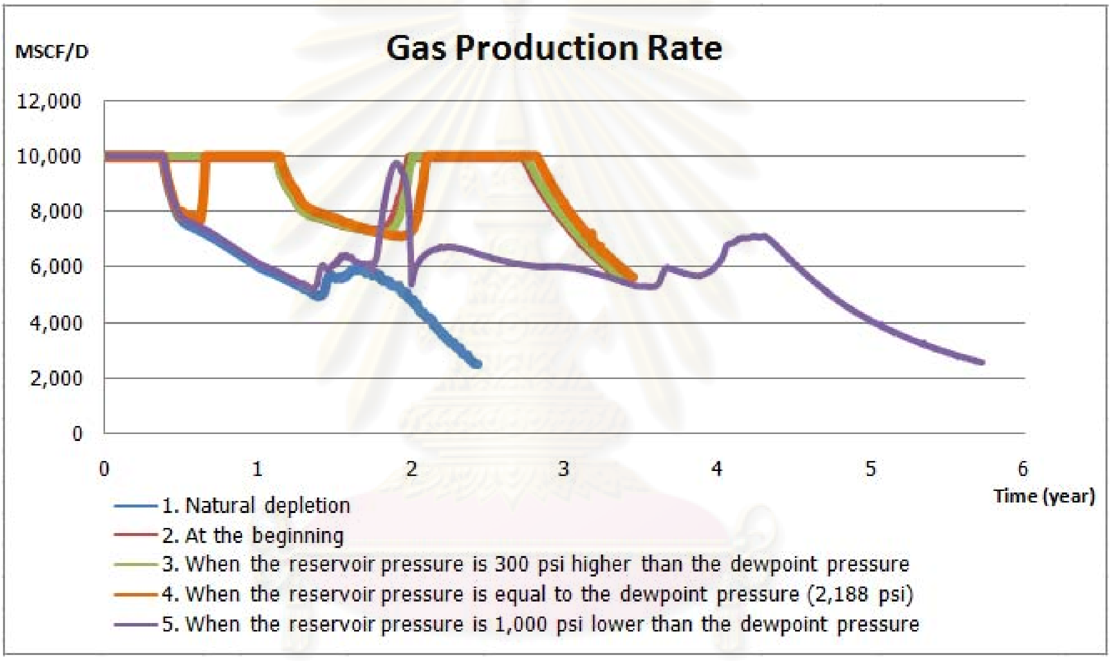

Figure 5.19: Gas production rate for different starting times of gas dump flood.

Figure 5.20 illustrates condensate production rate for different starting times of gas dump flood. In natural depletion case, we get only a short plateau period as discussed in Section 5.1. In all cases of gas dump flood, condensate production rate increases promptly when gas dump flood is started. Nevertheless, since flooding gas break the production well, the condensate production rate slightly increases because around the producing well area there exist only a small amount of condensate dropout. Consequently, after breakthrough, this small amount of condensate dropout revaporizes.

If gas dump flood is started when the reservoir pressure is 1,000 psi lower than the dewpoint pressure, the reservoir already contains a lot of condensate dropout prior to gas dump flood. After gas dump flood is started, condensate production rate increases slightly because pressure support from the source reservoir cannot sustain high level of production rate.

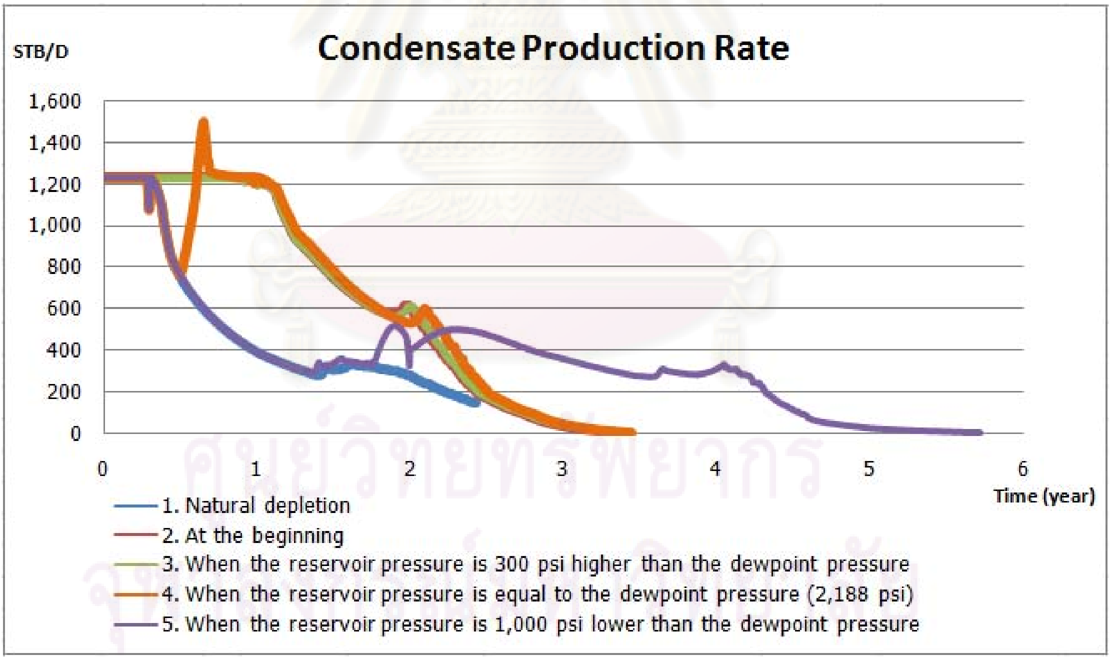

Figure 5.20: Condensate production rate for different starting times of gas dump flood.

As mentioned earlier, the main objective of gas dump flood is to maintain the reservoir pressure above the dewpoint pressure in order to prevent condensate dropout but different starting times of gas dump flood obtain different condensate saturation profiles during the production life as shown in Figure 5.21. If gas dump flood is delayed, the heavy component or condensate existing around the production well cannot flow and blocks the flow of fluid to the production well for a longer period, resulting in a decrease in total condensate production.

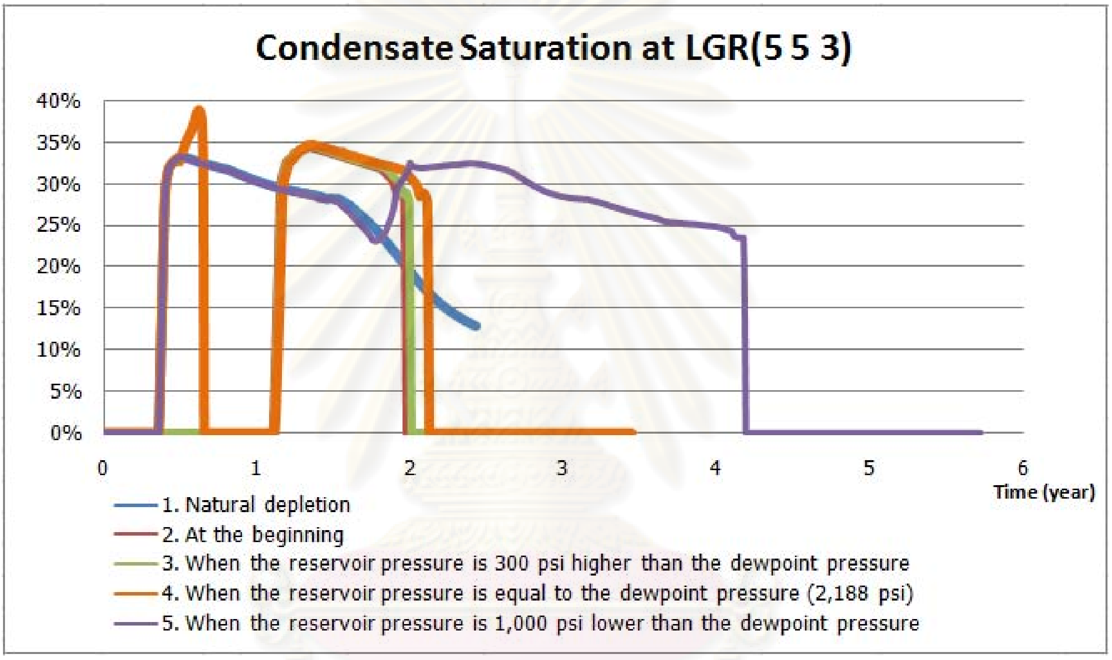

Figure 5.21: Condensate saturation at local grid (5, 5, 3) for different starting times of gas dump flood.

Table 5.1 shows the cumulative hydrocarbon gas production for gas dump flood being started at different times. There is a large increase in gas recovery when producing gas-condensate reservoir with gas dump flood compared with natural depletion case. If gas dump flood is started when the pressure is still higher than or equal to the dewpoint pressure, there is an increase of around 13% of gas recovery factor for all cases. However, by starting dump flood after the reservoir pressure is 1,000 psi lower than the dewpoint pressure, there is a larger increase in gas recovery. In these cases, the variation of starting time before the reservoir pressure drops the below dewpoint does not have much effect on increase in gas recovery.

Table 5.1: Cumulative hydrocarbon gas production and recovery factor for different starting times of gas dump flood

Starting time of gas dump flood	Cumulative hydrocarbon gas production (MSCF)	Recovery factor
1. None	5,522,105	71.54% *
2. At the beginning	9,051,136	84.45% **
3. When the reservoir pressure is 300 psi higher than the dewpoint pressure	9,046,614	84.41% **
4. When the reservoir pressure is equal to the dewpoint pressure (2,188 psi)	9,036,973	84.32% **
5. When the reservoir pressure is 1,000 psi lower than the dewpoint pressure	9,625,094	89.80% **

remark: * based on OGIP of target reservoir.

** based on OGIP of target and source reservoirs.

Table 5.2 illustrates the cumulative condensate production for gas dump flood started at different times. Condensate recovery increases by 40% approximately when gas dump flood is started at the pressure is equal to or higher than the dewpoint pressure. If gas dump flood is started later as in the case when the reservoir pressure is 1,000 psi below the dewpoint, there is less increment in cumulative condensate production.

Table 5.2: Cumulative condensate production and recovery factor for different starting times of gas dump flood

Starting time of gas dump flood	Cumulative condensate production (STB)	Recovery factor
1. None	454,939	47.88%
2. At the beginning	823,261	86.65%
3. When the reservoir pressure is 300 psi higher than the dewpoint pressure	823,504	86.67%
4. When the reservoir pressure is equal to the dewpoint pressure (2,188 psi)	823,470	86.67%
5. When the reservoir pressure is 1,000 psi lower than the dewpoint pressure	772,550	81.31%

In summary, gas dump flood started when the reservoir pressure is higher than the dewpoint pressure exhibits larger cumulative condensate production than gas dump flood started at a pressure below the dewpoint although cumulative gas production is less. Since the objective is to maximize condensate recovery, we should start gas dump flood before the pressure falls below the dewpoint.

5.4 Effect of CO_2 Concentration in Source Reservoir

As natural depletion causes condensate to drop out around the producer at early times, condensate still exists at high level in the reservoir until flooding gas arrives. In this section, the effect of the composition of the flooding gas on condensate recovery is investigated.

Four sets of composition are used as inputs in the source reservoir to investigate the effect of different CO_2 concentrations:

- $C_1:CO_2$ = 80:20 %mole
- $C_1:CO_2$ = 60:40 %mole
- $C_1:CO_2$ = 40:60 %mole
- $C_1:CO_2$ = 20:80 %mole

In this section, gas dump flood is performed when the reservoir pressure is 300 psi higher than the dewpoint pressure. The source reservoir is located 2,000 ft below the target reservoir. The effect of different CO_2 concentrations on condensate saturation in the grid blocks is shown in Figure 5.22.

Figures 5.22 and 5.23 depict condensate saturation profile at local grid (5, 5, 3) of the production well and cross flow rate for source gas containing different CO_2 percent moles, respectively. When the percent mole of CO_2 in the source reservoir is less, the movement of cross flow from the source reservoir to the target reservoir is faster because CO_2 has molecular weight heavier than methane. Consequently, flooding gas from the case of lower percent mole of CO_2 can maintain the reservoir pressure to prevent the condensate dropout in the reservoir slower than the case of higher percent mole of CO_2. However, when the flooding gas break through the production well, lower the percent mole of CO_2 shows the result that the condensate revaporizes slower than the case of higher the percent mole of CO_2. This is simply because CO_2 gas reduces the dewpoint of the resulting mixture. As the percent mole of CO_2 in the source reservoir increases, the percent mole of CO_2 in the produced gas increases as well as shown in Figure 5.24.

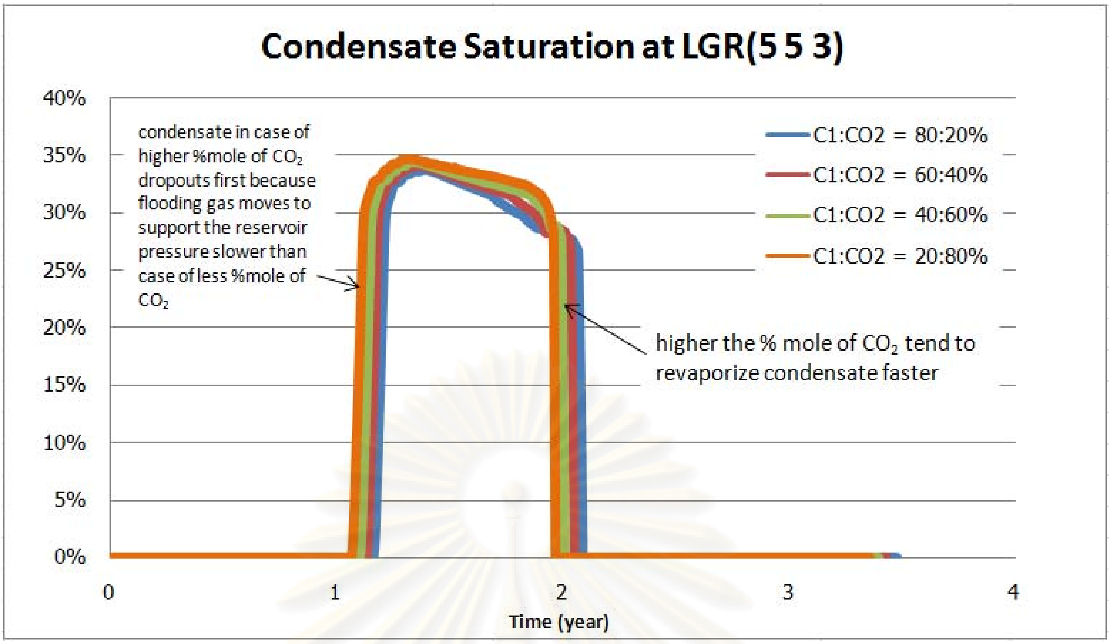

Figure 5.22: Condensate saturation at local grid (5, 5, 3) for different CO_2 %moles in the flooding gas.

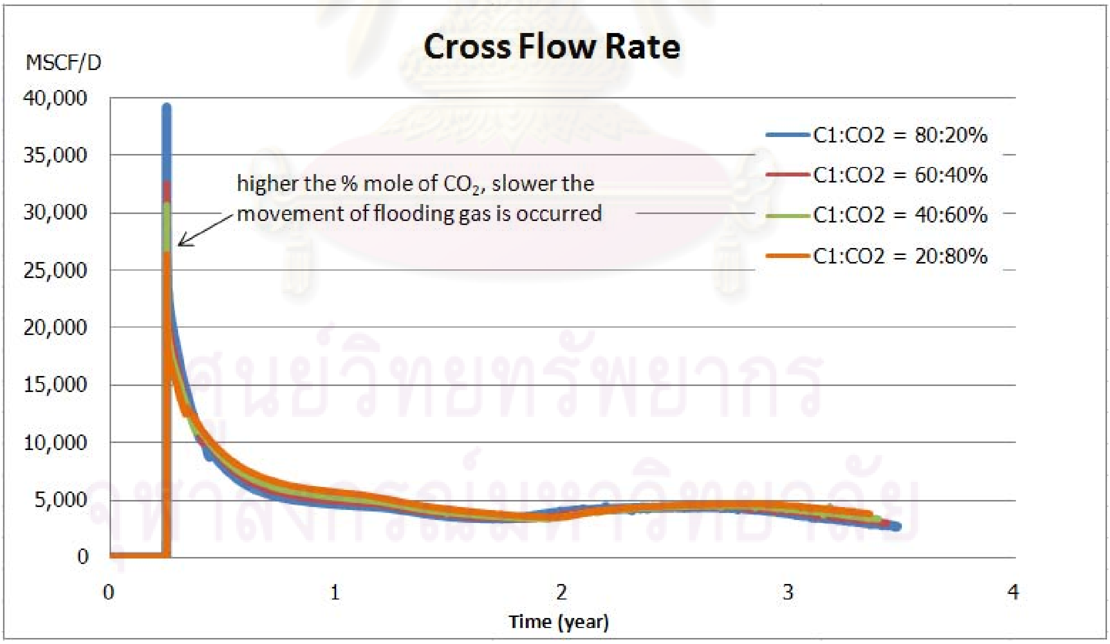

Figure 5.23: Cross flow rate from source to target reservoirs for different CO_2 %moles in the flooding gas.

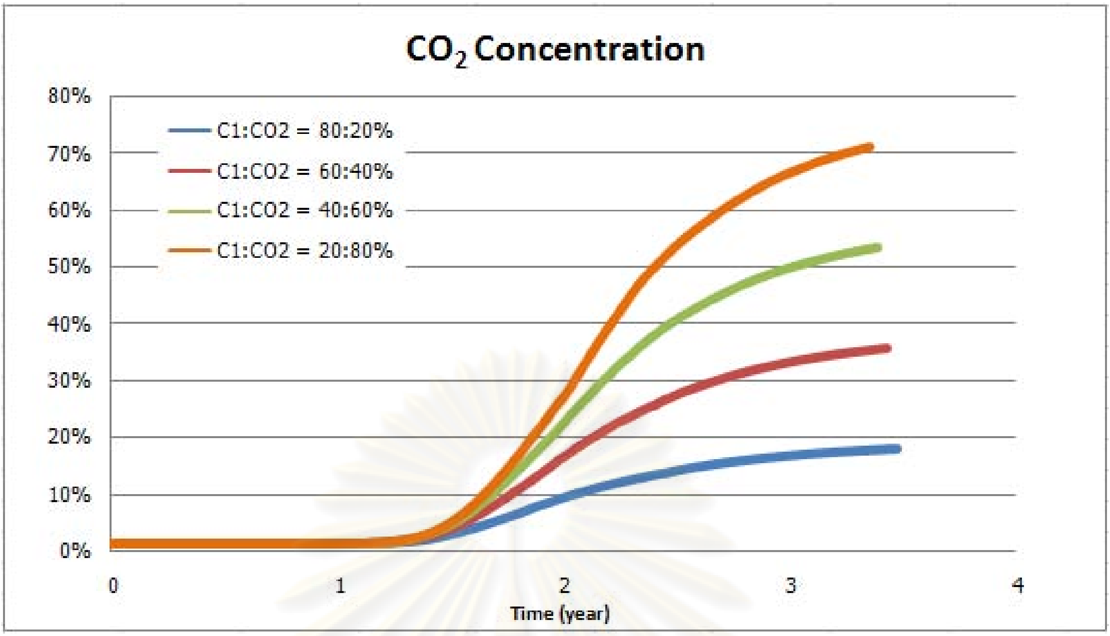

Figure 5.24: CO_2 concentration of produced gas for different CO_2 %moles in the flooding gas.

Table 5.3 shows the cumulative hydrocarbon gas production that higher CO_2 mole fraction results in higher hydrocarbon production because higher C_1 concentration causes an increased amount of hydrocarbon gas in place.

Table 5.3: Cumulative hydrocarbon gas production for different CO_2 %moles in the flooding gas

Case	Cumulative hydrocarbon gas production (MSCF)	Recovery factor
1. None	5,522,105	71.55%*
2. C_1:CO_2 = 80:20 %	10,487,606	76.45%**
3. C_1:CO_2 = 60:40 %	9,675,201	78.23%**
4. C_1:CO_2 = 40:60 %	8,931,477	83.33%**
5. C_1:CO_2 = 20:80 %	8,223,337	90.19%**

remark: * based on OGIP of target reservoir.

** based on OGIP of target and source reservoirs with different CO_2 %moles.

In terms of cumulative condensate recovery, higher CO_2 mole fraction results in slightly higher condensate recovery as depicted in Table 5.4. This is because higher CO_2 concentration causes an increased amount of condensate revaporization in the reservoir.

Table 5.4: Cumulative condensate production for different CO_2 %moles in the flooding gas

Case	Cumulative condensate production (STB)	Recovery factor
1. Natural depletion	454,939	47.88%
2. C_1:CO_2 = 80:20 %	826,116	86.95%
3. C_1:CO_2 = 60:40 %	830,393	87.40%
4. C_1:CO_2 = 40:60 %	833,792	87.76%
5. C_1:CO_2 = 20:80 %	836,582	88.05%

5.5 Effect of Depth Difference between Source and Target Reservoirs

To study the effect of difference in depths of the source reservoir and the target reservoir, simulation runs are performed for investigation in which gas dump flood is started when the reservoir pressure equals to the dewpoint pressure at 2,188 psi with CO_2 percent mole of 60% in the flooding gas. When the depth difference is higher, the difference in pressures between the two reservoirs becomes larger as well. The source and target reservoirs in the model are set to have depth difference as follows:

- 1,000 ft or 433 psi
- 2,000 ft or 866 psi

In order to account for the depth difference between source and target reservoirs as mentioned above, two sets of vertical flow performance curves are needed. In this case, VFP NO. 4 and NO. 8 (see Appendix B) are used for cases with depth difference of 1,000 and 2,000 ft, respectively. The effect of depth difference on gas production rate, condensate production rate, cross flow between the source and target reservoirs and cumulative condensate production are discussed in this section.

The gas production profile, condensate production profile, and cross flow between the source and target reservoirs for two depth differences are shown Figures 5.25, 5.26, and 5.27, respectively. The second gas production plateau rate after gas dump flood is extended when the depth or pressure difference between the source and target reservoirs is large. This results in a faster recovery of gas and condensate. In Figure 5.27, a higher cross flow from the source to the target reservoirs is seen when the depth difference becomes larger.

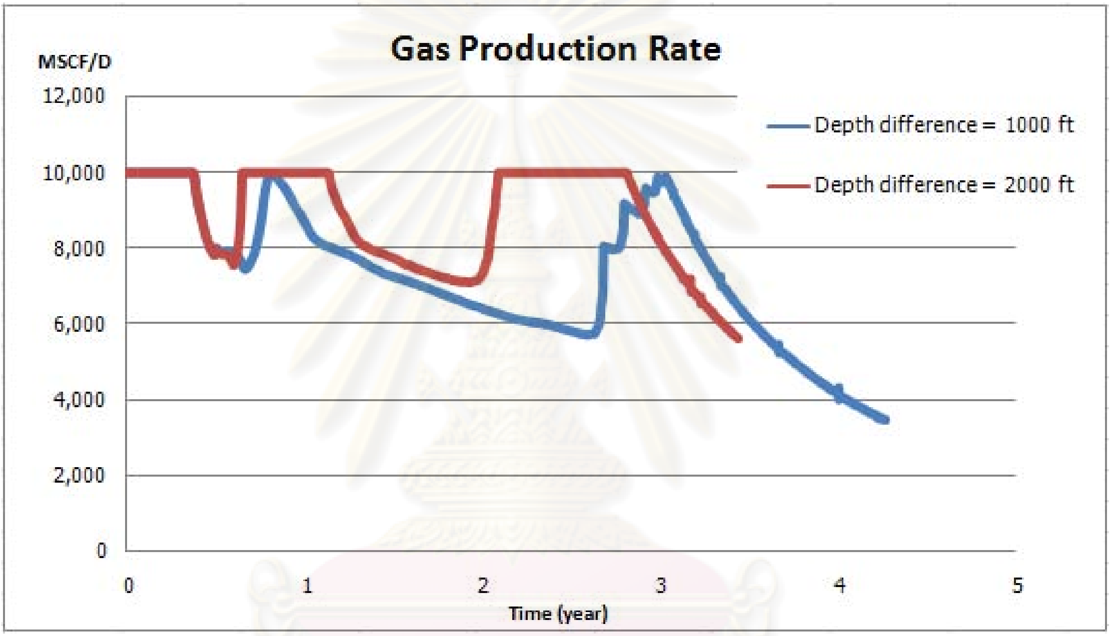

Figure 5.25: Gas production profile for various depth differences.

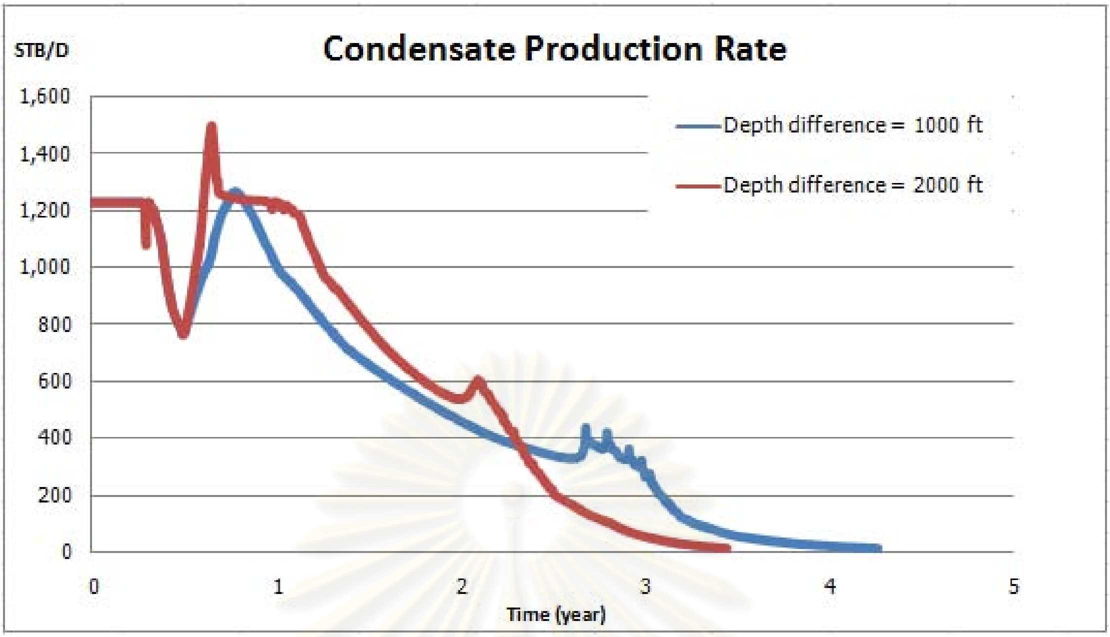

Figure 5.26: Condensate production profile for various depth differences.

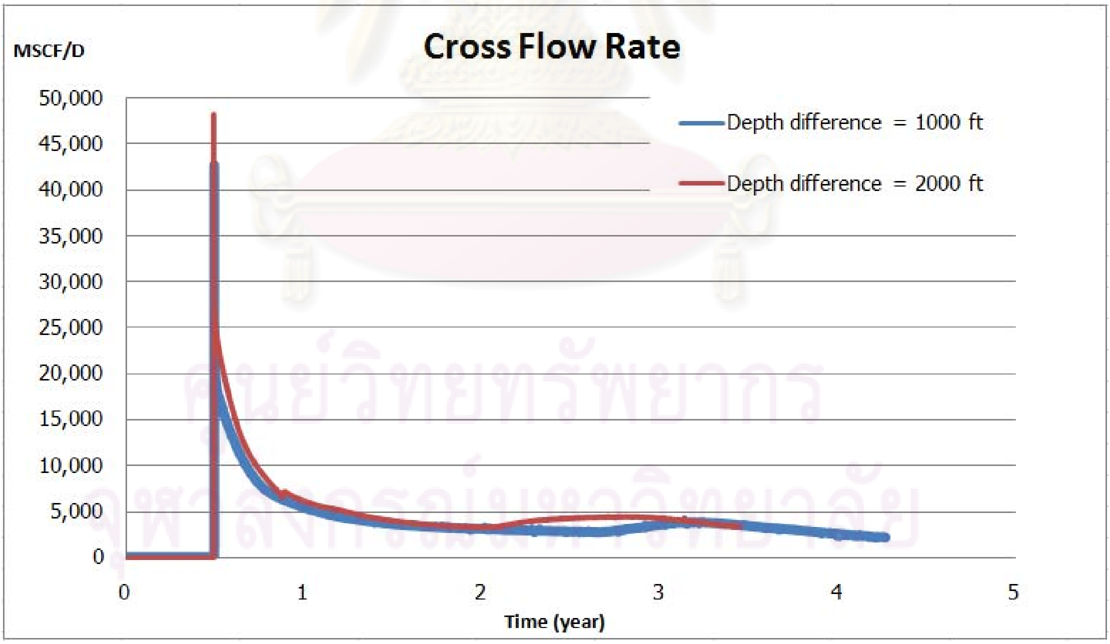

Figure 5.27: Cross flow rate from source to target reservoirs for various depth differences.

Figures 5.28 and 5.29 display condensate saturation at local grid and CO_2 concentration at the production well, respectively. The condensate dropout around the wellbore is revaporized faster when there is depth difference because flooding gas reaches the producing well faster as shown in Figure 5.28.

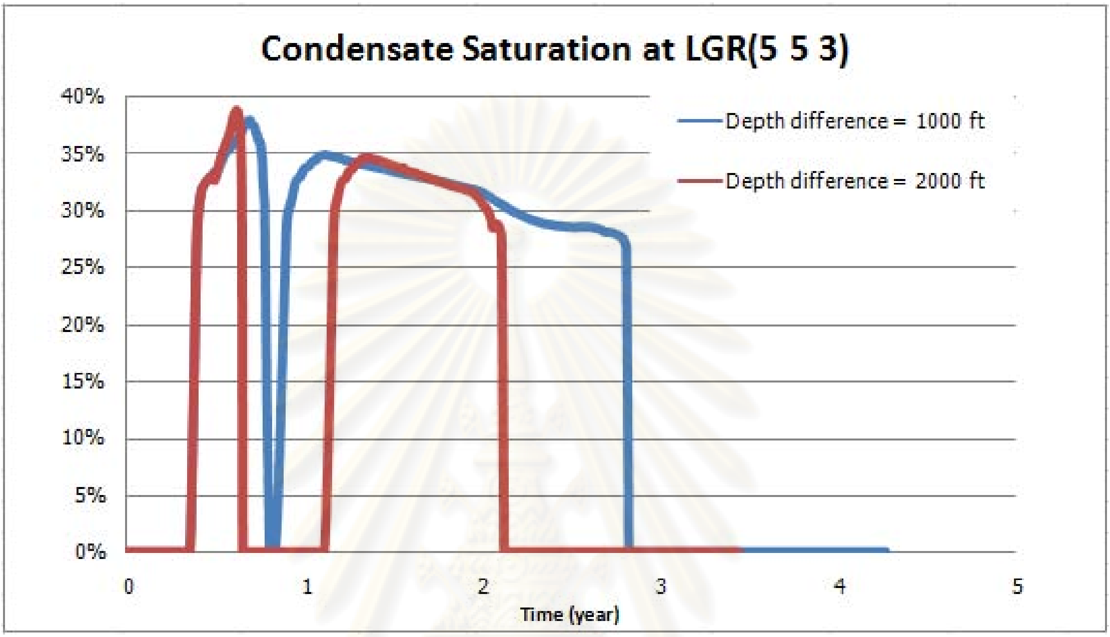

Figure 5.28: Condensate saturation profile at local grid (5, 5, 3) for various depth differences.

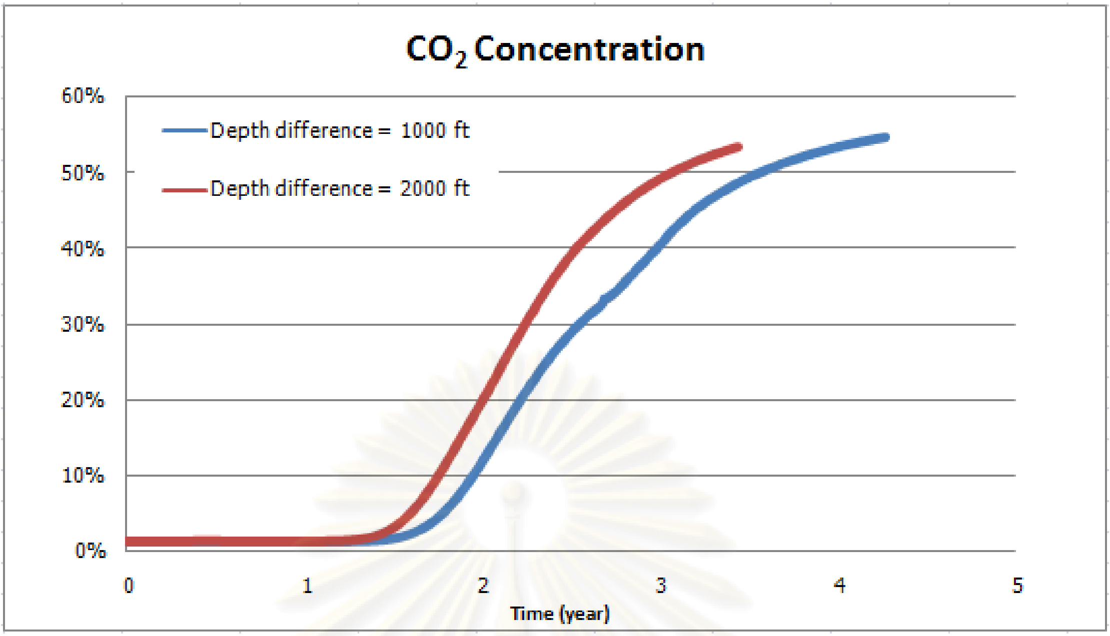

Figure 5.29: CO_2 concentration profile at local grid (5, 5, 3) for various depth differences.

Cumulative hydrocarbon gas and condensate production are shown in Tables 5.5 and 5.6, respectively. The results illustrate that the cumulative hydrocarbon gas and condensate production increases slightly when the depth difference between the two reservoirs changes from 1,000 ft to 2,000 ft.

Table 5.5: Cumulative hydrocarbon gas production for various depth differences

Case	Cumulative hydrocarbon gas production (MSCF)	Recovery factor
1. Natural depletion	5,522,105	71.55%*
2. Depth difference = 1,000 ft	9,036,973	84.32%**
3. Depth difference = 2,000 ft	8,915,864	83.19%**

remark: * based on OGIP of target reservoir.

** based on OGIP of target and source reservoirs with different depth.

Table 5.6: Cumulative condensate production for various depth differences

Case	Cumulative condensate production (STB)	Recovery factor
1. Natural depletion	454,939	47.88%
2. Depth difference = 1,000 ft	823,470	86.67%
3. Depth difference = 2,000 ft	834,365	87.82%

In summary, the effect of depth difference between source and target reservoirs can be summarized as follows:

a) The maximum gas and condensate production rate can be achieved easily by having higher depth difference because the potential of flooding gas in deeper depth is higher in flowing pressure from the source to the target reservoirs.

b) Even though the depth difference between the source and the target reservoirs has a slightly impact on cumulative hydrocarbon gas and condensate production but we can recover in case of high depth difference faster than in case of low depth difference due to the fact that higher difference in depth has a higher difference in pressure between the source and the target reservoirs.

5.6 Comparison between Gas Dump Flood and Conventional CO_2 Injection

In this scenario, gas injection cases were simulated in order to compare its performance with gas dump flood. We also investigated the effect injection rate on condensate recovery. According to the results in Section 5.3, the highest cumulative condensate production was obtained by starting gas dump flood at the reservoir pressure equal to or higher than the dewpoint pressure. Therefore, in this scenario, conventional CO_2 injection was implemented when the reservoir pressure equals to the dewpoint pressure of 2,188 psi. The injection rate was varied from 4,000 MSCF/D to 12,000 MSCF/D in a step of 2,000 MSCF/D increment. The location of injection well is the same as the source well in previous cases at coordinate (1, 1) in LGR grid (located at coordinate (1, 1) in the global grid). The maximum gas production rate which was set at 10,000 MSCF/D was used as the control variable. The gas production rate was kept constant as long as the reservoir pressure can sustain such rate with a tubing head pressure limit of 500 psia and vertical flow performance VFP NO.1 (see Appendix B) which is the same as in gas dump flood cases. Simulation runs stopped when the gas production rate reached abandonment rates of 100 MSCF/D or condensate production rate of 10 STB/D.

The gas and condensate production rates for different injection strategies are shown in Figures 5.30 and 5.31, respectively. At early time, gas and condensate production rates are constant while the bottomhole pressure declines as shown in Figures 5.32, 5.33, 5.34, 5.35 and 5.36 for the injection case of 4,000, 6,000, 8,000, 10,000, and 12,000 MSCF/D, respectively. After the bottomhole pressure drops below dewpoint pressure, gas and condensate production rates decrease and liquid starts to condense in the pore space. After that, the injection is performed when the reservoir pressure equal to dewpoint pressure.

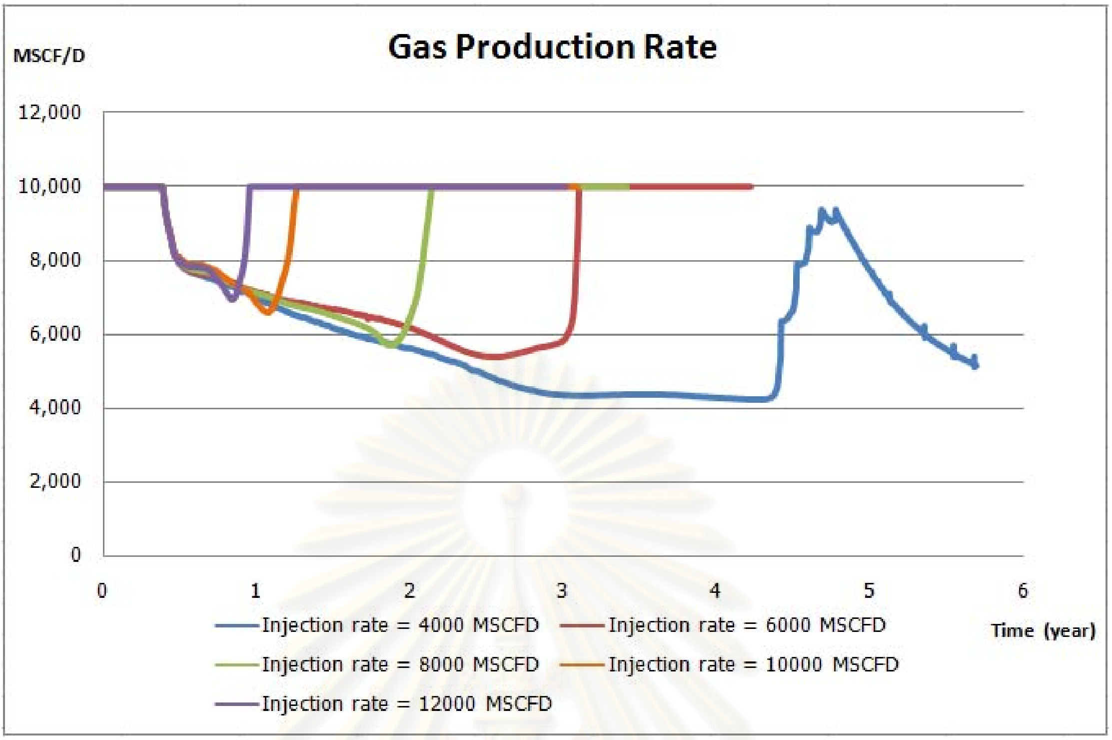

Figure 5.30: Gas production profile for injection cases with various injection rates.

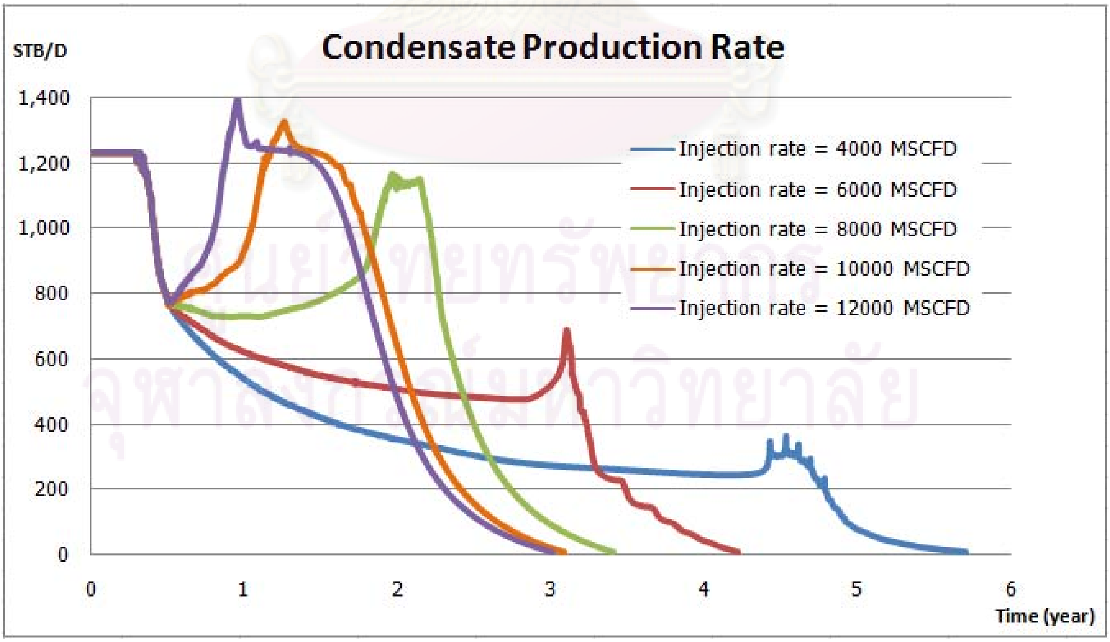

Figure 5.31: Condensate production profile for injection cases with various injection rates.

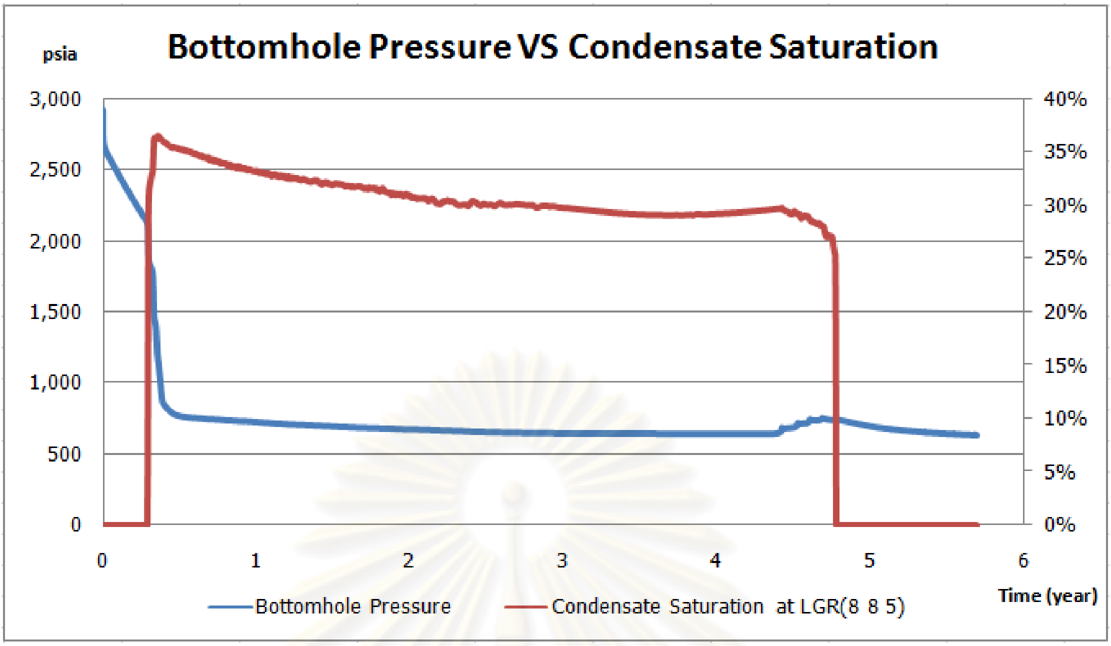

Figure 5.32: Bottomhole pressure and condensate saturation in LGR(8 8 5) for injection case of 4,000 MSCF/D.

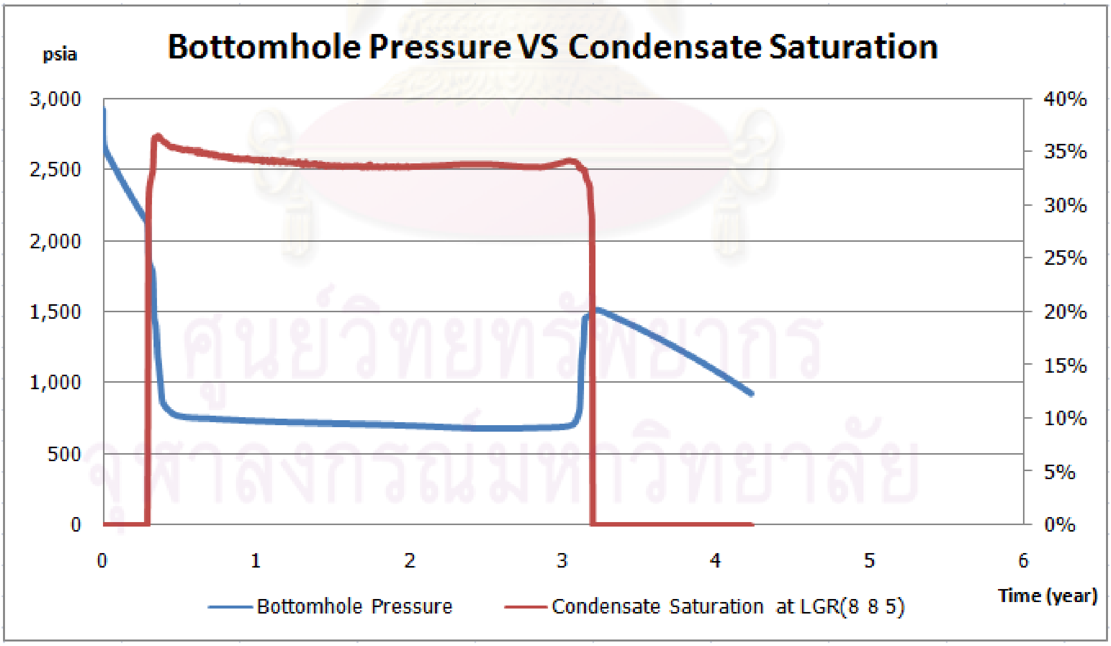

Figure 5.33: Bottomhole pressure and condensate saturation in LGR(8 8 5) for injection case of 6,000 MSCF/D.

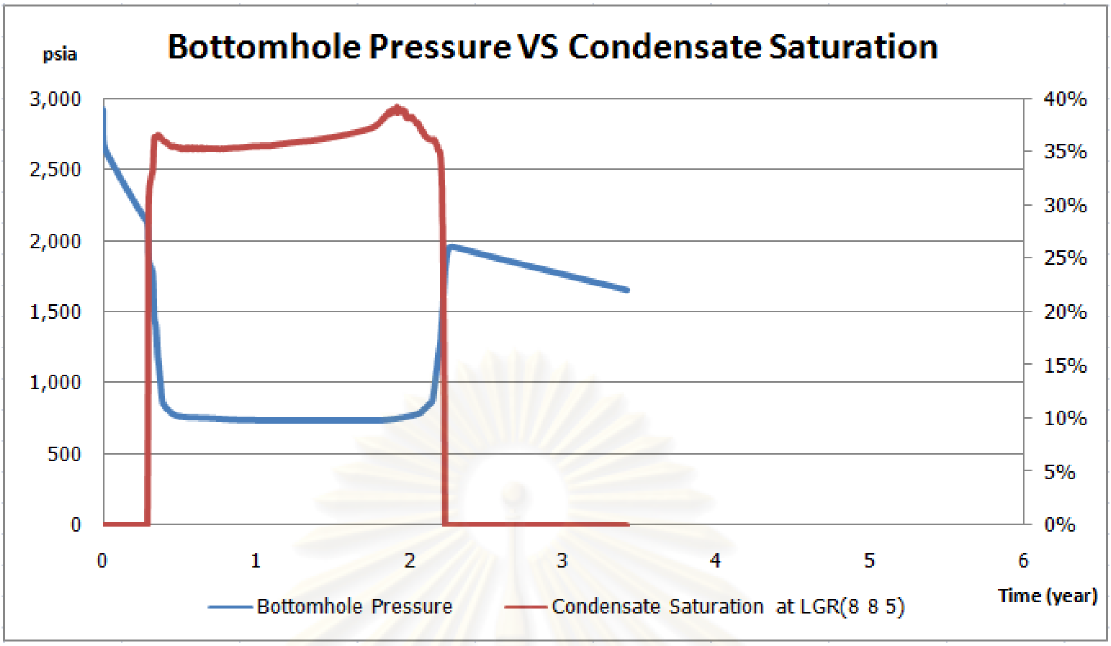

Figure 5.34: Bottomhole pressure and condensate saturation in LGR(8 8 5) for injection case of 8,000 MSCF/D.

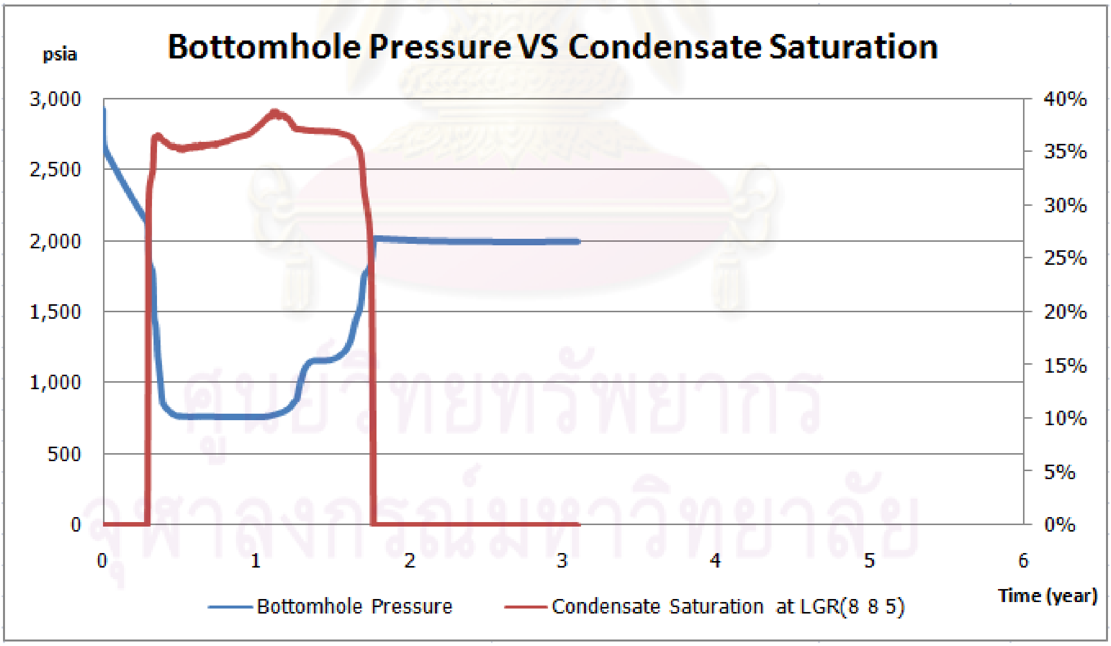

Figure 5.35: Bottomhole pressure and condensate saturation in LGR(8 8 5) for injection case of 10,000 MSCF/D.

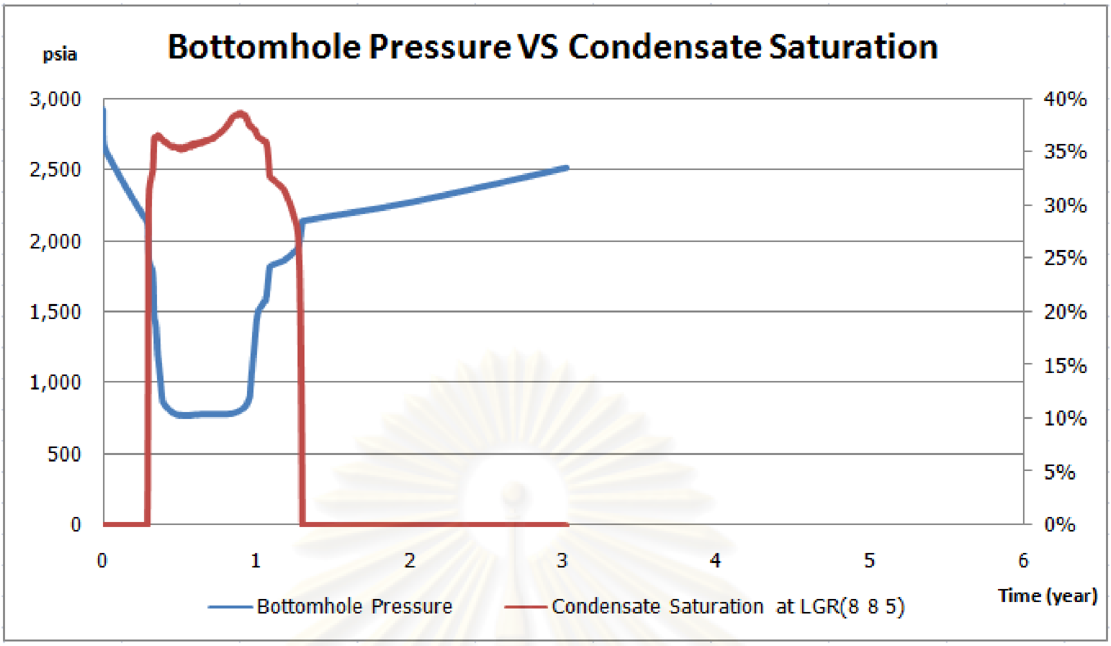

Figure 5.36: Bottomhole pressure and condensate saturation in LGR(8 8 5) for injection case of 12,000 MSCF/D.

Figures 5.32 to 5.36 also show that condensate saturation around the wellbore increases as condensate accumulates until it reaches the critical condensate saturation. Then, condensate revaporizes after the flooding gas breaks through the production well for some period of time and lowers the dewpoint pressure of the new mixture as discussed in Section 5.2. The production life is shorten when the injection rate increases because higher injection rate can maintain the reservoir pressure to achieve the maximum production rate until the simulation stop because condensate production rate reaches the abandonment rates of 10 STB/D.

Table 5.7 shows cumulative condensate production for various CO_2 injection rates. By increasing the injection rate, the cumulative condensate production gradually increases. This trend continues until gas injection rate reaches 8,000 MSCF/D. After that, an increase in gas injection rate has a negative effect on cumulative condensate production because higher injection rate results in less sweep efficiency as shown in Figure 5.37, leaving condensate in the lateral area of the target reservoir.

Table 5.7: Cumulative condensate production for various CO_2 injection rates

Case	Cumulative condensate production (STB)	Recovery factor
1. Natural depletion	454,939	47.88%
2. Injection rate 4,000 MSCF/D	783,122	82.42%
3. Injection rate 6,000 MSCF/D	807,606	85.00%
4. Injection rate 8,000 MSCF/D	846,828	89.13%
5. Injection rate 10,000 MSCF/D	842,208	88.64%
6. Injection rate 12,000 MSCF/D	833,152	87.69%

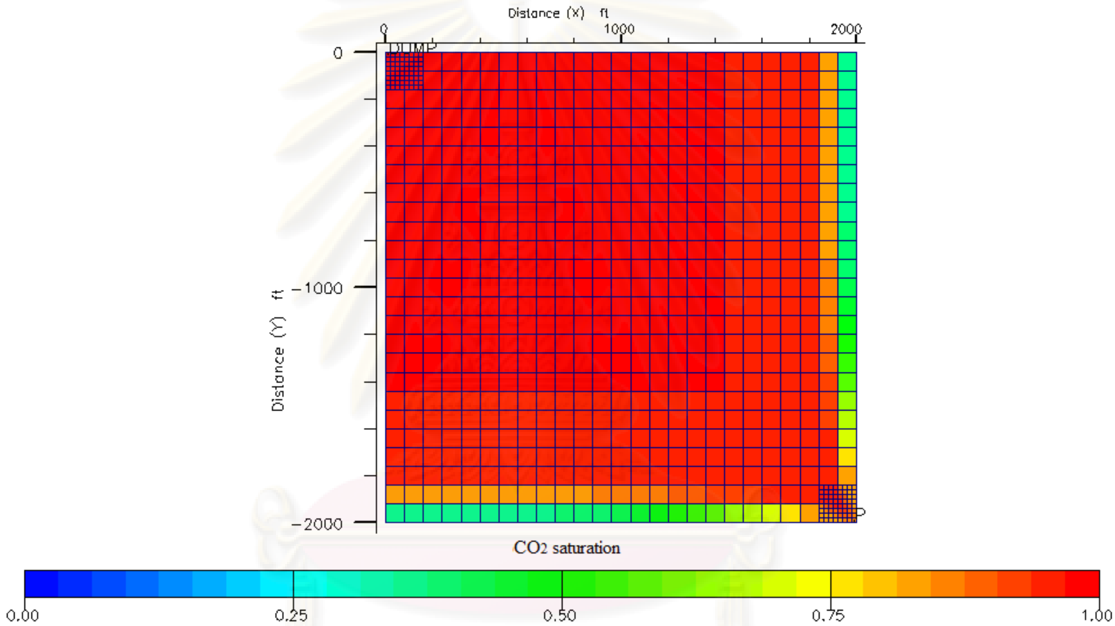

Figure 5.37: CO_2 saturation in the target reservoir.

Table 5.8 depicts cumulative hydrocarbon gas production for various CO_2 injection rates. The hydrocarbon gas recovery decreases when the CO_2 injection rate increases because higher injection rate results in less sweep efficiency as the same reason of less cumulative condensate recovery as mentioned above.

Table 5.8: Cumulative hydrocarbon gas production for various CO_2 injection rates

Methods	Cumulative hydrocarbon gas production (MSCF)	Recovery factor
1. Natural depletion	5,522,105	71.55%*
2. Injection rate 4,000 MSCF/D	7,690,185	99.64%*
3. Injection rate 6,000 MSCF/D	7,571,177	98.10%*
4. Injection rate 8,000 MSCF/D	7,391,255	95.77%*
5. Injection rate 10,000 MSCF/D	7,353,996	95.28%*
6. Injection rate 12,000 MSCF/D	7,295,113	94.52%*

remark: * based on OGIP of target reservoir.

After discussing the effect of injection rates on conventional CO_2 flooding in the gas condensate reservoir, the 8,000 MSCF/D of CO_2 injection case is selected for comparison with the gas dump flood case which has 60 percent mole of CO_2 and 2,000 ft in depth difference. Figures 5.38 and 5.39 display gas and condensate production rates for different recovery processes. As previously discussed, in the gas dump flood case, the cross flow rate is very high at the early time then rapidly decreases while the gas rate in the CO_2 injection case is stable. Therefore, the gas and condensate production rate of CO_2 injection case is less than those of the gas dump flood case at early and middle time as a consequence of difference in condensate saturation around the wellbore as shown in Figure 5.40 due to different degrees of pressure support from flooding gas.

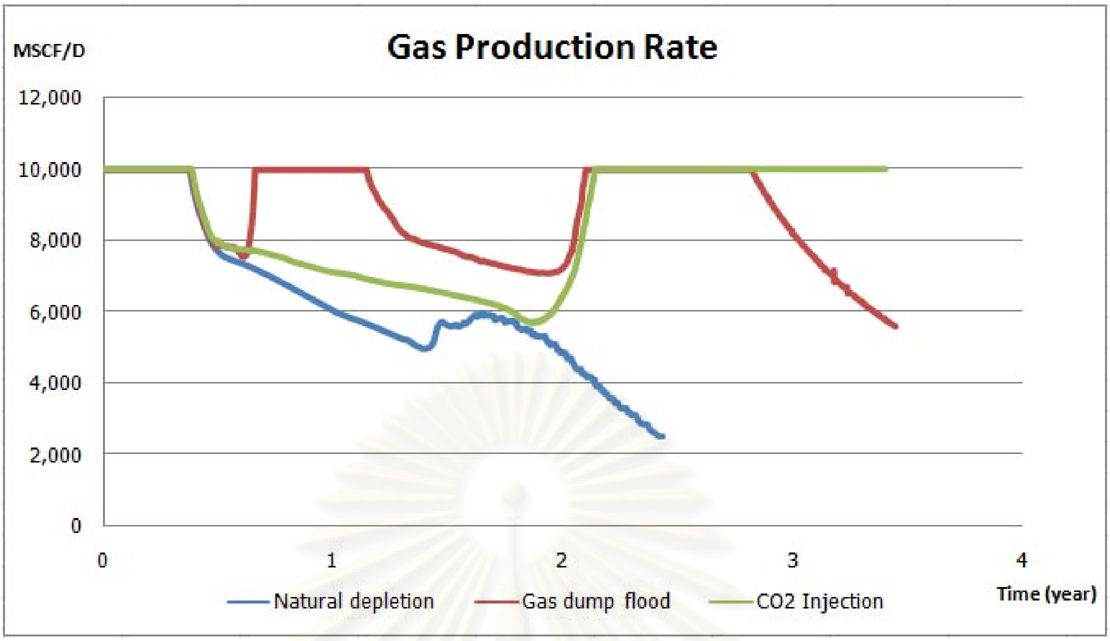

Figure 5.38: Gas production profile for different production strategies.

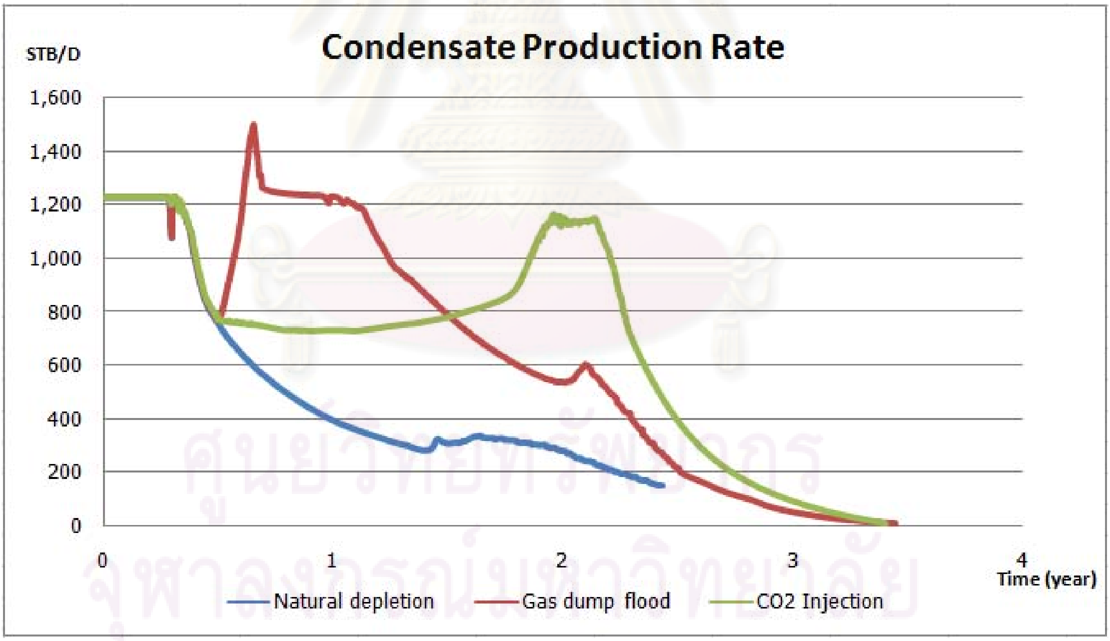

Figure 5.39: Condensate production profile for different production strategies.

Figure 5.40 and 5.41 illustrate the condensate saturation profile at local grid and bottomhole pressure for different recovery processes. The condensate saturation profile of injection case is more stable than that of gas dump flood case because the pressure maintenance process of CO_2 injection constantly sustains the bottomhole pressure along the production life. At late time of injection case or after CO_2 breakthrough, the reservoir fluid is changed by flooding process. At this period, flooding gas reduces the dewpoint pressure of the fluid in the target reservoir. As a consequence, condensate around wellbore revaporizes into gas phase.

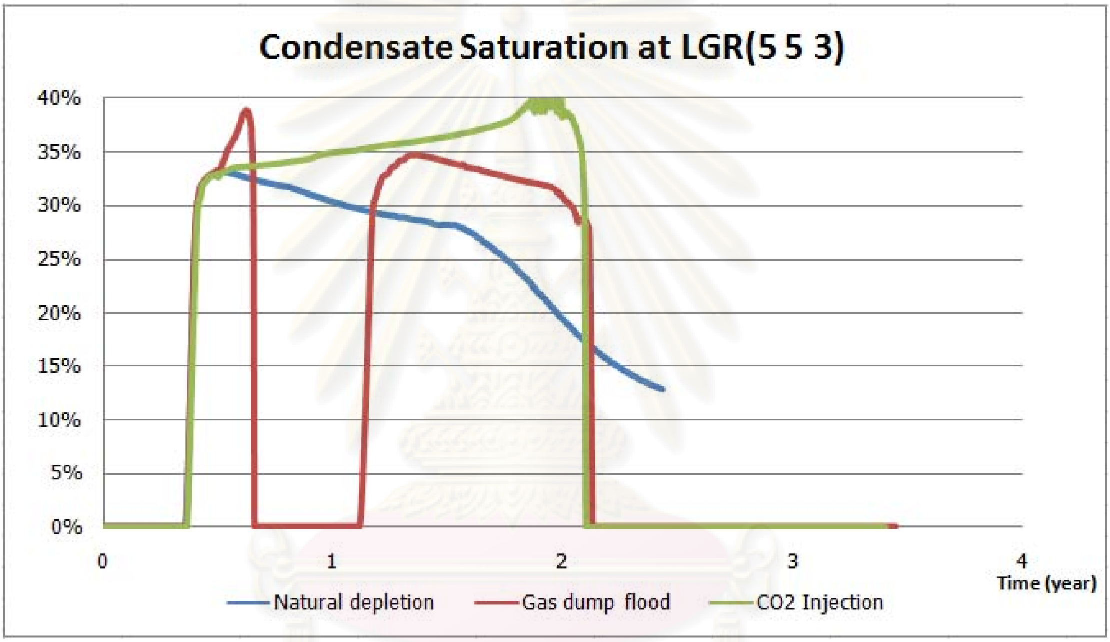

Figure 5.40: Condensate saturation profile for different production strategies.

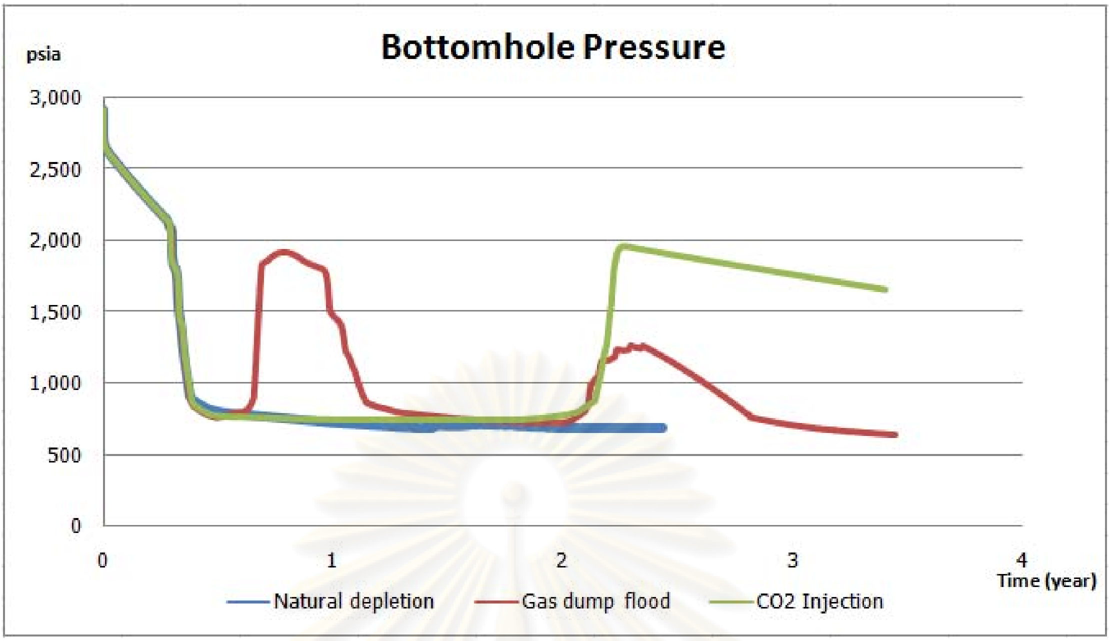

Figure 5.41: Bottomhole pressure for different production strategies.

Table 5.9: Cumulative hydrocarbon gas production for different production strategies

Case	Cumulative hydrocarbon gas production (MSCF)	Recovery factor
1. Natural depletion	5,522,105	71.55%*
2. Gas dump flood	8,915,864	83.19%**
3. CO_2 Injection	7,391,255	95.77%*

remark: * based on OGIP of target reservoir.

** based on OGIP of target and source reservoirs.

Table 5.10: Cumulative condensate production for different production strategies

Case	Cumulative condensate production (STB)	Recovery factor
1. Natural depletion	454,939	47.88%
2. Gas dump flood	834,365	87.82%
3. CO_2 Injection	846,828	89.13%

Tables 5.9 and 5.10 show comparison between gas dump flood and CO_2 injection cases. In term of hydrocarbon gas and condensate recovery, CO_2 injection has higher cumulative hydrocarbon gas and condensate recovery and slightly longer production life time. However, the disadvantage of CO_2 injection is that we need to invest on gas injection system.

CHAPTER VI

CONCLUSIONS AND RECOMMENDATIONS

In this chapter, general conclusions are drawn from the results of simulation runs for gas-condensate reservoir with emphasis on gas dump flood mechanism, effect of starting time of CO_2 dump flood, effect of CO_2 concentration in the source reservoir and effect of depth difference between source and target reservoirs. In addition, we discuss possible improvements of the current work.

6.1 Conclusions

Based on a specific set of input data, simulation results obtained from ECLIPSE 300 simulator, gas dump flood mechanism, effect of several variables on condensate recovery enhancement can be concluded as follows:

1. Gas dump flood can increase the condensate recovery by keeping the reservoir pressure high and revaporizing the liquid around the wellbore.
2. The best starting time to start CO_2 dump flood is anytime before the pressure of the gas-condensate reservoir falls below the dewpoint. Once the reservoir pressure falls below the dewpoint, the recovery of condensate becomes less effective.
3. The increase in concentration of CO_2 in the source gas has a slight effect on the recovery of condensate from the target reservoir. A higher concentration of CO_2 in the source gas results in a slightly higher condensate recovery.
4. Cases with low CO_2 concentration in the source gas yield higher hydrocarbon gas recovery than cases with high CO_2 concentration simply because the source gas has higher CH_4 concentration and it is produced together with the gas in the target reservoir. Gas from two reservoirs is being produced from one production well while another well is needed to connect the source to the target reservoir. Thus, a source reservoir with

high CH_4 concentration and low CO_2 concentration may be more attractive.

5. Larger depth or pressure difference between the source and target reservoirs slightly increases the condensate recovery. However, a larger difference in depths or pressures shortens the time required to recover gas and condensate from the target reservoir.
6. Gas dump flood process has less both hydrocarbon gas and condensate recovery than CO_2 injection. However, the disadvantage of CO_2 injection is that we need to invest on gas injection system.

6.2 Recommendations

As a number of assumptions and simplifications in this study such as homogeneous reservoir properties, no dip angle and normal five-spot flooding pattern were made in the simulation setup. Other than the lifting the assumptions, improvements can be made on the following aspects to better characterize the gas dump flood in gas-condensate reservoir:

First, changing the concentration of compositions in gas-condensate reservoir can be investigated by varying the heavy components.

Second, size of both gas-condensate and source reservoirs affect directly the recovery in the gas dump flood process.

Third, the location of source well and producing well may change the total results because of change in flooding pattern.

Future works should study the influence of these variables for more understanding on mechanism and performance of gas dump flood into a gas-condensate reservoir.

References

[1] AL-Abri, A., Sidiq, H., and Amin, R., Curtin University of Technology, Enhanced Natural Gas and Condensate Recovery by injection of Pure $SCCO_2$, Pure CH_4 and Their Mixtures: Experimental Investigation. Paper SPE 124145 presented at 2009 SPE Annual Technical Conference and Exhibition held in New Orleans, Louisiana, USA, 4-7 October 2009.

[2] Shi, C., Horne, R.N., and Li, K., Optimizing the Productivity of Gas/Condensate Wells. Paper SPE 103255 presented at 2006 SPE Annual Technical Conference and Exhibition held in San Antonio, Texas, U.S.A., 24-27 September 2006.

[3] Tangkaprasert, P., Enhancing Hydrocarbon Recovery from Gas condensate reservoir via carbon dioxide injection. 2008. Master's thesis, Department of Mining and Petroleum Engineering, Faculty of Engineering, Chulalongkorn University.

[4] Shtepani, E., CO_2 Sequestration in Depleted Gas/Condensate Reservoirs. Paper SPE 102284 presented at the 2006 SPE Annual Technical Conference and Exhibition held in San Antonio, Texas, U.S.A. September 2006.

[5] Shi, C., and Horne, R.N., Improved Recovery in Gas-Condensate Reservoirs Considering Compositional Variations. Paper SPE 115786 presented at the 2008 SPE Annual Technical Conference and Exhibition held in Denver, Colorado, USA, 21-24 September 2008.

[6] Chang, Y.B., Coats, B.K., and Nolen, J.S., A Compositional Model for CO_2 Floods Including CO_2 Solubility in Water. SPE Reservoir Evaluation & Engineering, 155-160. April 1998.

[7] Sengul, M., CO_2 Sequestration—A Safe Transition Technology. Paper SPE 98617 presented at the SPE International Conference on Health, Safety, and Environment in Oil and Gas Exploration and Production held in Abu Dhabi, U.A.E. April 2006.

[8] Al-Hashami, A., Ren, S.R., and Tohidi, B., CO_2 Injection for Enhanced Gas Recovery and Geo-Storage Reservoir Simulation and Economics. presentation at the SPE Europec/EAGE Annual Conference held in Madrid, Spain June 2005.

[9] Fan, L., Harris, B.W., and Jamaluddin, A., Understanding Gas-Condensate Reservoirs. 2006.

[10] Yisheng, F., Baozhu, L., and Yongle, H., Condensate Gas Phase Behavior and Development. Paper SPE 50925 Presented at the 1998 SPE International Conference and Exhibition in China held in Beijing. 2-6 November 1998.

[11] Roussennac, B., Gas Condensate Well Test Analysis. Master's thesis, Stanford University, Stanford, CA, 2001

[12] Forchheimer, P., "Wasserbewegung Durch Boden." Zeitschrift des Vereines Deutscher Ingenieure, 49:1736, 50:1981, 1901.

[13] Willhite G.P., Waterflooding. SPE textbook series Volume 3, Third Printing Society of Petroleum Engineers, Richardson, TX, 1986

[14] Craig Jr., F.F., The Reservoir Engineering Aspects of Waterflooding. Monograph Volume 3 of the Henry L.Doherty series. New York, U.S.A: Millet the printer, 1980.

APPENDICES

APPENDIX A

A-1) Reservoir model

Two reservoir models (high CO_2-content reservoir and gas-condensate reservoir) are generated by entering required data into ECLIPSE 300 reservoir simulator. The model used in this study composes of 25 x 25 x 11 blocks in the x-, y- and z- directions.

A-2) Case definition

Simulator:	Compositional	
Model dimensions:	Number of cells in the x-direction	25
	Number of cells in the y-direction	25
	Number of cells in the z-direction	11
Grid type:	Cartesian	
Geometry type:	Block centered	
Oil-Gas-Water options:	Water, gas condensate (ISGAS)	
Number of components:	10	
Pressure saturation options (solution type):	AIM	

A-3) Reservoir properties

<u>Grid</u>

Properties: Active grid blocks:	Gas-condensate reservoir				
		X, Y, Z	=	25, 25, 1-5	
	Source reservoir				
		X, Y, Z	=	25, 25, 7-11	
Inactive grid blocks:		X, Y, Z	=	25, 25, 6	
Porosity			=	0.17	
Permeability		k-x	=	50	mD
		k-y	=	50	mD
		k-z	=	5	mD

X Grid block sizes (All X = 1-25)	=	80 ft
Y Grid block sizes (All Y = 1-25)	=	80 ft
Z Grid block sizes (for Z = 1-5 and 7-11)	=	20 ft
Z Grid block sizes (for Z = 6)	=	1,000 ft or
	=	2,000 ft
Depth of top face (Top layer)	=	6,000 ft

Cartesian local grid refinement

LGR name	LGR coordinate			Number of refined cells		
	I	J	K	X	Y	Z
Producer	24-25	24-25	1-5	8	8	5
Source well	1-2	1-2	1-5,7-11	8	8	5

PVT table

Fluid densities at surface conditions	Oil density	40	lb/ft^3
	Water density	63	lb/ft^3
	Gas density	0.001	lb/ft^3
Rock properties	Reference pressure	3000	psia
	Rock compressibility	4.0E-6	/psi

A-4) Miscellaneous

Number of components	Number of components	10	
Standard condition	Standard temperature	60	˚F
	Standard pressure	14.7	psia
Component names	Component 1	CO_2	
	Component 2	C_1	
	Component 3	C_2	
	Component 4	C_3	
	Component 5	$i\text{-}C_4$	
	Component 6	$n\text{-}C_4$	
	Component 7	$i\text{-}C_5$	
	Component 8	$n\text{-}C_5$	
	Component 9	C_6	
	Component 10	C_{7+}	
PROPS reporting options	Oil PVT tables	No output	
	Gas PVT tables	No output	
	Water PVT tables	No output	

EoS Res tables

Pure component boiling points (Reservoir EoS)	Component CO_2	350.46	˚R
	Component C_1	200.88	˚R
	Component C_2	332.28	˚R
	Component C_3	415.98	˚R
	Component IC_4	470.34	˚R
	Component NC_4	490.86	˚R
	Component IC_5	541.80	˚R
	Component NC_5	556.56	˚R
	Component C_6	606.69	˚R
	Component C_{7+}	734.08	˚R
Critical temperature (Reservoir EoS)	Component CO_2	548.46	˚R
	Component C_1	343.08	˚R
	Component C_2	549.77	˚R
	Component C_3	665.64	˚R
	Component IC_4	734.58	˚R
	Component NC_4	765.36	˚R
	Component IC_5	828.72	˚R
	Component NC_5	845.28	˚R
	Component C_6	913.50	˚R
	Component C_{7+}	1061.3	˚R
Constant reservoir temperature	Initial reservoir temperature	293	˚F
Critical volume (Reservoir EoS)	Component CO_2	1.5057	ft^3/lb-mole
	Component C_1	1.5698	ft^3/lb-mole
	Component C_2	2.3707	ft^3/lb-mole
	Component C_3	3.2037	ft^3/lb-mole
	Component IC_4	4.2129	ft^3/lb-mole
	Component NC_4	4.0847	ft^3/lb-mole
	Component IC_5	4.9337	ft^3/lb-mole
	Component NC_5	4.9817	ft^3/lb-mole
	Component C_6	5.6225	ft^3/lb-mole
	Component C_{7+}	7.509	ft^3/lb-mole
Overall composition for region 1	Component CO_2	1.2302	%
	Component C_1	59.991	%
	Component C_2	8.4326	%
	Component C_3	6.3988	%
	Component IC_4	3.4127	%
	Component NC_4	3.8989	%
	Component IC_5	1.4286	%
	Component NC_5	1.3988	%
	Component C_6	7.2718	%
	Component C_{7+}	6.5366	%

Critical pressure (Reservoir EoS)	Component CO_2	1071.3	psia
	Component C_1	667.78	psia
	Component C_2	708.34	psia
	Component C_3	615.76	psia
	Component IC_4	529.05	psia
	Component NC_4	550.66	psia
	Component IC_5	491.58	psia
	Component NC_5	488.79	psia
	Component C_6	436.62	psia
	Component C_{7+}	403.29	psia
Equation of state (Reservoir EoS)	Equation of State Method	PR (Peng-Robinson)	
Molecular weights (Reservoir EoS)	Component CO_2	44.01	
	Component C_1	16.043	
	Component C_2	30.07	
	Component C_3	44.097	
	Component IC_4	58.124	
	Component NC_4	58.124	
	Component IC_5	72.151	
	Component NC_5	72.151	
	Component C_6	84	
	Component C_{7+}	115	
Acentric factor (Reservoir EoS)	Component CO_2	0.225	
	Component C_1	0.013	
	Component C_2	0.0986	
	Component C_3	0.1524	
	Component IC_4	0.1848	
	Component NC_4	0.201	
	Component IC_5	0.227	
	Component NC_5	0.251	
	Component C_6	0.299	
	Component C_{7+}	0.38056	

A-5) SCAL

Gas/Oil relative permeabilities

where:

k_{rg} is relative permeability to gas

k_{ro} is relative permeability to oil

k_{rw} is relative permeability to water

S_w is saturation of water

S_g is saturation of gas

p_c is capillary pressure

S_g	k_{rg}	k_{ro}
0	0	0.897
0.03515	7.63E-05	0.705923
0.0703	0.00061	0.544104
0.10545	0.002059	0.409125
0.1406	0.00488	0.298553
0.17575	0.009531	0.209941
0.2109	0.01647	0.140865
0.24605	0.026154	0.0889
0.2812	0.03904	0.051603
0.31635	0.055586	0.026534
0.3515	0.07625	0.011275
0.38665	0.101489	0.003398
0.4218	0.13176	0.000433
0.45695	0.167521	0
0.4921	0.20923	0
0.52725	0.257344	0
0.5624	0.31232	0
0.59755	0.374616	0
0.6327	0.44469	0
0.66785	0.522999	0
0.703	0.61	0

Oil/Water relative permeabilities

S_w	k_{rw}	k_{ro}
0.297	0	0.897
0.319026	1.76E-05	0.769065
0.341051	0.000141	0.653913
0.363077	0.000476	0.55087
0.385102	0.001128	0.459264
0.407128	0.002203	0.378422
0.429154	0.003807	0.307671
0.451179	0.006045	0.246339
0.473205	0.009024	0.193752
0.49523	0.012849	0.149238
0.517256	0.017625	0.112125
0.539282	0.023459	0.081739
0.561307	0.030456	0.057408
0.583333	0.038722	0.038459
0.605358	0.048363	0.024219
0.627384	0.059484	0.014016
0.649410	0.072192	0.007176
0.671435	0.086592	0.003027
0.693461	0.102789	0.000897
0.715486	0.12089	0.000112
0.737512	0.141	0
1	1	0

A-6) Initialization equilibration

Equilibration Region	Keywords	EQUIL(Equilibrium Data Specification)	
EquilReg 1	Equilibrium Data Specification	Datum Depth	6,000 ft
		Pressure at Datum Depth	3,000 psia
		Oil-Water Contact	9,000 ft
EquilReg 2	Equilibrium Data Specification	Datum Depth	7,000 or 8,000 ft
		Pressure at Datum Depth	3,433 psia or 3,866 psia
		Oil-Water Contact	9,000 ft

Region/Array

Initial water saturation (SWAT) : 0.297

Initial gas saturation (SGAS) : 0.703

Initial pressure : 3,000 psia

Dewpoint pressure : 2,188 psia

A-7) Region

Keywords	Region	Cell		
		X	Y	Z
Equilibration region numbers	1	1 - 25	1 - 25	1 - 5
	2	1 - 25	1 - 25	7 - 11
EOS region numbers	1	1 - 25	1 - 25	1 - 5
	2	1 - 25	1 - 25	7 - 11
FIP region numbers	1	1 - 25	1 - 25	1 - 5
	2	1 - 25	1 - 25	7 - 11

A-8) Schedule

Production well

LGR Well Specification (PROD) [WELSPECL]

Well	PROD
Group	-
LGR	PROD_LGR
I location	8
J location	8
Datum depth	6,000 ft
Preferred phase	Gas
Inflow equation	STD
Automatic shut-In instruction	Shut
Cross flow	Yes
Density calculation	SEG
Type of well model	STD

Amalgamated LGR Well Comp Data (PROD) [COMPDATL]

Well	PROD
LGR	PROD_LGR
K upper	1
K lower	5
Open/Shut flag	Open
Well bore ID	0.2916667 ft.
Direction	Z

Production well control (PROD) [WCONPROD]

Well	PROD
Open/Shut flag	Open
Control	GRAT
Gas rate	10000 MSCF/D
THP target	500 psia
VFP pressure table	1

Production well economics limits [WECON]

Well	PROD
Minimum oil rate	10 STB/D
Minimum gas rate	100 MSCF/D
Workover procedure	None
End run	YES

Source well (Dump flood case)

LGR well specification (DUMP) [WELSPECL]

Well	DUMP
Group	-
LGR	DUMP_LGR
I location	1
J location	1
Preferred phase	Gas
Inflow equation	STD
Automatic shut-in instruction	Shut
Cross flow	Yes
Density calculation	SEG
Type of well model	STD

Amalgamated LGR well comp data (DUMP) [COMPDATL]

Well	DUMP
K upper	1
K lower	5
Open/Shut flag	Open
Well bore ID	0.2916667 ft
Direction	Z

Amalgamated LGR well comp data (DUMP) [COMPDATL]

Well	DUMP
K upper	7
K lower	11
Open/Shut flag	Open
Well bore ID	0.2916667 ft
Direction	Z

Production well control (DUMP) [WCONPROD]

Well	DUMP
Open/Shut flag	STOP
Control	-
Gas rate	-
THP target	0
VFP pressure table	2, 3, 4, 5, 6, 7, 8 and 9

Injection well (Injection case)

Well specification (Inj1) [WELSPECS]

Well	DUMP
Group	-
LGR	DUMP_LGR
I location	1
J location	1
Preferred phase	Gas
Inflow equation	STD
Automatic shut-in instruction	Shut
Cross flow	Yes
Density calculation	SEG
Type of well model	STD

Amalgamated LGR well comp data (DUMP) [COMPDATL]

Well	DUMP
K upper	1
K lower	5
Open/Shut flag	Open
Well bore ID	0.2916667 ft
Direction	Z

Injection well control (Inj1) [WCONINJE]

Well	Inj1
Injector type	Gas
Open/Shut flag	Open
Control mode	Rate
Gas surface rate	4000, 6000, 8,000 MSCF/D

Nature of injection gas (Inj1) [WINJGAS]

Well	DUMP
Injection fluid	STREAM
Well stream	1

Injection gas composition [WELLSTRE]

Well stream	1
Comp1	1

APPENDIX B

B-1) Vertical Flow Performance (VFP)

The vertical flow performance curves are generated by production and system performance analysis software (PROSPER) in order to put the proper pressure traverse calculations in the simulation cases.

VFP NO.1

Well : PROD

Fluid : Concentration of each composition is shown in Table 4.2

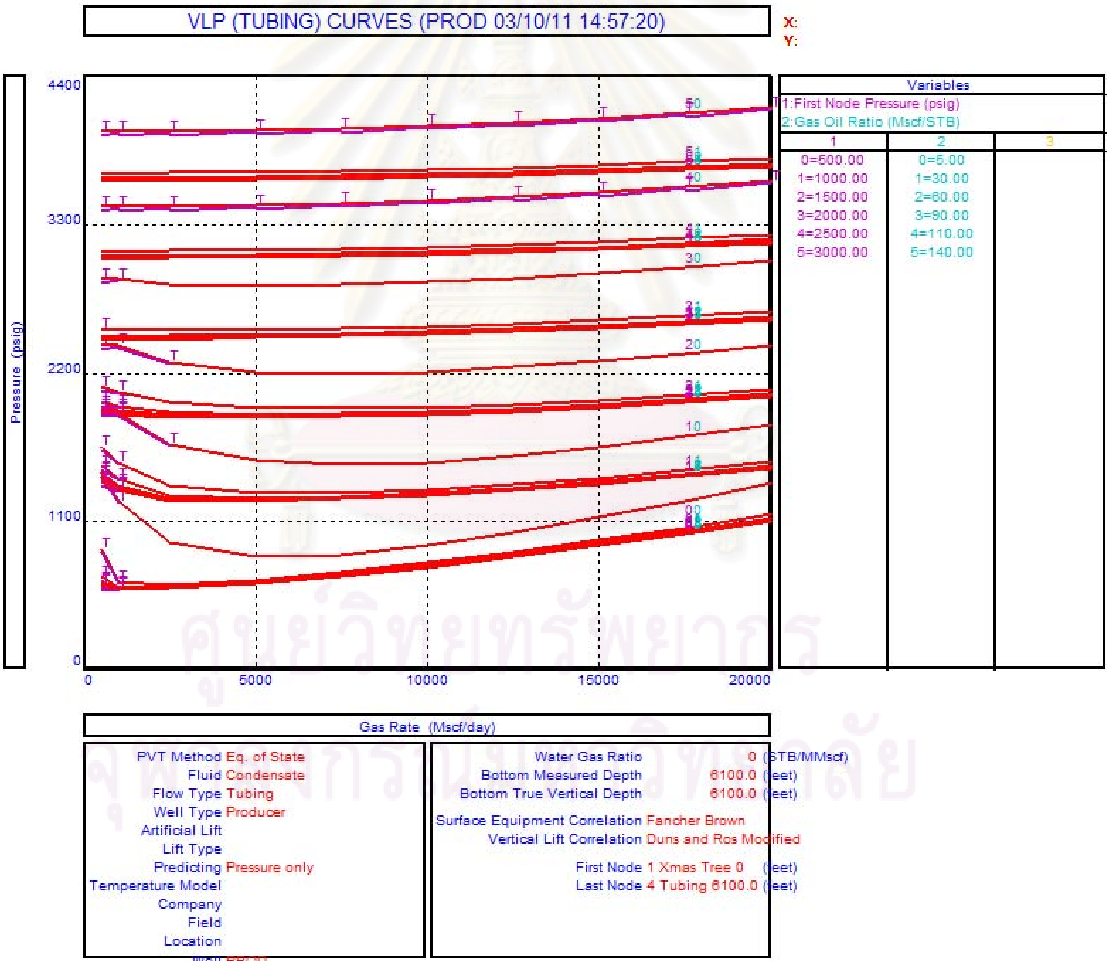

VFP NO.2

Well	: DUMP
Fluid	: C_1:CO_2 = 80:20%
Depth difference	: 1,000 ft

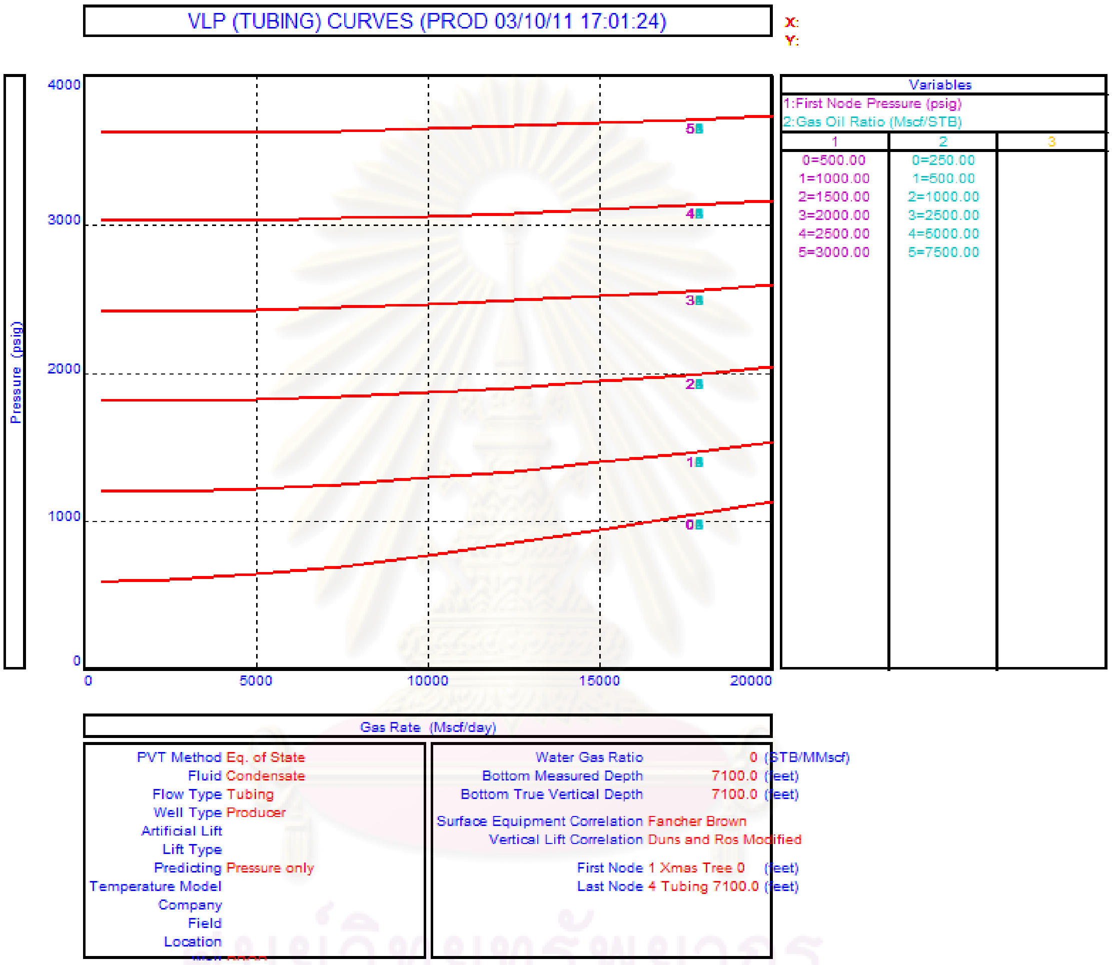

VFP NO.3

Well : DUMP

Fluid : C_1:CO_2 = 60:40%

Depth difference : 1,000 ft

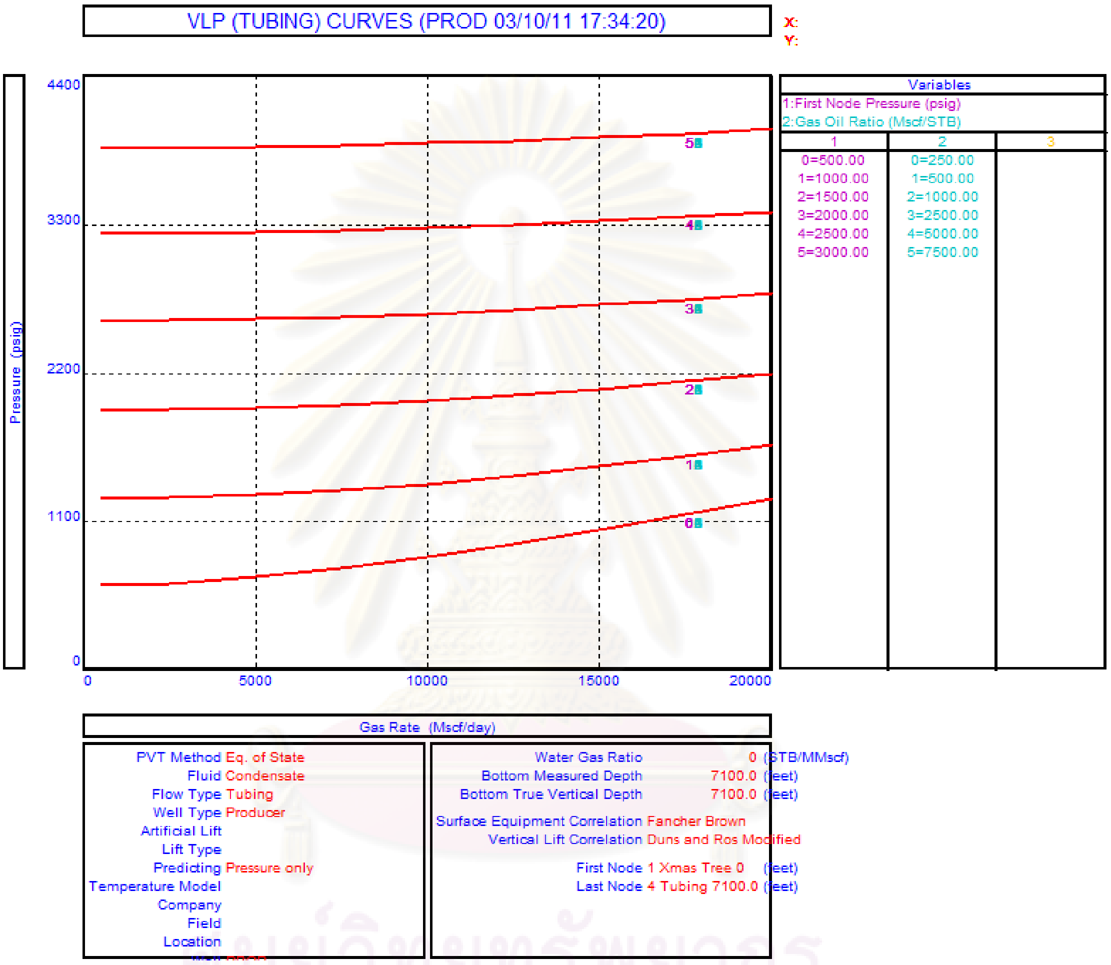

VFP NO.4

Well	: DUMP
Fluid	: C_1:CO_2 = 40:60%
Depth difference	: 1,000 ft

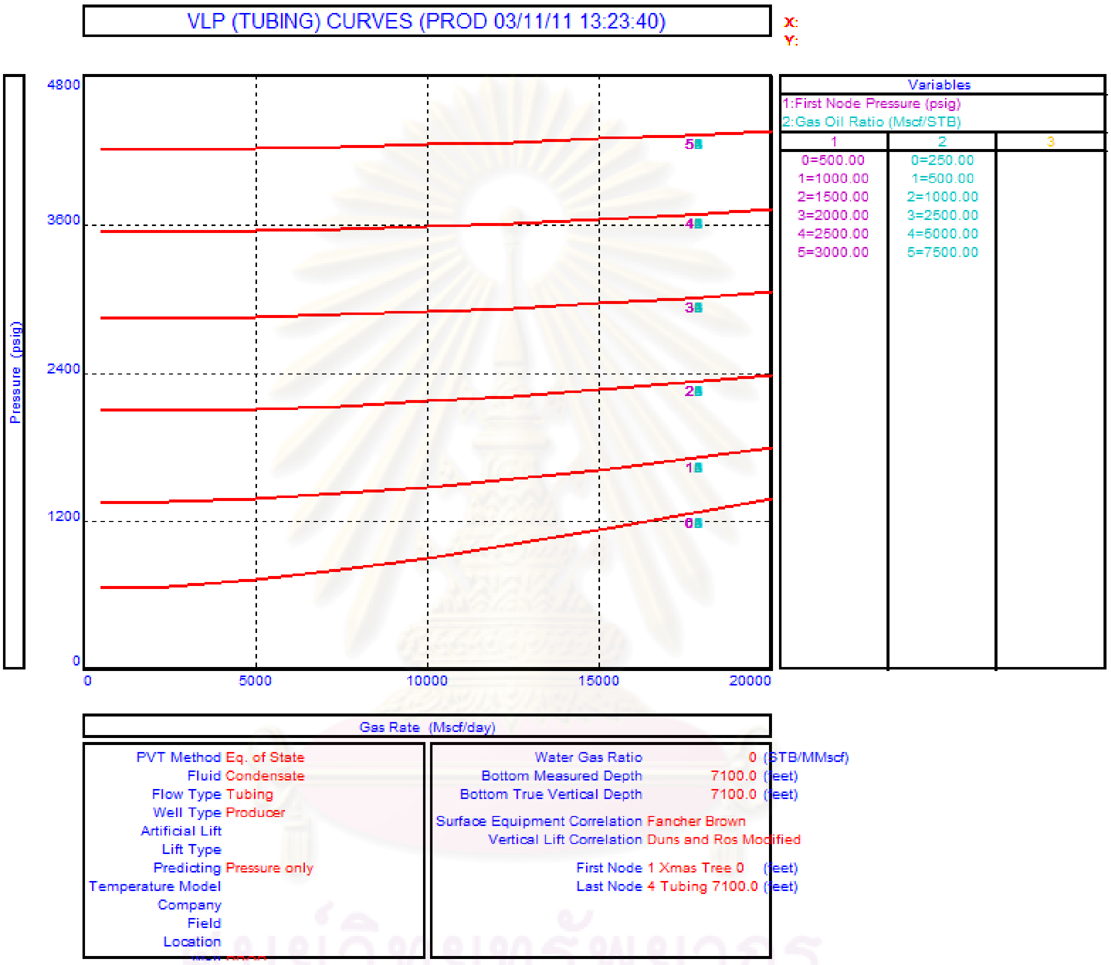

VFP NO.5

Well : DUMP

Fluid : C_1:CO_2 = 20:80%

Depth difference : 1,000 ft

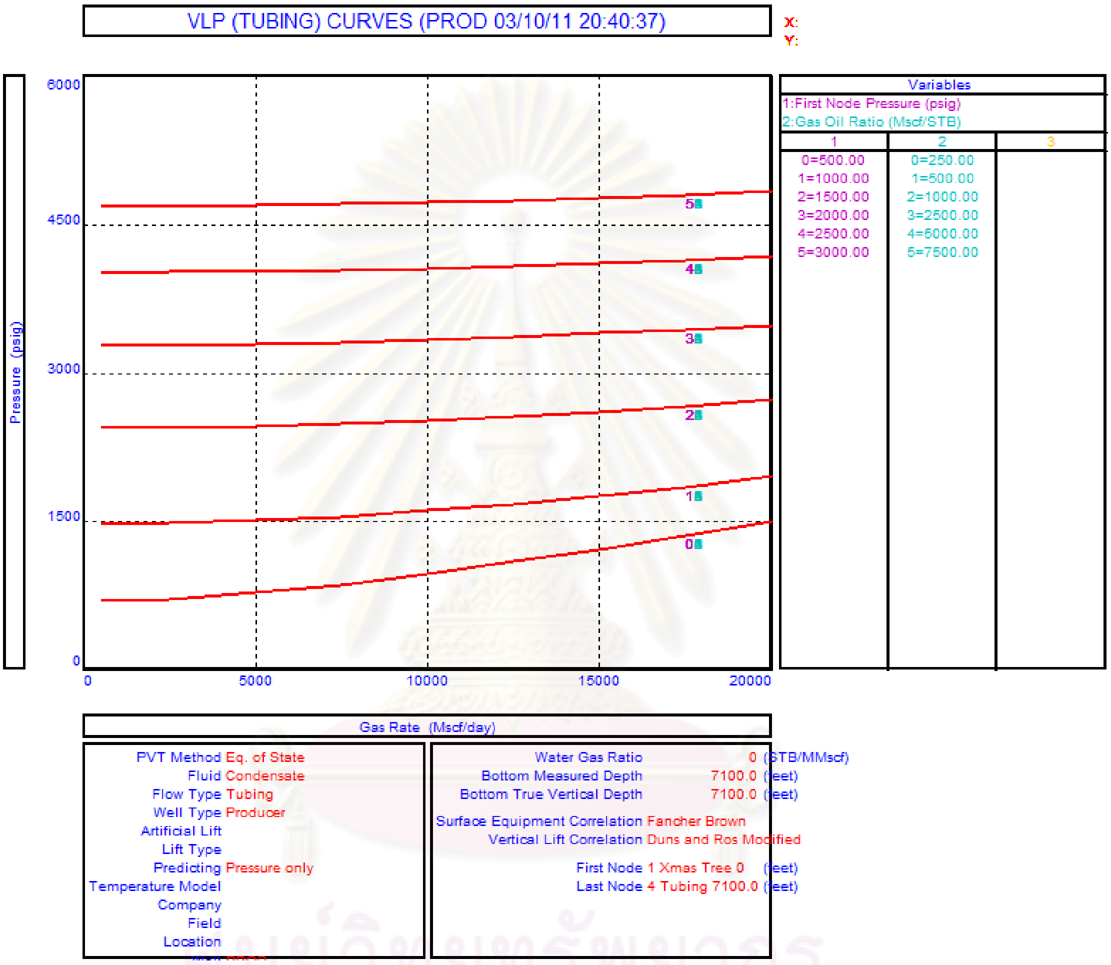

VFP NO.6

Well	: DUMP
Fluid	: C_1:CO_2 = 80:20%
Depth difference	: 2,000 ft

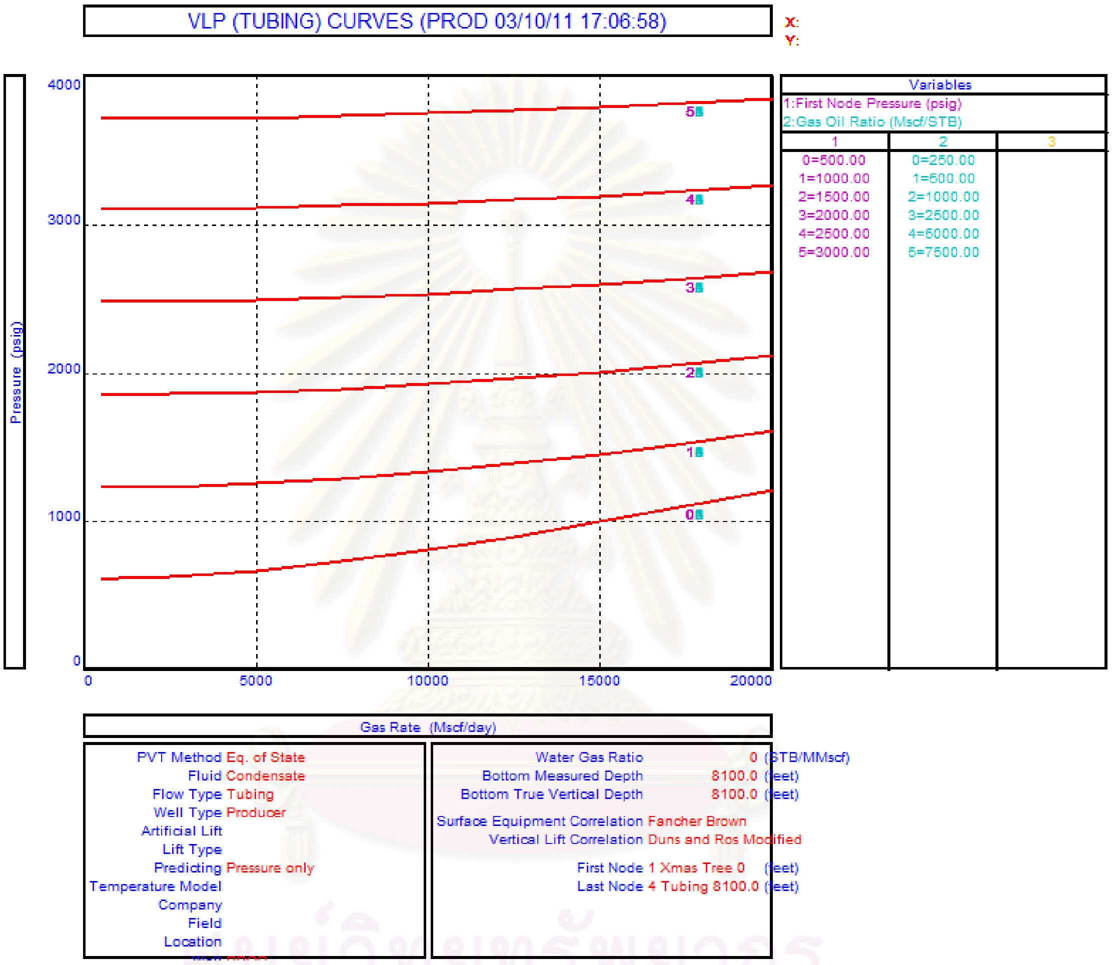

VFP NO.7

Well : DUMP

Fluid : C_1:CO_2 = 60:40%

Depth difference : 2,000 ft

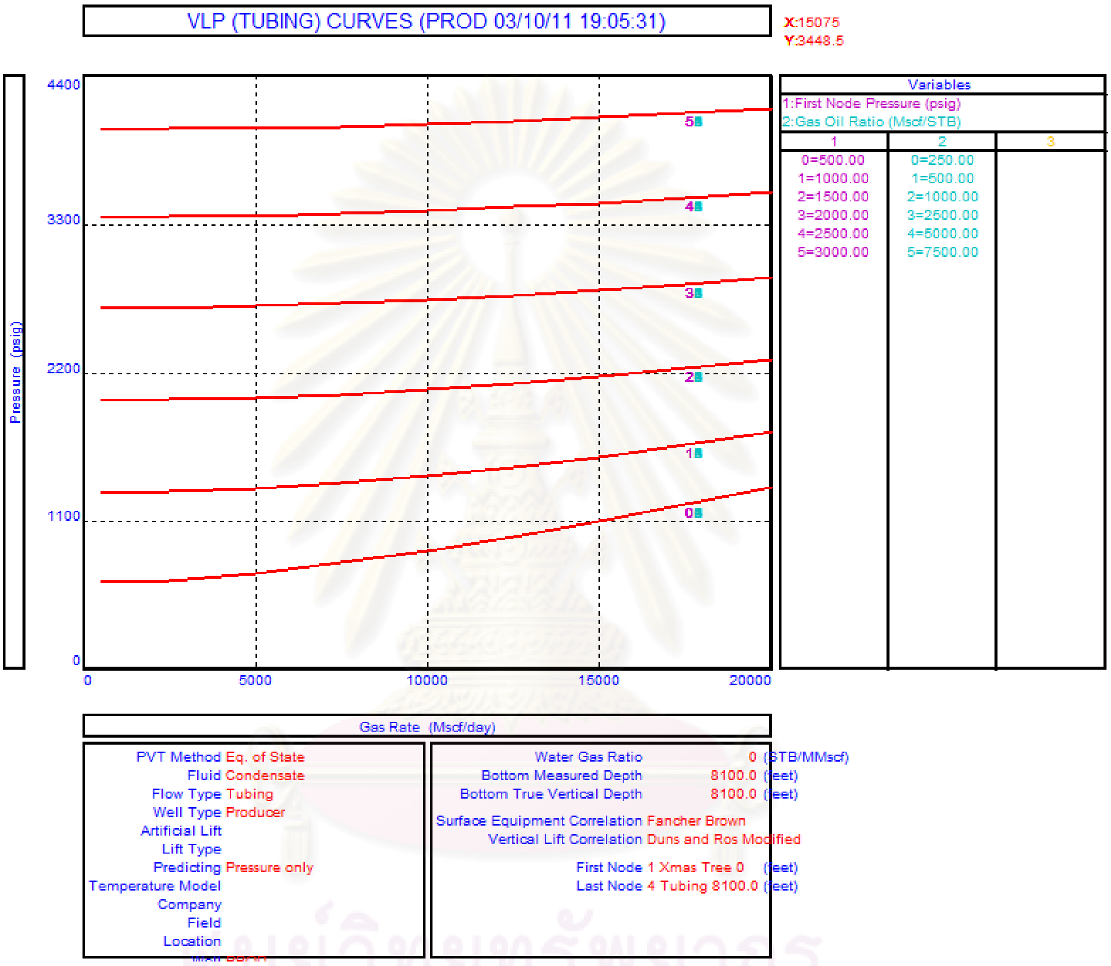

VFP NO.8

Well : DUMP

Fluid : C_1:CO_2 = 40:60%

Depth difference : 2,000 ft

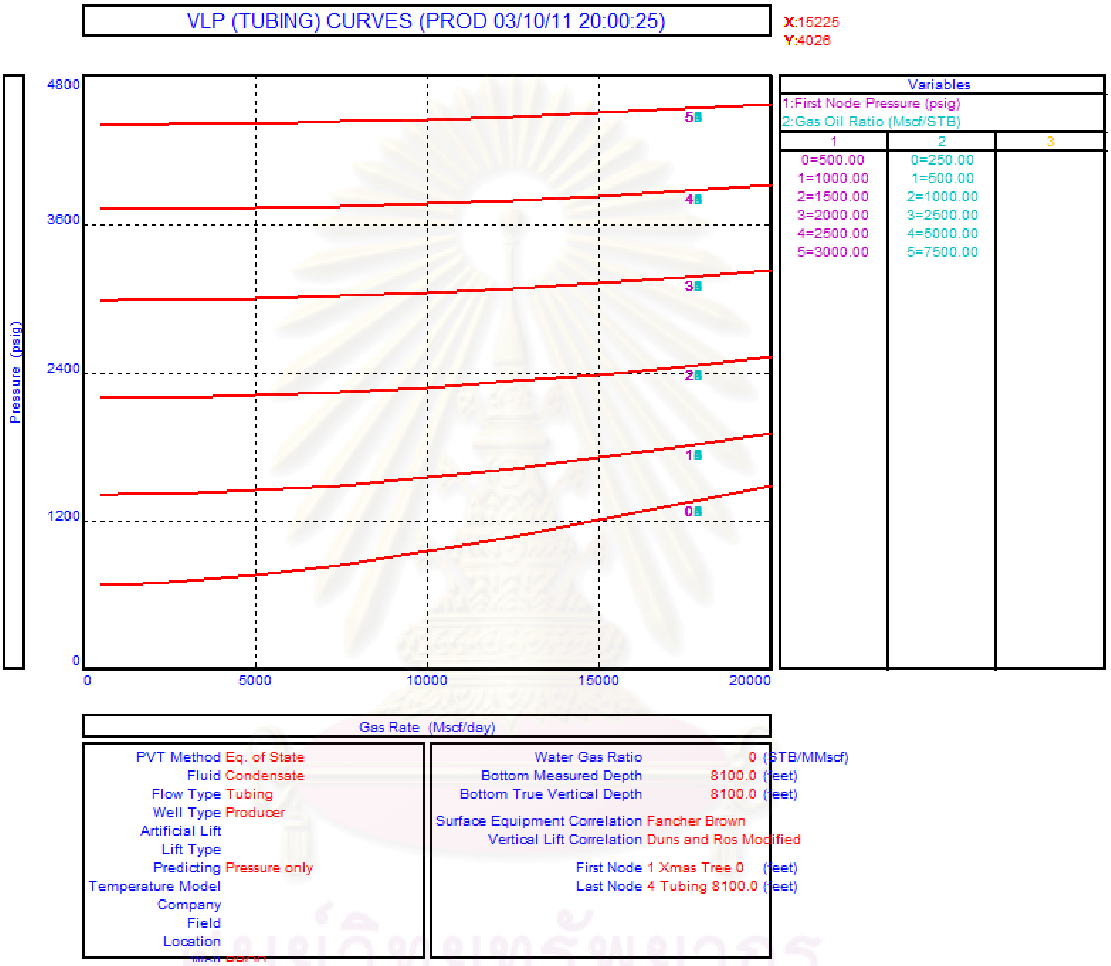

VFP NO.9

Well : DUMP

Fluid : C_1:CO_2 = 20:80%

Depth difference : 2,000 ft

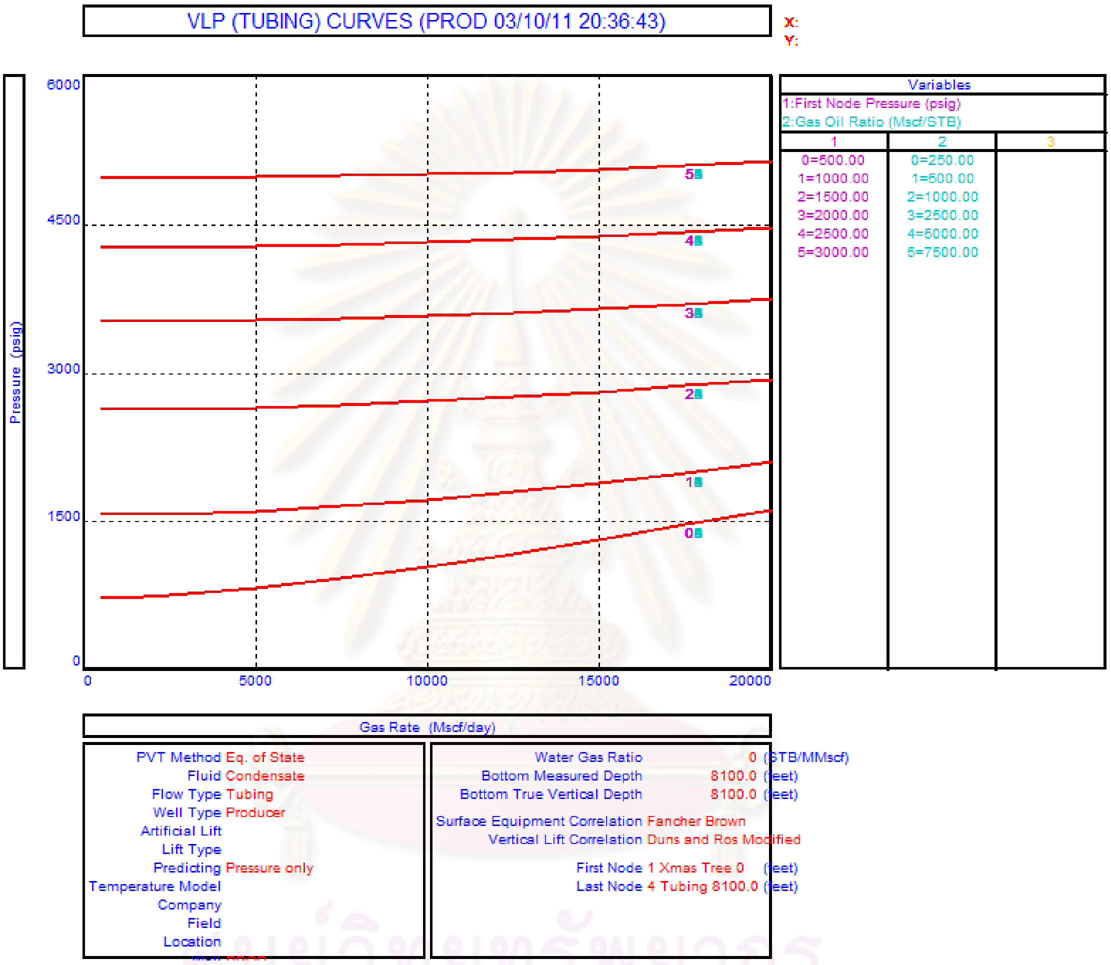

Vitae

Nitichatr Kridsanan was born on April 16th, 1985 in Bangkok, Thailand. He received his degree in Bachelor of Engineering in Electrical Engineering from the Faculty of Engineering, King Mongkut's Institute of Technology Ladkrabang in 2007. He has been a graduate student in the Master's Degree Program in Petroleum Engineering of the Department of Mining and Petroleum Engineering, Chulalongkorn University since 2009.